Western Australian School of Mines: Minerals, Energy and Chemical Engineering

Anti-diabetic Action of Lupinus Angustifolius Seed Proteins and Peptides

Mrunmai Tapadia

This thesis is presented for the Degree of

Doctor of Philosophy

of

Curtin University

March 2019

Declaration

To the best of my knowledge and belief this thesis contains no material previously published by any other person except where due acknowledgment has been made.

This thesis contains no material which has been accepted for the award of any other degree or diploma in any university.

Signature:

Date: 05/03/2019

Acknowledgements

I want to express my deepest gratitude to A/Prof Ranjeet Utikar for his support and guidance throughout the course of my research work. He has been a constant source of encouragement, and his motivation on self-learning over getting direct answers has made me able to solve problems both in academic and personal fronts.

I would like to extend my thanks to Prof. Philip Newsholme for guiding me throughout my PhD tenure and providing me with the infrastructure and scientific inputs in my work. His brilliant suggestions have immensely helped to enhance the standard of this research work. I am grateful to Dr. Rodrigo Carlessi for introducing me to different cell culture techniques, helping me to design experiments for labwork and for providing constant support and guidance at every step of my PhD work. I would like to thank A/Prof. Stuart Johnson for all his suggestions and enabling me to develop an idea from different perspectives.

I am grateful to thank Prof. Vishnu Pareek for providing the facilities, his advice and support during my research work. My special thanks to Dr. Sandeep Kale for recommending me to Curtin University. I am thankful to Prof. Karam Singh for gifting me the primary antibody of γ-conglutin. My appreciation extends to Prof. Marco Falasca for providing valuable suggestions in γ-conglutin bioactivity studies and providing me with INS-1E cell lines. I appreciate the help provided by Dr. Scott Bringans for all the discussions related to MS studies and Mr Russell Nicholls for IP commercialisation.

I gratefully acknowledge Department of Chemical Engineering, Curtin University for providing funding during my PhD. I am thankful to the technical staff of Chemical Engineering, Curtin Health Innovation Research Institute (CHIRI) and School of Public Health for their assistance during the tenure of my work.

The path wouldn't have been easy with company of special friends around me. My special thanks to Manjushree for constantly supporting me like an elder sister, hearing to all my problems and making me feel confident. I would like to extend thanks to Sharmilee for her valuable inputs in the project and helping me to design experiments for lab-work. My special thanks to Sanket, Adhirath and Himanshu for their constant

Abstract

Lupinus Angustifolius, a protein rich legume seed, is gaining global attention due to its blood glucose lowering properties in animals and humans. This research focuses on exploring *in-vitro* anti-diabetic potential of proteins extracted and purified from *Lupinus angustifolius* seed. The proteins extracted from lupin seeds were initially hydrolysed by digestive enzymes to mimic oral gastrointestinal proteolytic digestive condition. The insulin secretory property of protein extract in rat derived pancreatic β cell lines (BRIN-BD11 and INS-1E) was explored. The extract hydrolysate exhibited glucose permissive insulin secretion along with enhanced glucose metabolism subsequently leading to membrane depolarisation and insulin secretion in pancreatic β cell. Also, a novel insulin secretory mechanism of extract hydrolysate mediating through $G\alpha_q$ protein signalling transduction by activating PLC-PKC pathway and increasing downstream intracellular Ca^{2+} levels was established.

The glucose modulating property of lupin has been attributed to a particular seed protein 'γ-conglutin' as reported from different clinical studies in animal and humans. Despite its potential value in diabetes, its application in nutraceutical and functional foods is limited. The conventional methods for purification of γ-conglutin from lupin seed extract involves number of steps which increases the overall cost of the process. Also, the purity of γ-conglutin is either not reported or calculated on the basis of semi-quantitative techniques. Thus, an in-house γ-conglutin purification method was further improved with an objective to achieve pure γ-conglutin fractions. The identity of purified γ-conglutin was confirmed by western blotting and mass spectrometry and its purity was determined by sodium do-decyl sulphate polyacrylamide gel electrophoresis (~100%) and reverse-phase high performance liquid chromatography (95.2%) techniques.

In order to evaluate its effect as oral supplements, the purified fraction of γ-conglutin was hydrolysed by gastrointestinal proteolytic enzymes. Later, γ-conglutin peptides were evaluated for their anti-diabetic properties in pancreatic β-cells and primary human muscle cells. γ-conglutin peptides did not exhibit insulin secretory action in β cells but exhibited potent insulin-mimetic action by activating different branches of

insulin signalling pathway responsible for glycogen and protein synthesis and glucose transport in muscle cells. Peptides also inhibited dipeptidyl peptidase 4 enzyme. This inhibitory action can potentially increase the blood levels of incretin hormones responsible for triggering insulin secretion in pancreatic β cells.

The current research has identified lupin seed proteins as a valuable source of anti-diabetic biomolecules that can improve glucose homeostasis in type 2 diabetic patients. The results presented herein substantiate the health benefits achieved from lupin seeds which can be one of the preliminary steps in driving the current market of lupins as stockfeed, towards lupin-based food products for human consumption.

Publications and conferences

Peer reviewed journals

- Tapadia, M. T., Carlessi R., Utikar, R.P., Johnson, S., Newsholme, P. (2019). Lupin seed hydrolysate promotes G-protein-coupled receptor, intracellular Ca2+ and enhanced glycolytic metabolism-mediated insulin secretion from BRIN-BD11 pancreatic beta cells. *Molecular and cellular endocrinology,* 480 (2019): 83-96. (*Impact Factor – 3.9*).

Conferences

- Tapadia, M. T., Carlessi R., Utikar, R.P., Johnson, S., Newsholme, P. Insulinotropic effects of lupin protein hydrolysates, Science on the Swan 2017, Perth, Western Australia (*poster presentation*).

- Tapadia, M. T., Carlessi R., Utikar, R.P., Johnson, S., Newsholme, P. Lupin hydrolysate as emerging insulinotropic agent, Australian Islet Society Group meeting 2017, Perth, Western Australia (*oral presentation*).

Patent and Award

Patent application

- A process patent application is being filed for purification of γ-conglutin from lupin protein extract (chapter 3)

Curtin Commercial Innovation Award 2017

- 'Extraction of anti-diabetic from the humble lupin' Curtin Commercial Innovation Awards 2017, Health Science Prize.

Chapter 3 (section 3.5.4) and chapter 4

Statement of authorship

Title of Paper	Lupin seed hydrolysate promotes G-protein-coupled receptor, intracellular Ca^{2+} and enhanced glycolytic metabolism-mediated insulin secretion from BRIN-BD11 pancreatic β cells
Publication Status	Published
Publication Details	https://doi.org/10.1016/j.mce.2018.10.015
Journal	Molecular and cellular endocrinology (2019; volume 480; pages 83-96

Author information and contribution

Author 1	Mrunmai Tapadia (primary / first author)
Affiliation	HDR student, Curtin University, Australia
Contribution	Conducted literature review, carried out all the experiments, data analysis and wrote the manuscript
Declaration	This paper reports on the original research I conducted during the period of my Higher Degree by Research candidature and is not subjected to any obligations or contractual agreements with a third party that would constrain its inclusion in this thesis. I acknowledge the contribution stated above are accurate to the best of my knowledge.
Signature	██████ Date 26/02/19

Author 2	Dr. Rodrigo Carlessi (corresponding author)
Affiliation	Research Fellow, School of Pharmacy and Biomedical Sciences, Curtin Health Innovation Research Institute Biosciences, Curtin University, Australia
Contribution	Assisted in experimental design related to investigation of insulin secretion mechanism, data analysis from experiments and manuscript development
Declaration	I acknowledge the contribution stated above are accurate to the best of my knowledge.
Signature	██████ Date

Author 3	A/Prof. Stuart Johnson (co-author)		
Affiliation	Associate Professor, School of Molecular and Life Sciences, Curtin Health Innovation Research Institute, Australia		
Contribution	Assisted in lupin protein extraction, data analysis and reviewed manuscript		
Declaration	I acknowledge the contribution stated above are accurate to the best of my knowledge.		
Signature	■■■■■	Date	27/02/2019

Author 4	A/Prof Ranjeet Utikar (co-author)		
Affiliation	Associate Professor, WASM: Minerals, Energy and Chemical Engineering, Curtin University, Australia		
Contribution	Assisted in lupin protein extraction, characterisation of lupin hydrolysate, data analysis from experiments, reviewed manuscript.		
Declaration	I acknowledge the contribution stated above are accurate to the best of my knowledge.		
Signature	■■■■■	Date	26/02/2019
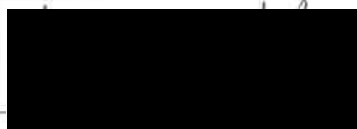
Author 5	Prof. Philip Newsholme (corresponding author)		
Affiliation	Professor, School of Pharmacy and Biomedical Sciences, Curtin Health Innovation Research Institute Biosciences, Curtin University, Australia		
Contribution	Assisted in the cellular experimental design related to investigation of insulin secretion mechanism, data analysis from experiments and manuscript development.		
Declaration	I acknowledge the contribution stated above are accurate to the best of my knowledge.		
Signature	■■■■■	Date	26th February 2019

Table of Contents

Nomenclature

Acronyms

2-NBDG	2-(N-(7-nitrobenz-2-oxa-1,3-diazol-4-yl) amino)-2-deoxyglucose
AC	Adenylate cyclase
ADP	Adenosine diphosphate
Akt	Protein kinase B
AMC	Aminomethylcoumarin
ANOVA	Analysis of variance
ATP	Adenosine triphosphate
BCA	Bicinchoninic acid
BSA	Bovine serum albumin
BW	Body weight
cAMP	Cyclic adenosine monophosphate
CREB	cAMP regulatory element binding
CV	Column volume
DAG	Diacyl glycerol
DH	Degree of hydrolysis
DMEM	Dulbecco's modified Eagle's medium
DNA	Deoxyribo nucleic acid
DPP4	Dipeptidyl peptidase 4
ECAR	Extracellular Acidification Rate
ECL	Enhanced chemiluminescence
EDTA	Ethylenediaminetetraacetate
eIF4E	Eukaryotic translation initiation factor
ELISA	Enzyme-linked immunosorbent assay
EPAC2	Exchange protein directly activated by cAMP
ERK	Extracellular signal-regulated kinase
FCCP	Carbonilcyanide p-triflouromethoxyphenylhydrazone
FSC	Forward scatter

G6Pase	Glucose-6-phosphatase
GAPDH	Glyceraldehyde-3-phosphate dehydrogenase
GDP	Guanosine diphosphate
GIP	Gastric inhibitory peptide
GLP-1	Glucagon like peptide 1
GLP-1R	$G\alpha_s$ protein coupled receptor specific to GLP-1
GLUT2	Glucose transporter 2
GLUT4	Glucose transporter 4
GPCR	G-protein coupled receptor
GPR	$G\alpha_q$ protein receptors
Grb2	Growth factor receptor bound 2
GS	Glycogen synthase
GSIS	Glucose-stimulated insulin secretion
GSK3β	Glycogen synthase kinase-3β
GTP	Guanosine triphosphate
HMW	High molecular weight
HOMA-IR	Homeostatic model assessment- insulin resistance
HRP	Horseradish peroxidase
HSMM	Human skeletal muscle myotubes
IMW	Intermediate molecular weight
IP3	Inositol triphosphate
IR	Insulin receptor
IRS	Insulin receptor substrate
K-ATP	ATP dependent potassium channels
KRBB	Krebs Ringer bicarbonate buffer
LC-MS	Liquid chromatography mass spectrometry
LDL	Low-density lipoproteins
LMW	Low molecular weight
m/z	Mass to charge ratio
MAPK	Mitogen-activated protein kinases

MCT	Monocarboxylate transporter
MRM-MS	Multiple reaction monitoring mass spectrometry
mRNA	Messenger ribonucleic acid
MS	Mass spectrometry
mTOR	Mammalian target of rapamycin
mTORC2	Mammalian target of rapamycin complex 2
MTT	(3-(4,5-dimethylthiazol-2-yl)-2,5-diphenyl tetrazolium bromide)
MW	Molecular weight
MWCO	Molecular weight cut off
NADPH	Nicotinamide adenine dinucleotide phosphate reduced
OCR	Oxygen Consumption Rate
OPA	o-phthalaldehyde
OPP	O-propargyl-puromycin
p70S6K	Ribosomal protein S6 kinase
PBS	Phosphate buffer saline
PDK-1	3-phosphoinositide-dependent protein kinase 1
PEPCK	Phosphoenol pyruvate carboxykinase
pH(I)	Isoelectric point
PI	Propidium iodide
PI3K	Phosphoinositide kinase-3
PI3K	Phosphoinositide-3-kinase
PIP2	Phosphatidylinositol 4,5 biphosphate
PKA	Protein kinase A
PKC	Protein kinase C
PLC	Phospholipase C
pNPG	p-nitrophenol-α-D-glucopyranoside
PVDF	Polyvinylidene fluoride
RIPA	Radioimmunoprecipitation buffer
RP-HPLC	Reverse phase high-performance liquid chromatography
RPMI	Roswell Park Memorial Institute medium

S6	S6 ribosomal protein
SD	Standard deviation
SDS-PAGE	Sodium do-decyl sulphate polyacrylamide gel electrophoresis
SEC	Size exclusion chromatography
SPR	Surface plasma resonance
SSC	Side scatter
STZ	Streptozotocin
T2D	Type 2 diabetes
TBST	Tris-buffered saline with 0.05% Tween 20
TFA	Trifluoroacetic acid
TSC	Tuberous sclerosis complex
UV	Ultraviolet

Symbols

α	Alpha
β	Beta
γ	Gamma
δ	Delta
R^2	Regression coefficient
Rs	Resolution factor
V_R	Retention volume
$W_{0.5}$	Peak width measured at half height
As	Asymmetry factor
HETP	Height equivalent to theoretical plate

List of Figures

List of Tables

Chapter 1

Introduction

1.1 INTRODUCTION

In humans, after food intake, there is a rapid rise in blood glucose levels peaking about one hour after the meal. Insulin helps to transport the circulating glucose from the blood into the cells for the production of storage molecules such as glycogen or triacylglycerol, thus achieving blood glucose homeostasis. Diabetes is a chronic condition in which the production and/or function of insulin is impaired, subsequently leading to a high blood glucose level i.e. hyperglycaemic condition. Type 1 diabetes is an autoimmune condition where the body's own immune system attacks pancreatic β cell inducing progressive depletion in β cell mass and low levels of insulin in the blood [1]. In type 2 diabetes, the body cells develop resistance to the normal effects of insulin. Due to this, pancreatic β cells produce more insulin to maintain glucose homeostasis and the overproduction of insulin eventually results in wear and tear of β cells. By the time an individual is diagnosed, there is already a loss of ~50-70% of β cells [2]. Thus, type 2 diabetes is a combination of early insulin resistance and progressive loss of β cells leading to insufficient amounts of insulin in blood [3].

Type 1 and type 2 diabetes represents about 10-15% and 85-90% of all diabetes cases respectively [4]. Type 1 diabetes, known as juvenile-onset diabetes, most frequently begins in childhood and the peak age of diagnosis is 10-14 years [4]. It is treated by injecting insulin several times a day or by using insulin pumps. Type 2 diabetes generally affect adults over the age of 45-55 years. This condition can be initially managed by changing lifestyle and managing diet, maintaining a healthy weight, and regular physical activity [5]. Later, blood glucose levels can be maintained by proper medications. The medications used for the treatment of type 2 diabetes work by either improving body cell's sensitivity to insulin and/or decrease glucose production in the liver and/or increase insulin secretion from pancreatic β cells [6]. Drugs inhibiting dipeptidyl peptidase 4 (DPP4) enzyme increases the level of incretin hormone responsible for triggering insulin secretion in pancreatic β cells and drugs inhibiting α-glucosidase enzyme in intestine delays the degradation of starch into glucose [7, 8].

As a result, inhibition of these enzymes directly or indirectly regulate blood glucose level in hyperglycaemic conditions.

A diabetic condition can increase the risk of heart attack, stroke, visual impairment, kidney failure, amputation, depression, stress and anxiety [4]. Because of all the complications associated with diabetes, it is recorded as the seventh major leading cause of death [9]. According to the International Diabetes Federation, 1 in 11 adults worldwide has diabetes (425 million) and 1 in 2 diabetic adults is undiagnosed [10]. Medication and treatments related to diabetes are a major source of household expenditure in many parts of the world. The total economic cost of diagnosed diabetes in the USA (2017) was $327 billion [11]. People diagnosed with diabetes have medical expenditure 2.3 times more than people with the absence of diabetes. Also, due to the increasing prevalence of diabetes, the economic costs of diabetes has raised by 26% from 2012 to 2017 [11]. All this has imposed a huge economic burden on diabetic patients and/or healthcare systems in society.

To prevent and control pathophysiological changes in diabetes, dietary interventions with supplements as well as functional foods are being encouraged for type 2 diabetes patients [12, 13]. The objectives of the dietary treatments in diabetes are to help bring blood glucose and lipid levels under control, prevent/reduce diabetes-related complications and improve health and fitness by providing balanced nutrition [14]. An anti-diabetic agent improves blood glucose homeostasis by (a) enhancing insulin secretion from pancreatic β cells (insulinotropic), (b) mimicking/improving insulin action in peripheral tissues (insulin-mimetics) or (c) exhibiting extra-pancreatic effects by inhibiting the enzymes (α-glucosidase and DPP4) which can contribute to the regulation of blood glucose levels [15]. Before the introduction of therapeutic drugs for diabetes, its treatment relied heavily on dietary supplements using traditional plant therapies like extracts from roots, leaves, and bark [16, 17] consisting of different bioactives like proteins, polypeptides, alkaloids and glycosides [18-20]. Bioactive compounds from plants are currently regaining the momentum as compared to synthetic medicines for the treatment of diabetes due to their abundant availability, efficacy and fewer side effects [21, 22].

Grain legumes are the source of protein, minerals, vitamins, dietary fibres and anti-oxidants that have important health protective benefits [23]. Lupin (*Lupinus angustifolius*) is one of the largest legume seed crops grown in Australia and a major rotation crop in Western Australia [24]. It is crucial for sustainable grain production through its nitrogen-fixing ability [25]. Its balance of essential amino acids is complementary to cereal proteins. In recent years, leguminous seeds have played a primary role in the search for vegetable sources of proteins as a replacement for animal proteins [26]. Australian sweet lupin has recently been recognized as such a source due to its low cost, non-genetically modified status, and low levels of potentially hazardous phytoestrogenic compounds and alkaloids [27]. This has resulted in increased commercial interest in lupin as a health food ingredient and nutraceutical.

1.2 MOTIVATION

The majority of lupin production is consumed as ruminant, pigs and poultry feed [28]. Recently, however, the emerging health benefits of lupins has shifted the focus towards human consumption [29]. Lupin has high protein and fibre content with negligible sugar and starch and thus can lower the glycaemic load of the diet [26, 30]. Clinical studies in animals and humans focusing on hypoglycaemic actions of lupin seed based food preparations (bread, pasta, beverages) and/or proteins have been reported [31-35]. This stimulated research in exploring the hypoglycaemic mechanism of action of lupin seed proteins.

Identification of a bioactive is relatively straightforward as compared to investigating its mechanism of action. Only a few studies have demonstrated the insulinotropic property of lupin seed extract/protein with very limited focus on its mechanism of action [36, 37]. As a result, investigating signaling pathways responsible for insulin secretory action of lupins in pancreatic β cells will provide scientific substantiation for its health benefits and will help in the promotion of lupin seed as human food.

The glucose modulating property of lupin has been attributed to a specific seed protein component 'γ-conglutin' as evaluated from different cellular and animal models and human post-prandial studies. In spite of its potential value in diabetes, application of γ-conglutin protein as a nutraceutical and pharma food is still commercially restricted.

This undervaluation is due to lack of an efficient food-grade scalable γ-conglutin purification process. The conventional method for lupin protein isolation is alkaline extraction of proteins from defatted lupin flour, separation of insoluble fibres remaining after extraction, and acidification of the extract at the isoelectric point of major lupin globulins (α and β) [38]. The precipitated globulins (α and β) are recovered by centrifugation, whereas the supernatant enriched with γ-conglutin is further purified by a combination of chromatographic processes (anion exchange followed by cation exchange coupled with zinc and insulin affinity chromatography) [38]. This existing lab-scale purification method involves a number of steps which increases the total operating cost. Also, zinc affinity chromatography can lead to contamination of purified γ-conglutin with leached zinc making it unfit for human consumption. In literature, the purity of γ-conglutin used for deducing hypoglycaemic mechanism of action is either not reported or calculated based on semi-quantitative technique like gel electrophoresis. In order to address all the above short-comings in the purification processes, a cost-effective purification process for selective extraction and purification of γ-conglutin from *L. angustifolius* seed flour with a minimum number of steps was previously optimised in our laboratory [39]. However, there is a need to further develop this process to improve the purity of γ-conglutin. The development of such a purification process yielding high purity γ-conglutin can drive the market of lupins from a cattle feed to anti-diabetic nutraceutical or bio-pharmaceutical agent.

The insulin-mimetic property of γ-conglutin peptides in derived muscle, liver and fat cell lines has been studied in detail [40-42]. γ-conglutin activated insulin signalling pathways responsible for muscle energy metabolism, glucose transport, and protein and glycogen synthesis in derived mouse muscle myoblasts. However, these insulin-mimetic effects of γ-conglutin have not been validated in primary human muscle cells. Also, exploring other γ-conglutin antidiabetic activities like insulinotropic action in pancreatic β cells and inhibitory action on enzymes (α-glucosidase and dipeptidyl peptidase 4) responsible for directly or indirectly increasing blood glucose levels can help in better understanding the glucose modulating action of γ-conglutin peptides. Further fractionation and identification of bioactive peptide(s) can guide the development of innovative peptide-based nutraceuticals from lupin.

1.3 AIMS AND OBJECTIVES

The primary aim of this thesis is to gain a deep insight into mechanisms underlying the anti-diabetic action of lupin proteins in crude extract and in purified form. Following are the specific objectives of this research:

- To deduce insulin secretory (insulinotropic) mechanism of action of lupin extract in pancreatic β cell lines – BRIN-BD11 and INS-1E.

- To improve the in-house cation exchange chromatography purification process with an objective to achieve pure γ-conglutin fractions.

- To characterize the purified γ-conglutin by a range of analytical methods such as sodium do-decyl sulphate polyacrylamide gel electrophoresis (SDS-PAGE), western blot, reverse phase high-performance liquid chromatography (RP-HPLC) and mass spectrometry.

- To explore different potential anti-diabetic action of γ-conglutin like insulinotropic action in pancreatic β cells, insulin-mimetic action in human muscle cells, and enzyme (DPP4 and α-glucosidase) inhibitory action.

1.4 THESIS STRUCTURE

The thesis is divided into 6 chapters as summarised in Figure 1.1 and explained in the text:
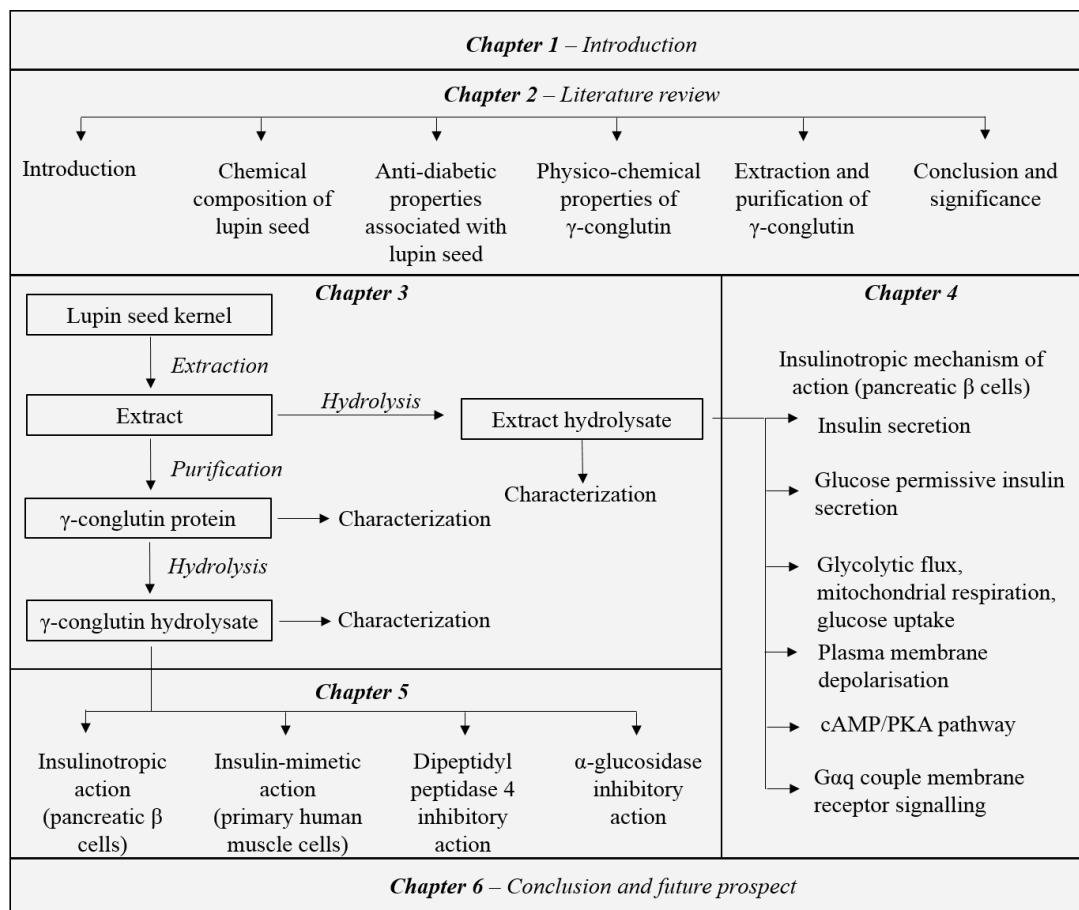
Figure 1.1 Outline of thesis chapters

- Chapter 1 gives a brief introduction to the research problems along with the motivation and objectives of the research work

- Chapter 2 presents a comprehensive literature review in relation to production and market for lupin seeds, bioconstitutents present in the seed, their physicochemical properties and bioactivities associated with them. It also provides an overview of existing extraction and purification methods devised for separation of lupin proteins, in particularly, γ-conglutin. The chapter is concluded by identifying research gaps in existing research and by formulating different set of questions as starting point for further investigation.

- Chapter 3 (experimental) focuses on extraction, purification, and hydrolysis of lupin proteins. First, the established in-house process protocol for extraction of lupin proteins and purification γ-conglutin is summarised and discussed. Later, this purification process is further developed and improvised with an objective to achieve maximum possible pure γ-conglutin. The identity and purity of eluted γ-

conglutin fraction is determined using different analytical techniques. In order to evaluate the effect of both the extract and γ-conglutin as oral supplements, they are subjected to proteolytic gastrointestinal digestion (hydrolysis). The anti-diabetic action of the hydrolysates obtained at the end of hydrolysis is evaluated in further chapters.

- Chapter 4 (experimental) is based on deducing the insulinotropic mechanism of action of crude lupin extract hydrolysate in BRIN-BD11 pancreatic β cells. This chapter focuses on the identification of the insulin secretory action of hydrolysate in β cells. Effect of the hydrolysate on glucose metabolism and classical membrane depolarisation mechanism involved in insulin exocytosis is discussed. Detailed investigation of different signalling pathways responsible for the hydrolysate's insulinotropic action in β cells is accomplished. This chapter, for the first time, provides the evidence of insulinotropic action of lupin hydrolysate via G-protein receptor-mediated signal transduction ($G\alpha_q$/PLC/PKC pathway) in β cells.

- Chapter 5 (experimental) is focused on exploring potential anti-diabetic actions of peptides (hydrolysate) obtained from hydrolysis of pure γ-conglutin protein. Insulinotropic (insulin secretion) action of peptides in pancreatic β cells (BRIN-BD11) is studied. Effect of the peptides on different branches of insulin signal transduction pathway in primary muscle myotubes is also investigated. Lastly, the inhibitory effect of peptides on the enzymatic activity of DPP4 and α-glucosidase enzymes is evaluated.

- Chapter 6 is an overall conclusion of the research work by highlighting important new knowledge, potential outcomes and areas of improvement and suggestion for the future work.

Chapter 2

Literature review

2.1 INTRODUCTION

Legumes include all forms of peas, beans, lentils, peanuts and other types of plants with seeds in pods used as food. The seeds accumulate a large number of proteins in their development stage that provides amino acids, carbon, and nitrogen skeleton to the developing seedling in its germination stage [43]. Proteins in legume seed constitute about ~20% (dry weight) in pea and beans with an exceptionally high amount (35-40%) in lupins and soybeans and can, thus, be regarded as one of the richest sources of plant proteins for animal and human consumption [26]. Apart from being a source of amino acids, legume proteins also play an important role as sources of bioactives and may protect against health problems in humans such as diabetes, cardiovascular disease, obesity, digestive malfunctions, and hypocholesterolemia [26].

This chapter describes various health benefits of a legume seed, lupin. Initially, the chapter discusses the agricultural production and market for lupin seeds, the bioconstitutents present in the seed, their physicochemical properties, and bioactivities associated with them. Then, an overview of existing extraction and purification methods for separation of lupin proteins, particularly, γ-conglutin along with the associated challenges are presented. The chapter concludes by identifying the research gaps in current literature and the areas that need further exploration.

2.1.1 Lupin taxonomy

Lupinus, commonly known as 'lupin' (in Australia and Europe) or 'lupine' (in North America), is an ancient, large and diverse genus in the leguminous family. Taxonomically, lupins are classified within the class Magnoliophyta, order Fabales, family Fabaceae (or leguminosae), tribe Genisteae and genus *Lupinus L.* [44]. The number of species in this genus is not well defined and is estimated to be more than 1000. However, the existing well recorded lupin species are around 280 with 164 of them accepted officially as species in Integrated Taxonomic Information System [28, 45]. Out of these species, only four of them are of agronomic interest - *L. angustifolius*,

L. albus, *L. luteus,* and *L. mutabilis* and are produced in Australia, Denmark, Chile, Poland, Germany, USSR, USA, and Ukraine [46]. *L. angustifolius*, known as blue or narrow-leafed lupin, is extensively grown in Australia, whereas *L. albus* (white lupin) and *L. luteus* (yellow lupin) are native to Europe and Mediterranean region respectively [46] and *L. mutabilis*, known as Andean or Tarwi or pearl lupin, belongs mostly to the Andean region of Ecuador, Peru, and Bolivia [47]. Recently developed varieties of *L. angustifolius* are known as 'Australian sweet lupin' due to their low alkaloid content (<200mg/kg) compared to other wild lupin types (5,000 – 40,000mg/kg alkaloids) [27].

2.1.2 Production

Australia is the largest lupin producer contributing to 85% of lupin production in the world. Other leading producers include Chile, Belarus, Russian Federation and European Union producing lupin which contribute a lesser percentage as compared to Australia [30]. Western Australia is the leading exporter of lupin producing 80% of Australia's lupin in the wheat belt tracts while the remainder is grown in southwestern slopes of Victoria and South Australia [29, 30]. The majority of *L. angustifolius* variety is grown in Western Australia while the *L. albus* variety is grown in New South Wales and Victoria [48].

L. angustifolius prefer sandy acidic soil (pH 4.5-7) with a supply of manganese and potassium for high yield and grain quality [25]. Being a leguminous crop, they fix nitrogen in the soil with the deep root system and, thus, can tolerate infertile soil. Since lupins have hard seed coat and low moisture content they can be stored for several years. Lupin production in Australia peaked in 1980s and 1990s before the prevalence of weed issues [25]. Eventually, due to low prices, growers opted for canola cultivation instead of lupin as a rotation crop. As a result, the production of lupin fell from 1200,000 hectares/tonnes in 1998 to 700,000 hectares/tonnes in 2016 [29]. Optimistically, cultivation of new varieties resistant to different pests and viruses coupled with continuous awareness and promotion of health benefits from lupin seeds should escalate lupin production again in the near future.

2.1.3 Market

The majority of lupin production is primarily consumed as ruminant feed followed by pigs and poultry feed with small percentage used in aquaculture [28]. Western Australia is a leading exporter of lupin to Germany, Japan, Malaysia, Netherland and South Korea [30]. Lupins are valued at 70 to 75% of soybean meal price in the export market [29]. Even though a decreased percentage of lupin production (~4%) is consumed in human food, it is estimated that around 500,000 tonnes of food (bread, pasta, noodles) with lupin flour, flakes, hull, splits, and kibble is increasingly being produced each year in European countries [29]. Overall, lupins are being used as animal feed in most of the markets, however, emerging health benefits in diabetes, cardiovascular and obesity diseases in recent years is increasing the development of lupin-based food products for human consumption [49, 50].

2.1.4 Allergens

Due to high protein and fibre content, there is a growing development of lupin in food products for human consumption and thus allergenicity to lupin-based products should be considered. 'Lup an 1' (55-61 kDa β-conglutin protein from *L. angustifolius*) and 'Lup a 5' (15 KDa profilin peptide from *L. albus*) allergens have been identified and recorded in the International Union of Immunological Societies database [51, 52]. Since, the properties of these allergens are found similar to major peanut allergen, Ara h1, people allergenic to peanuts might also show a reaction to lupin [53]. The prevalence of lupin allergy seems to be very low (<1%) in the population that have consumed lupin-based food products. Only a few reports [54, 55] on lupin allergy in Australia has been accounted and there is a further need to establish a clinical assessment for lupin allergenicity in order to help with its risk management. In 2017, lupin was added in the list of allergens to be declared on food products in Australia to inform potentially sensitive consumers of the risks [56].

2.2 CHEMICAL COMPOSITION OF LUPIN SEEDS

Lupin seeds are dicotyledonous in structure. The seed is composed of ~25% hull (seed coat) and 75% cotyledons (kernels). The cotyledons are made of outer thickened cell

wall region (25-30%) consisting of pectin like dietary fibres whereas the inside region comprises of proteins, fats, oligosaccharides, starch, phytic acid, and water [46, 57]. Different chemical constituents present in the seed are discussed below:

2.2.1 Carbohydrates

Lupins seeds have low starch content (<1.5%) and the major carbohydrate content (~40%) consist of non-starch polysaccharides (dietary fibres) [58]. Lupin hulls predominantly comprise non-starch polysaccharides like cellulose, hemicellulose, and pectins with small amounts of proteins and lipids. The outer region of cotyledons contains non-starch polysaccharides consisting mainly of galactose, arabinose, and uronic acids whereas the inner region contains ~5-12% of oligosaccharides like raffinose (trisaccharide), stachyose (tetrasaccharide), verbascose (pentasaccharide), and ajugose (hexasaccharide) [59]. Raffinose has one galactose linked to sucrose whereas stachyose, verbascose, and ajugose have 2, 3, and 4 such galactose residues respectively [59]. Lupins have high protein and fibre content with negligible sugar and starch. It can lower the glycaemic load of the diet legumes thus having positive implications in the treatment of diabetes [27].

2.2.2 Lipids

The fat content varies considerably within different lupin species with a maximum in *L. albus* (~10.7% of seed) and minimum in *L. angustifolius* and *L. luteus* (5.6-5.9% of seed) [59, 60]. The major fatty acids (% of oil) present in these species are palmitic acid (0.6-7.6%), stearic acid (1.5-3.0%), oleic acid (31.5-47.6%), linoleic acid (20.3-46.9%), and linolenic acid (2.6-9.2%) [61]. Apart from the fats and fatty acids, the other components like triglycerides, phospholipids, sterol, wax esters, and hydrocarbons are also present in lupin oil [28]. Lupin oil can be used in bakery, meat and sausage goods. Due to the presence of high oleic acid content, it has also been used in anti-wrinkle cosmetic formulations [62].

2.2.3 Proteins

Lupin is one of the richest source of proteins (35-40% w/w of seeds) among legumes [27]. Lupin proteins, when combined with cereal proteins, makes them almost

nutritionally equivalent to animal proteins [27]. This legume has relatively less anti-nutritional properties such as proteinase inhibitors or hemagglutinins compared to other legume grains like soybean, peas, string beans [63]. Lupin, when mixed with wheat flour, increases the amino acid score equivalent to egg proteins. Moreover, lupin proteins have excellent emulsifying properties and thus are used as egg substitute in different bakery products [64]. The amino acid profile of proteins in lupin seed is high in leucine, lysine, arginine, and phenylalanine as compared to soybean seed proteins [58].

The majority of proteins in legumes are located in the storage vacuoles of cotyledons and are referred to as storage proteins serving as basic carbon and nitrogen source to the growing plantlet. According to Osborne classification, these seed proteins can be divided into four classes depending on their solubility: albumin (water soluble), globulins (soluble in 10% NaCl), prolamins (alcohol-water soluble) and glutenins (dilute acid/alkali soluble) [65]. Lupin seed proteins are majorly classified into albumin and globulin present in ~1:9 (albumin/globulin) ratio [66]. Minor fractions of prolamins have also been detected [67]. Albumins are represented as functional proteins of the seed due to their role in plant defence systems (hydrolase inhibitors and lectins) or as metabolic enzymes related to storage function of cotyledonary tissues, whereas, globulins are generally seed storage proteins and are referred as 'conglutins' [68].

Molecular features of lupin conglutins

On the basis of electrophoretic mobility, Blagrove and Gillespie further separated lupin conglutins into four major fractions as α and β-conglutins (major fraction), γ and δ-conglutins (minor fraction) [66]. Structural molecular features lupin conglutins' (*L. albus*) has been summarised in Table 2.1.

Table 2.1 Summary of lupin conglutins' (L. albus) molecular features. Source: [38]

Cong-lutin	% of total globulins	Native protein			Monomer composition			Glycosylat-ion
		Mol. wt.	pI	Quaternary structure	Subunit name	Mol. wt.	pI	
α	35-37	330-430	5.1-5.8	Hexamer	Acidic[a]	42-52	4.5-4.7	Yes/No[b]
					Basic[a]	20-22	6.7-8.6	No
β	44-45	143-260	5.0-6.0	Trimer	HMW	53-64	5.1-5.7	Yes
					IMW	25-46	5.3-8.4	Yes/No[b]
					LMW	17-20	4.2-5.0	Yes/No[b]
γ	4-5	200	7.9	Tetramer	Large[a]	29	8.2-8.9	Yes
					Small[a]	17	5.8-6.6	No
δ	10-12	13	Acidic	monomer	Large[a]	9	4.1-4.3	No
					Small[a]	4	n.d.	No

Mol. Wt.: Molecular weight, pH(I): isoelectric point, HMW: High molecular weight, IMW: Intermediate molecular weight, LMW: Low molecular weight.

[a] covalently linked disulphide bond(s).

[b] not all peptides are glycosylated.

α-conglutin, belonging to 11S globulin family (legumin like globulin), accounts for 35-37% of total globulins in lupin seeds (*L. albus*) [69]. It is a hexameric oligomer acidic protein (330-430KDa) consisting of acidic (42-52KDa) and basic subunits (20-22KDa) as observed in reducing and non-reducing SDS-PAGE analysis (Figure 2.1; lane 1 and 2) [38]. Some of the acidic subunits of α-conglutin are glycosylated [70]. The α-conglutin is located in the storage vacuoles of cotyledons and functions as storage protein for the plantlet's development [71].

β-conglutin, the most abundant protein among globulins (44-45%), belongs to 7S globulin family called as vicilin-like globulin [69]. The native conformation of β-conglutin is a trimer (143-260KDa) consisting of a number of monomeric polypeptides in the range from 16 – 70KDa. The reducing and non-reducing SDS-PAGE profile of β-conglutin indicates the absence of any disulphide bonds (Figure 2.1; lane 3 and 4) [38]. Like α-conglutin, β-conglutin is also a storage protein found in cotyledonary protein bodies [71].

γ-conglutin, unique basic 7S protein, accounts for 4-5% of total proteins in lupin seeds [69]. It is equally soluble in water and in salt solutions. At neutral pH, γ-conglutin exists in its native tetrameric [72] or hexameric [66] form. The transition from tetramer

(200Kda) to monomer (48Kda) occurs when the pH shifts from neutral to acidic (pH 4.5) [73]. Each monomer is composed of a heavy subunit (29kDa) and a light subunit (17KDa) linked together by disulphide bonds (Figure 2.1; lane 5 and 6) [74]. The heavy subunit is glycosylated by link to mannose and glucosamine sugar units [75]. Like other conglutins, γ-conglutin is also located in the protein bodies of developing seeds. However, its unusual resistance to degradation during germination and proteolysis (*in-vitro*) suggests that protein probably has non-storage role like other basic 7S globulins storage protein [70].

δ-conglutin, a 2S sulphur-rich albumin, is present in very low content (~3-4%) in lupin seeds [69]. It is a monomeric low molecular weight (13KDa) protein consisting of heavy (9KDa) and light (4Kda) polypeptide subunits connected by disulphide linkages (Figure 2.1; Lane 7 and 8) [38]. Its location in seed and biological function are not yet known.
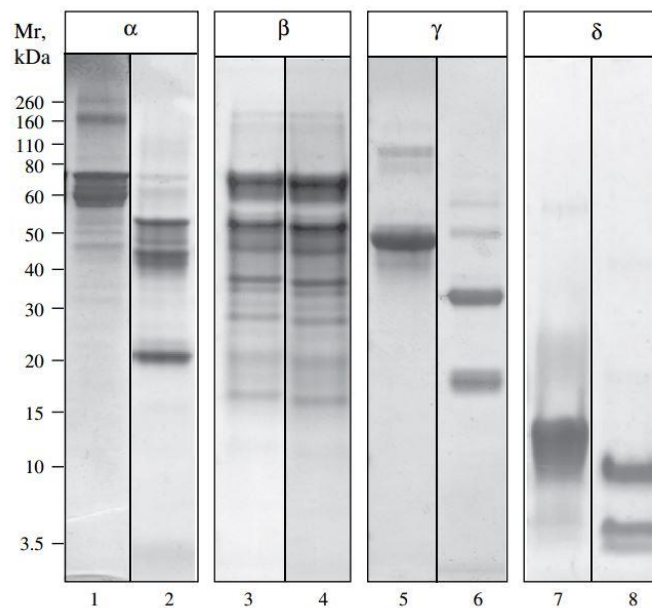
Figure 2.1 Non-reducing (lane 1,3,5 and 7) and reducing (2,4,6 and 8) SDS-PAGE profile of purified L. albus conglutins (α, β, γ, and δ)

2.2.4 Alkaloids

The total alkaloid content in lupin range between $0.01 - 4\%$ (%w/w of seed) depending on the species and its cultivation conditions [76]. The quinolizidene (and its

derivatives) alkaloids predominate in the lupin species of agricultural importance. Australian sweet lupins contain 4 types of alkaloids: lupanine 0.98 to 73.0 %, 13-hydroxy lupanine 15.6 – 71.1 %, angustifoline 0 – 49.8 % and isolupanine 0 – 34.0 % of total alkaloid content [77]. Alkaloids extracted from the lupin seed was reported to exert hypoglycaemic effects in type 2 diabetic humans and rats and increased insulin secretion from pancreatic islets [78, 79].

2.2.5 Other components

Carotenoids are the pigments synthesized by plants. Recent studies have explored their antioxidant activity, role in regulating the immune system and controlling cell growth and differentiation [80]. The total carotenoids in different lupin species range from 53μg/g to 229.73μg/g (weight of seed) with predominant forms being lutein, zeaxanthin, β-carotene, and lycopene [81]. Lupin seeds also show the presence polyphenolics, tocopherols, and tannins which have anti-oxidant activity [82]. The mineral content of lupin (*L. angustifolius*) varies from 3.2-4.6g/100g dry matter, typically containing calcium, magnesium, sodium, and potassium ions and trace elements like iron, zinc, and copper [27].

2.3 ANTI-DIABETIC PROPERTIES ASSOCIATED WITH CONSTITUENTS IN LUPIN SEEDS

After food intake, starch breaks down into glucose molecules by the gastrointestinal enzymes. In the absorptive stage, the intestinal cells absorb glucose resulting in a rise in blood glucose level. In the post-absorptive stage, glucose from blood gets transported into cells and is metabolised to generate energy and excess glucose is stored as glycogen. Subsequently, the blood glucose level falls. The normal physiological fasting glucose concentration lies between 3.3-6.1 mmol/L. Glucose concentration below and above this range results in hypoglycaemia and hyperglycaemia respectively. In the absorptive stage, an increase in glucose concentration triggers the release of insulin from pancreatic β cells. Insulin stimulates glucose transport into muscle, adipose, and liver cells. Insulin also promotes glycolysis (glucose metabolism to release energy), glycogenesis (conversion of glucose to glycogen for storage), and inhibition of lipolysis (breakdown of lipids to release

energy), thus, overall reducing blood glucose level. Several hours after food intake, in the post-absorptive stage, both levels of insulin and glucose fall down. This triggers the release of glucagon from pancreatic α cells. Glucagon, as opposite to insulin's function, increases blood glucose level by stimulating glycogenolysis (conversion of glycogen into glucose) and gluconeogenesis (production of glucose from lactic acid and other metabolites) in liver cells. Besides insulin and glucagon, other hormones also help in blood glucose homeostasis. Increased post-prandial glucose concentration causes the release of somatostatin from pancreatic δ cells. Somatostatin inhibits gut motility, nutrient absorption and release of pancreatic digestive enzymes. On contact with food, intestinal cells release gastrin, cholecystokinin and incretin hormones that stimulate insulin secretion from pancreatic β cells. In this manner, through negative and positive feedback mechanisms glucose concentration is maintained in blood [83].

Pancreatic β cells secrete insulin in a glucose-dependent manner. With an increase in plasma glucose levels, glucose enters pancreatic β cells through the glucose transporter 2 (GLUT2) and the enzyme glucokinase, glucose sensor, allows the β cell to respond to a physiological rise in glucose concentration. Glucose is subsequently metabolised via glycolysis, citric acid cycle and mitochondrial oxidative phosphorylation pathways which generate different coupling factors and increases adenosine triphosphate (ATP) / adenosine diphosphate (ADP) ratio [84]. ATP is one of the important signalling molecules in β cells with respect to insulin secretion. Increase in ATP/ADP ratio causes closure of ATP dependent potassium channels (K-ATP) leading to a rise in β cell membrane potential [84]. The membrane depolarisation eventually opens the voltage-dependent L-type calcium channels followed by the influx of calcium ions in the cells. This elevation of calcium ions can drive insulin exocytosis in the presence of ATP and other metabolic signalling molecules ultimately increasing blood insulin levels [85].

The evidence for nutritional and health benefits of lupin is growing rapidly. Various reviews have showcased its health benefits in different metabolic dysfunction conditions like diabetes, hyperlipidaemia, and cardiovascular disease [38, 86, 87]. The anti-diabetic action i.e. hypoglycaemic effect of lupin has been explored in detail in different animal and cell models. The in-vivo animal studies involve usage of different normal (healthy) and diabetic animal models. Streptozotocin, an anti-neoplastic agent

particularly damages pancreatic β cells, thus, hampering production of insulin [88]. This induces hypoinsulinemic and hyperglycemic conditions in animals resulting in development of diabetic model. Insulin resistant model is generated by feeding animals with either high carbohydrate (fructose/sucrose) or high fat (free fatty acids) diet for a long period of time until they develop resistance to insulin [89].

Reduction in glucose and insulin levels with positive effects on satiety, palatability, and food intake was observed in volunteers consuming lupin (*L. angustifolius*) bread breakfast compared to volunteers eating white bread breakfast [33-35]. Decreased acute glycaemic response and increased insulin and C-peptide serum levels were found in type 2 diabetic individuals consuming lupin and soy (protein and fibre) beverages [32]. Prolonged administration of *L. albus* dry extract (manufactured by Vital laboratory; Ben Arous, Tunisia) for 12 weeks improved the fasting and post-prandial serum glucose concentration and insulin sensitivity in type 2 diabetic Tunisian patients [90]. Also, lupin seed powder when combined with anti-hyperglycaemic drugs like metformin and gliclazide displayed a synergistic hypoglycaemic effect in diabetic rats and improved the overall biochemical parameters like body weight, serum insulin, glycated hemoglobin, and lipid profile [91, 92]. All these animal and clinical trial studies indicated that bio-constituents in lupin seed might have a significant beneficial role in diabetes prevention and control. However, a thorough investigation in understanding its mode of action is necessary before its application as a nutraceutical agent. An insulinotropic (insulin release or secretion) study of lupin extract reported an increase in insulin secretion at high glucose concentration in pancreatic β cells [36]. Lupin extract is a mixture of macro (proteins, peptides, carbohydrate) and micro (alkaloids, polyphenols, amino acids, di-tri saccharide) biomolecules which either alone or in combination might be responsible for its anti-diabetic action. Out of these biomolecules, alkaloids and proteins from lupin extract have been reported to modulate serum glucose levels. Anti-diabetic properties associated with them have been discussed in following sections.

2.3.1 Alkaloids

Low levels of quinolizidene alkaloids are present in *L. albus and L. angustifolius* seed. Alkaloids extracted from the lupin seeds demonstrated a hypoglycaemic effect in type

2 diabetic humans and rats [79, 93]. These alkaloids also improved insulin secretion in rat islets by mediating their action through closure of K-ATP channels and stimulated insulin secretion in glucose-dependent manner [36, 37]. Similar insulinotropic action along with an increase in expression of gene encoding insulin (*Ins-1*) was observed in derived insulin secreting β cell line – INS-1E on treatment with lupanine and its derivatives [94]. Lupanine reduced blood glucose levels and improved glycaemic control in streptozotocin-treated diabetic rats [94]. Thus, the anti-diabetic action of lupin can, at least partially, be attributed to alkaloids present in the extract, however, further investigation in deducing their mechanism of action is required.

2.3.2 Proteins

Dietary proteins have shown to attenuate the postprandial hyperglycaemia by either slowing down gastric emptying rate or delaying absorption of glucose or stimulating insulin secretion by releasing incretin hormones that augment insulin release from pancreatic β cells [95-97]. Lupin proteins and peptides, apart from being an amino acid suppliers, exhibited their role in controlling blood pressure (hypertension), plasma lipids (hypercholesterolemia) and glucose concentrations (hyperglycaemia) in different mechanistic ways [49, 50]. Here, the clinical, animal, cellular and molecular studies related to the anti-diabetic action of lupin proteins is discussed.

The lupin protein responsible for hypoglycaemic action has been identified to be γ-conglutin in most of the reports except for two that attribute the anti-diabetic action of lupin proteins to β-conglutin [98, 99]. Isoforms of recombinant β-conglutins (β1, β3, and β6) (a) increased the glucose uptake which subsequently improved insulin secretion, (b) up-regulated mRNA expression of key mediators involved in insulin signalling pathway, (c) activated intracellular insulin receptor substrate (IRS) / phosphoinositide kinase-3 (PI3K) pathway involved in glucose homeostasis and (d) improved cell oxidative stress in an insulin-resistant pancreatic β cell model [98, 99]. Apart from these reports, γ-conglutin has been identified as the main anti-hyperglycaemic component in lupin seed. This information has been summarised in Table 2.2 and is discussed below:

2.3.2.1 γ-conglutin protein

Clinical and Animal studies

Pasta enriched with γ-conglutin peculiarly diminished the serum glucose concentration after glucose overload compared to pasta with other lupin isolates (α+β+δ conglutins), or ovalbumin control [31]. In addition, reduction in food intake and bodyweight was observed in rats consuming pasta supplemented with lupin protein isolates. Also, the structure of γ-conglutin was not degraded during the preparation process of pasta [31]. In another report, a dose-dependent reduction of blood glucose levels was observed on acute oral administration of purified γ-conglutin in rats [100]. Similar acute hypoglycaemic effect was also detected in healthy mouse models and human volunteers administered with γ-conglutin enriched preparations [101]. Like the acute effects, chronic treatment of γ-conglutin exhibited a reduction in plasma glucose and insulin levels in rats supplied with 10% D-glucose water for 3 weeks [92]. Increased levels of *Ins-1* gene expression and pancreatic β cell insulin content was reported in streptozotocin-induced type 2 diabetic rat models after administration of γ-conglutin [102]. In all these studies, γ-conglutin displayed its hypoglycaemic action only at high glucose concentration and not at normal glucose concentration, thus, preventing hypoglycaemic episodes at normal glucose concentration. These studies highlighted the potential use of γ-conglutin in food supplements for diabetic patients. The major tissues responsible for clearing glucose from blood are muscle, liver and adipocyte tissues which become insulin resistant in type 2 diabetes [103] and, thus, these cell models were used to investigate the insulin-mimetic mechanism of action of γ-conglutin.

Mechanistic studies in hepatocytes/liver cell lines

The liver maintains blood glucose levels by creating a balance between glucose production (gluconeogenesis) and glucose storage in the form of glycogen (glycogenesis). Observation of the internalization of intact γ-conglutin and its phosphorylation at multiple sites in human liver carcinoma cell line (HepG2) was proposed as the first step in hypoglycaemic mechanism of action [104]. HepG2 cells, on exposure to γ-conglutin for 24 to 48 hours, increased glucose consumption when cultured in high glucose concentration [92]. GLUT2, a primary transporter of glucose

between blood and liver, is encoded by the *Slc2a2* gene [105]. The γ-conglutin treatment increased the expression of this gene in the hepatic tissue of type 2 diabetic rat model and augmented glucose uptake/consumption in liver cells [106].

A typical characteristic of type 2 diabetes is abnormally high glucose production by the liver [107]. Hepatic glucose-6-phosphatase (G6Pase) and phosphoenol pyruvate carboxykinase (PEPCK) are the key enzymes activating the hepatic gluconeogenic pathway. In type 2 diabetes, overexpression of these enzymes increase the rate of glucose production and consequently augment the release of glucose into the blood [108]. It was reported that γ-conglutin reduced the expression of *G6pc* and *Pck1* genes (responsible for encoding G6Pase and PEPCK enzymes respectively) in hepatic tissues isolated from an insulin-resistant rat model resulting in attenuation of liver glucose production [109]. A recent publication corroborated similar reduction of gluconeogenesis and PEPCK expression levels in HEPG2 cells on treatment with γ-conglutin hydrolysates absorbed through intestinal epithelial cells [40].

Usually, diabetic patients have the same total cholesterol level and high-density lipoproteins as the general population but the levels of low-density lipoproteins (LDL) and triglycerides in the blood are higher. Sirtori et al., found that γ-conglutin stimulated LDL receptor-mediated uptake of LDL in HepG2 cells, thus, extrapolating its potential use in hypercholesterolemia [110].

Mechanism studies in muscle cell lines

The insulin-mimetic property of γ-conglutin was explored in the immortalized mouse myoblast cell line C2C12. Figure 2.2 summarises the activation of different intracellular proteins of the insulin signalling pathway by γ-conglutin in this cell line [41]. In brief, γ-conglutin phosphorylated IRS leading to activation of PI3K and phosphorylation of protein kinase B (Akt-1) eventually associated with glucose homeostasis. Like insulin, γ-conglutin also stimulated cellular protein synthesis by activating downstream targets such as phosphorylation of ribosomal protein S6 kinase (p70S6K) and eukaryotic translation initiation factor (eIF4E). It also increased flotillin-2 and caveolin levels which are responsible for translocation of intracellular glucose transporter 4 (GLUT4) vesicles to the membrane, thus, facilitating glucose

transport from serum into the cell [111]. Lastly, γ-conglutin influenced muscle cell differentiation and regulated muscle energy metabolism [41].
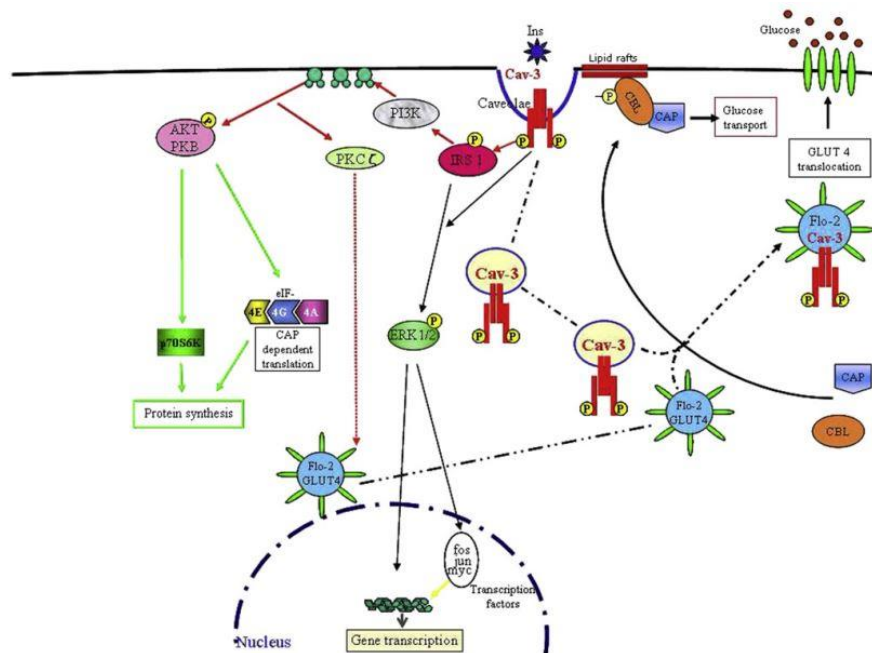
Figure 2.2: Activation of different intracellular proteins of the insulin signalling pathway by γ-conglutin in C2C12 cells [41]

Mechanism studies in adipocytes

Overweight and obese patients are often found to be present with metabolic disorders and diseases such as dyslipidemia, cardiovascular problems, risk of stroke, high cancer risk, and risk of type 2 diabetes. In these patients, an excess of fat deposition in tissues results from hypertrophy and hyperplasia of adipocytes and differentiation of pre-adipocytes into mature adipocytes [112]. γ-conglutin suppressed differentiation of pre-adipocytes (3T3-L1 cells) into mature fat cells by (a) downregulating the mRNA expression of adipogenic transcription factors (Pparγ, C/ebpα, Fabp4, leptin) involved in the differentiation process and (b) decreasing accumulation of lipid content in the cells [42]. The γ-conglutin peptides, absorbed through intestinal epithelial cells (Caco-2) assisted in translocation of GLUT-4 receptors to the membrane, thus, increasing glucose uptake in adipocytes in an *in vitro* model [40].

Table 2.2 literature reported hypoglycaemic actions of γ-conglutin from lupin seeds

Animal	Diet/Model	Treatment period and groups	γ-conglutin characterisation	Test	Outcomes of γ-conglutin treatment	Reference
Clinical study						
Healthy human volunteers	Healthy diet	Acute treatment (30mins): • Control (placebo) • γ-conglutin enriched extract (750, 1500, 3000 mg/volunteer)	60.0±7% γ-conglutin in the extract (by SDS-PAGE)	• Oral glucose overload test	• All hemodynamic parameters stable. • Dose-dependent reduction in blood glucose level (75% and 79% of placebo with 1500 and 3000mg/kg concentration respectively). • No modification in overall insulin response.	[101]
Animal studies						
Rat	Standard rat diet	Acute treatment (30mins): • Control (vehicle) • Metformin (50mg/kg) • γ-conglutin (30, 60, 120 mg/kg BW)	γ-conglutin analysed by SDS-PAGE (purity not mentioned)	• Oral glucose overload test	• Dose dependent reduction in blood glucose level.	[100]
Rat	Standard rat diet	Acute treatment (30mins): • Control (vehicle) • Metformin (50mg/kg)	60.0±7% γ-conglutin in extract (by SDS-PAGE)	• Oral glucose overload test	• Dose dependent reduction in blood glucose level (14%, 42%, 64% reduction with 50, 100 and 200mg/kg concentration respectively compared to control).	[101]

		• γ-conglutin enriched extract (50, 100, 200 mg/kg BW)				
Rat	10% D-glucose in drinking water for 1 week (2-3g daily intake/rat)	Chronic treatment (3 weeks): • Control (vehicle) • D-glucose+ γ-conglutin enriched preparation (100mg/kg BW) • D-glucose + vehicle	28% (w/w) γ-conglutin in preparation (by SDS-PAGE)	• Blood glucose and insulin level • Oral glucose overload test	• Attenuation in the rise of blood glucose (1.9 fold) and insulin (1.8 fold) levels compared to D-glucose + vehicle group. • Reduction in insulin resistance (expressed by HOMA-IR**) by 2.3fold compared to D-glucose + vehicle group. • Glucose overload test – Reduction in blood glucose level (by 25%) compared to D-glucose + vehicle group.	[92]
Rat	STZ induced T2D model	Chronic treatment (1 week): • Control (vehicle) • Glibenclamide (10mg/kg BW) • γ-conglutin (120mg/kg BW)	γ-conglutin analyzed by SDS-PAGE (purity not mentioned)	• Blood glucose and insulin level • β cell insulin content and • *Ins-1*gene expression	• Reduction in serum glucose level (17%) and an increase in insulin level (63%) compared to glucose level before treatment. • Increase in % insulin content than control. • Increase in Ins-1 gene expression (1.77 fold) than control.	[102]
Rat	<u>IR Group</u>-Insulin resistant rat model – 30% sucrose in	Chronic treatment (1 week): • Control (vehicle) • Metformin (300mg/kg BW)	γ-conglutin analysed by SDS-PAGE (purity not mentioned)	• Serum glucose and insulin level • Gene expression of enzymes involved in hepatic gluconeogenesis	• Increase in glucose level (27% - IR group and 16% - STZ group) compared to control • Decrease in insulin level in IR group (38%) and increase in STZ group (46%) compared to control. • No renal and hepatic damage/lesions observed.	[109]

	drinking water for 20 weeks <u>STZ Group-</u> STZ induced T2D model	• γ-conglutin (120mg/kg BW) (treatments for IR and STZ group)		(*G6pc, Pck1, Fbp1*)	• Increase of *G6pc* expression in IR and STZ group, decrease of *Pck1* expression in IR group and increase in STZ group, decrease of *Fbp1* expression in IR group and increase in STZ group.	
Rat	STZ induced T2D model	Chronic treatment (1 week): • Control (healthy) • STZ control group • STZ group + γ-conglutin (120mg/kg BW)	γ-conglutin analysed by SDS-PAGE (purity not mentioned)	• Serum glucose level • GLUT2 content in pancreatic islets • *Slc2a2, Pdx-1, Gck* gene expression in islets and hepatic tissue	• Reduction in serum glucose level (18%) compared to glucose level before treatment. • Reduction in GLUT2 protein content (1.6 fold) compared to STZ control group. • Pancreatic tissue – increase in expression of *Slc2a2* (1.7 fold) and *Pdx-1* (1.12 fold) compared to STZ control; Gck expression was not quantifiable. • Hepatic tissue – increase in expression of *Slc2a2* (1.26 fold) but decreased levels of *Gck* (0.56 fold).	[106]
Cellular mechanism studies						
HepG2	-	• Control • Insulin • Metformin • γ-conglutin (10µM) with and without insulin and metformin	γ-conglutin analysed by SDS-PAGE (purity not mentioned)	• Glucose consumption at 5.5,11.1, 16.5mM glucose concentration in 24 to 48 hour	• At normal glucose concentration (5.5mM) - no glucose consumption by cells. • At high glucose concentration – increase in cellular glucose consumption (γ-conglutin in presence and absence of Met and Insulin).	[92]
HepG2	-	• Control • γ-conglutin (10mM)	-	• Time course (0.5, 3, 6, 24hours) study of γ-conglutin uptake	• Intracellular accumulation of γ-conglutin at 6hr incubation with cells (confocal microscopy).	[104]

					• Detection of intact γ-conglutin in the cell lysate (2D electrophoresis). • Phosphorylation of internalised γ-conglutin (Mass spectrometry).	
Dual layered Caco-2 with HepG2	-	• Control • Metformin • γ-conglutin hydrolysates (5 and 2mg/ml)	γ-conglutin analysed by SDS-PAGE and immunoblot (purity not mentioned)	• Glucose production (gluconeogenesis) • expression of phosphoenol pyruvate carboxykinase in cell lysate	• Co-culturing of Caco-2 and HepG2 cells to mimic gastrointestinal digestion absorption condition. • Decrease in glucose production in HepG2 cells (effect similar to metformin) by absorbed peptides through Caco-2 cell monolayer. • Decrease in phosphoenolpyruvate carboxykinase expression.	[40]
HepG2	-	• Control (Lipoprotein deficient serum) • Total protein extract (125, 250, 500mg/ml) • γ-conglutin (125, 250, 500mg/ml)	-	• Detection of isoflavones in lupin protein extract and γ-conglutin • LDL receptor mediated uptake and degradation	• Isoflavones below limit of detection (mass spectrometry). • Upregulation of LDL-receptor (21-53%) thus involved in mechanism for reduction of cholesterolemia.	[110]
C2C12 myoblasts	-	• Control • γ-conglutin (10 μM) • Insulin • Metformin	γ-conglutin analysed by SDS-PAGE and immunoblot (purity not mentioned)	• Exploring activation of intracellular kinases in insulin signalling pathway at 5, 10, 20 , 30 mins)	• Activation of IRS-1/PI-3K pathway involved in glucose homeostasis. • Activation of eIF4E and p70S6K responsible for cell protein synthesis. • Increase in levels of follitin-2 and caveolin-3 associated with GLUT-4 translocation.	[41]

					• Increase in the accumulation of myosin heavy chain and myogenin (differentiation markers) in myotubes.	
3T3-L1	-	• Control • γ-conglutin (1, 2.5, 5μM)	-	• mRNA expression of adipogenic transcription factors • lipid content	• Suppression of pre-adipocyte differentiation into mature fat cells by (a) downregulation of adipogenic transcription factors (Pparγ, C/ebpα, Fabp4, leptin) and (b) diminished lipid accumulation	[42]
Dual layered Caco-2 with 3T3-L1	-	• Control • Insulin • γ-conglutin hydrolysates (5 and 2mg/ml) with and without insulin	γ-conglutin analysed by SDS-PAGE and immunoblot (purity not mentioned)	• Glucose uptake • GLUT-4 translocation	• Co-culturing of Caco-2 and 3T3-L1 cells to mimic gastrointestinal digestion absorption condition. • Absorbed peptides through Caco-2 cells increased glucose uptake into the cell in presence and absence of insulin and stimulated GLUT-4 translocation to the plasma membrane	[40]

STZ: Streptozotocin; T2D: Type 2 Diabetes; SDS-PAGE: Sodium do-decyl sulphate gel electrophoresis; BW: Body weight; HOMA-IR: Homeostatic model assessment- insulin resistance; IR: Insulin resistance

As discussed above, majority of the γ-conglutin cellular mechanism studies were focused on its insulin-mimetic property. There are no studies reporting the direct or indirect (via incretins) action of γ-conglutin on insulin release from pancreatic β cells. On contact with food, intestinal cells release incretin hormones that stimulate insulin secretion from pancreatic β cells (Kim & Egan, 2008). Exploring the mechanism of γ-conglutin peptide induced insulin secretion by (a) either stimulating incretin release from intestinal cells or (b) directly triggering insulin release from pancreatic β cells can lead to a greater understanding of its hypoglycaemic action.

The common current oral anti-diabetic treatments also include inhibition of metabolic enzymes like α-glucosidase and DPP4. The α-glucosidase hydrolyses carbohydrates to glucose in the intestinal tract, which causes a rise in blood glucose levels [8]. DPP4 is a metabolic enzyme that cleaves and degrades glucagon like peptide 1 (GLP-1) incretin resulting in decreased insulin secretion [113]. γ-conglutin peptides were reported to inhibit DPP4 enzyme *in-vitro* [40]. This could potentially improve the stability and half-life of GLP-1. However, the purity of γ-conglutin was not reported in this study and, hence, if the action is resultant of γ-conglutin peptides or other lupin peptides known to exhibit similar action is still an open question [114]. In the DPP4 assay, the fluorogenic substrate Gly-Pro-aminomethylcoumarin (AMC) is used to measure DPP4 activity. The enzyme cleaves the substrate into dipeptides and releases free AMC fluorogenic group which can be analysed. Inhibition of DPP4 can result in decreased cleavage of fluorogenic substrate resulting in reduced fluorescence. In the above report, the researchers did not cross-examine if γ-conglutin peptides were also potential DPP4 substrates. If this hypothesis holds true then γ-conglutin peptides, instead of inhibiting DPP4 enzyme, would be competing with the fluorogenic substrate thus preventing DPP4 enzyme's accessibility to fluorogenic substrate. This eventually would decrease the fluorescence and lead to misinterpretation of results as inhibitory effect.

2.4 CHARACTERISTIC PHYISCO-CHEMICAL PROPERTIES OF γ-CONGLUTIN

2.4.1 Resistance of γ-conglutin to enzymatic hydrolysis

γ-conglutin, a unique basic 7S globulin, exhibited an unusual resistance to proteolysis both during *in-vivo* seed germination and *in-vitro* trypsin and pancreatin proteolytic conditions [71]. Both glycosylated and non-glycosylated forms of γ-conglutin were found to be resistant to trypsin [115]. On the other hand, the unfolded glycosylated form of γ-conglutin refolded at a faster rate compared to non-glycosylated form in renaturing conditions [70]. Thus, it was concluded that the N-linked carbohydrate saccharide moieties (glycosylation) were not responsible for γ-conglutin's resistant property but facilitated the structural re-organisation bringing γ-conglutin back to trypsin resistant conformation [116]. The oligomeric conformation at neutral or slightly acidic pH remained unaffected on prolonged heat treatment below a critical temperature (<60°C), thus, contributing to the overall stability of this protein [72].

γ-conglutin was observed to be resistant to proteolysis at pH greater than 4.25 below which it was susceptible to proteolytic degradation. It was hypothesized that a sharp conformation transition occurred from pH 3 to 4.25 transforming γ-conglutin from cleavable to uncleavable conformation [117]. At pH ≤4.5, the global positive charge on protein due to protonation of basic amino acids (histidine, lysine, and arginine) residues resulted in charge repulsion among monomeric units, thus, preventing their aggregation. However, a small drift to less acidic pH 5.5 reduced the positive charge and dissociation of acidic amino acid glutamate residue side groups eventually triggered the formation of salt-bridges leading to dimerization of monomeric units. A further shift to pH 6.5 balanced out the positive (protonation of lysine and arginine) and negative (dissociation of aspartate and glutamate) charges. As a result, electrostatic repulsion among proteins decreased and formation and stabilization of inter and intra salt-bridges increased. This phenomena at neutral or slightly acidic pH led the molecules to associate and adopt a compact tetramer oligomeric structure making it resistant to proteolysis [73]. However, γ-conglutin was found to be prone to proteolytic degradation by pepsin at acidic pH and chymotrypsin at neutral pH cleaving the protein at 97 and 124 sites respectively [118]. In addition, γ-conglutin has

relatively few peptide cleavage sites for trypsin and pancreatin enzymes and its oligomer conformation at neutral pH blocked the enzyme's accessibility to these cleavage sites. These observations indicated that resistance of γ-conglutin to proteolytic digestion is not related only to the oligomerisation phenomena. Another hypothesis suggested that flavonoids released from other proteins during hydrolysis might have affected its susceptibility to proteolytic digestion [119]. At neutral pH, partially ionised flavonoids (apigenin glycosides) interacted with positively charged lysine and arginine residues of γ-conglutin leading to blockage of amino acids and preventing accessibility to cleavage sites for trypsin and pancreatin [118].

2.4.2 γ-conglutin interaction with metal ions

Protein interaction with metal ions results in aggregation and precipitation of the protein molecules [120]. γ-conglutin precipitated in the presence of different divalent metal ions, specifically, Zn^{2+}, Hg^{2+} and Cu^{2+} (1mM) at neutral pH [121]. However, after addition of chelating agent like ethylenediaminetetraacetate (EDTA), γ-conglutin re-solubilised indicating that the metal-induced precipitation did not lead to denaturation. The protein precipitation effect was observed only at neutral pH (7.5), whereas, below pH 6.0 the protein was completely soluble even at higher Zn^{2+} concentration (10-20mM). As a result, acidic pH buffer or chelators like EDTA/imidazole were used to elute γ-conglutin absorbed on zinc-coupled affinity chromatography columns during γ-conglutin purification [121].

2.4.3 γ-conglutin interaction with insulin

γ-conglutin protein exhibited an electrostatic binding interaction with insulin immobilised on agarose gel matrix and was eluted at higher ionic concentration (200mM NaCl) [100]. While loading lupin protein extract on the column, γ-conglutin specifically bound to insulin immobilised matrix indicating that other components in the extract did not affect this interaction. This binding property of γ-conglutin with insulin was observed only in its native conformation between pH 7.5 to 4.2. The equilibrium dissociation constant of γ-conglutin insulin interaction (10^{-5} M) was found to be in moderate affinity range of the protein-ligand interaction as recorded by real-time Surface Plasma Resonance (SPR) analysis of γ-conglutin with insulin [100]. However, γ-conglutin dissociated from insulin at a low concentration of NaCl (40-

85mM) and, thus, its binding capacity with insulin under physiological condition (154mM Na$^+$ and Cl$^-$) needs to be assessed further.

2.5 EXTRACTION AND PURIFICATION OF γ-CONGLUTIN

Being a 'glucose modulating agent' (as discussed in section 2.3.2.1), processes for separating γ-conglutin from lupin seeds have been developed. Depending on the physicochemical properties of the desired protein, the extraction and purification steps are tailored. A recent review on the extraction and purification of lupin conglutins, especially γ-conglutin, has elaborated the basic steps used for its purification such as (a) seed pre-treatment, (b) extraction, (c) membrane filtration and (d) chromatographic purification [39].

2.5.1 Defatting of lupin flour

As discussed in section 2.2.3, the majority of protein (~95%) is located in cotyledons of lupin seeds. Thus, at first, the lupin hulls are separated from the cotyledons (kernels). Next, cotyledons are milled and sieved to obtain flour of desired particle size. Defatting is required before extraction of proteins because lupin flour contains different saturated and unsaturated aldehydes, carboxylic acids, fats and fatty acids, and lipids that get co-extracted with the proteins during extraction, thus, decreasing the process efficiency [122, 123]. Defatting of flour is usually performed with hexane using either soxhlet apparatus [124] or by agitation/stirring method [125]. Removal of fats increase the stability of the extract and minimises the risk of the off-flavour product generation [39]. Later, the fat extracted in hexane is separated by distillation method and used for the production of lupin oil which can be further used in bakery and cosmetic industries.

2.5.2 Extraction of defatted lupin flour

Since the hypoglycaemic action of lupin proteins is attributed to γ-conglutin, the major focus of this section is to review different γ-conglutin extraction and purification methodologies. Lupin conglutins – α, β, and δ have acidic isoelectric point (pH(I)) in the range 5.1-6.0, whereas γ-conglutin has pH(I) 7-8. When pH is equal to pH(I), the protein surface has no net charge and thus has minimum solubility in solution. The

solubility of α, β and δ conglutin is minimum in acidic pH and in alkaline conditions these proteins are charged and maximally soluble. Conventionally, alkaline extraction of defatted lupin flour (step 1) was followed by acidic precipitation of proteins in supernatant (step 2) [38]. The alkaline extraction (step 1) yielded major conglutin proteins (α and β) in the precipitate while the supernatant consisted of γ-conglutin along with other impurities. In this alkaline extraction step, γ-conglutin was not completely extracted [126] and was preferentially bound to dietary fibres [127], thus, leading to incomplete recovery. Acidic precipitation of γ-conglutin in supernatant of step 1 yielded 10.3g of protein per kg flour with 53% γ-conglutin (purity based on densitometric scanning of SDS-PAGE analysis) [124]. γ-conglutin in the supernatant of step 1 was also be precipitated with zinc ions (section 2.4.2). However, for nutraceutical application of γ-conglutin removal of the metal ions from solution or in conjugation with the protein is necessary.

Separation of lupin globulins was first reported by Blagrove and Gillespie (1975). Initially, defatted lupin seed flour was extracted with water resulting in 10% protein yield (albumins). Next, sodium chloride solution (10%) was used to extract residual proteins (globulins) followed by fractionation of individual globulins (α, β, and γ) using different percentages of saturated ammonium sulphate solution in multiple steps [66]. However, scaling up a process involving large number of precipitation and extraction steps is tedious.

Micellisation method was also used to purify total lupin protein isolates [128]. In the micellisation method, the lupin flour was extracted with 1M NaCl followed by the conventional extraction (alkaline extraction followed by acidic precipitation) of the residue. The supernatants in both the steps were pooled and allowed to stand for 18 hours at 4°C. Both the micellisation and conventional extraction methods applied to prepare sweet and bitter lupin isolates resulted in relatively comparable nutritional (chemical score, essential amino acid, crude protein and ash content, alkaloid content) and functional (Fat and water absorption capacity, emulsification capacity, foam capacity) properties [128]. However, this report was focused on extraction of total proteins and not isolation or separation of different conglutin fractions.

In order to remove toxic quinolizidene alkaloids, pigments, and other non-protein components, aqueous methanol/ethanol solutions were used for extraction of lupin in consecutive, counter-current or semi counter-current manner [129]. Extraction with ethanol/methanol solution (80% v/v in water) resulted in lupin protein concentrates with 70% protein yield and 0.1-0.2% alkaloids. However, extraction of proteins with alcohols can lead to their denaturation in turn affecting their bioactivity [130].

2.5.3 Isolation and purification of lupin γ-conglutins

Based on conventional extraction method, a semi-industrial extraction process for isolation of conglutins was developed by Fraunhofer Institute (Germany) [131]. This method involved protein extraction in alkaline conditions followed by precipitation of α, β and δ conglutin at acidic pH. The precipitated proteins were recovered by large scale centrifugation (Type E) and have excellent emulsifying properties. γ-conglutin in the supernatant was recovered from other non-protein small molecules by ultrafiltration using zirconium oxide membrane (molecular weight cut-off 15KDa) maintained at pH 7-8. The retentate fraction (Type F) had outstanding foaming properties [131]. This method separated protein isolates on pilot scale level for specific food application, but, individual conglutin purity in different fractions was not reported. Moreover, SDS-PAGE analysis of type F protein reported by Mane et al. (2018) showed different protein impurities in 45-14KDa range [132] along with the target protein (γ-conglutin).

Ion exchange chromatography is used for protein purification in order to achieve a high level of purity by manipulating the surface charge of proteins. In ion exchange chromatography, the selection of appropriate resin matrix for protein purification depends on the protein charge which varies with surrounding pH and conductivity. The separation is based on reversible oppositely charged surface ionic interactions between the resin matrix and the protein. Below their pH(I), proteins are positively charged and binds to negatively charged cation exchanger and vice versa. At first, the protein samples (feed) are loaded on the ion exchange column (loading step). The charged protein from the feed binds to the oppositely charged resin matrix at low ionic strength and the unbound proteins (flowthrough) are washed out of the column. The bound proteins are gradually released (eluted) out of the column by increasing the ionic

strength of the medium in the column, thus, weakening ionic interaction of the protein with the resin (elution step). Any remainder bound proteins are later completely removed by passing very high ionic strength medium (1M NaCl/ 1M NaOH) through the column (regeneration step) [133].

At present, a lab-scale purification method using a combination of chromatography techniques is being used for separation of conglutins [38]. In these methods, first, defatted lupin flour was extracted at neutral pH with 0.5M NaCl followed by centrifugation. The supernatant was desalted using a gel filtration column (Whatman DE 52 DEAE-cellulose to remove low molecular weight components. The desalted extract was loaded on anion exchange column at pH 7.5. At this pH, all conglutins except γ-conglutin, having acidic pH(I) were retained on the weak anion exchange column, whereas, the γ-conglutin passed the column in the flowthrough. Among the retained conglutins, β-conglutin eluted at 0.27M NaCl and both α and δ conglutin eluted at 0.37M NaCl. For further separation of α and δ conglutin, the mixture was loaded on concanavalin A affinity chromatography for capturing glycosylated α-conglutin protein whereas the unglycosylated δ-conglutin passed out in the flowthrough. The anion exchange flowthrough fraction containing γ-conglutin was adjusted to pH 4.5 and loaded on the cation exchange column. At this pH, positively charged γ-conglutin interacted with negatively charged resin matrix and was eluted at 0.35M NaCl. γ-conglutin was reported to bind with insulin (pH 4.2-7.5) [100] and Zn^{2+} (pH 7.5) [121] and, thus, Zn^{2+} or insulin-mobilized affinity chromatography was used as polishing step to achieve desired purity. Insulin affinity chromatography, apart from being used in the polishing step, was also used for capturing γ-conglutin from crude protein extract as discussed earlier (section 2.4.3) [100]. However, the % purity of γ-conglutin eluted after loading crude extract was not reported. Also, there is a possibility of contamination of γ-conglutin fraction with zinc ions leaching from zinc-mobilized affinity chromatography column. This can make the final purified γ-conglutin fraction unfit for human consumption.

Using a combination of several techniques make the process scale-up design difficult and less efficient. As a result, a single step extraction process yielding γ-conglutin enriched extract and selective capturing of γ-conglutin by one step chromatography

process should be formulated and optimized to achieve high purity, yield, and production with easy scale up.

2.6 CONCLUSION AND RESEARCH GAPS

As discussed in this chapter, lupin is one of the major Australian rotation crops. Australia contributes to 85% of lupin production in the world with Western Australia being the lead exporter. At present the majority of lupin production is used as stockfeed [29]. Despite its beneficial effects in different metabolic dysfunctions like diabetes, hypercholesterolemia, obesity, and cardiovascular diseases only 4% of lupin production is consumed as human food by incorporating low-cost lupin ingredients in wheat-based bakery items [49]. Though significant clinical trials and animal studies report positive health promoting effects of lupin seed proteins, their mechanism of action has not been investigated in detail. Out of the many health benefits, this research focuses on establishing anti-diabetic mechanism of action of lupin seed proteins.

The hypoglycaemic effect of lupin-based food preparations or the extract obtained from lupin seeds has been investigated in healthy and diabetic animal model *in-vivo* (section 2.3). Only few reports have studied the insulinotropic property (insulin secretory action) of lupin seeds [36, 94]. These reports focused only on the activation of ionic mechanisms i.e. closure of K-ATP channel and opening of Ca^{2+} channels involved in membrane depolarisation pathway in pancreatic β cells. Effect of lupin extract on energy metabolism and different signalling pathway in pancreatic β cells needs a further detailed investigation.

The globulin protein fraction, γ-conglutin, is of particular interest due to its *in vivo* glucose modulating action in animals and humans [100, 101]. In spite of its beneficial action, the protein is not available commercially as nutraceutical supplement in the market. As discussed in section 2.5.3 the conventional lab scale purification process involves multiple steps (anion exchange coupled with cation exchange followed by polishing steps) making the process difficult to scale-up and also increases the overall process cost. In addition, the purity of γ-conglutin is quantified based on semi-quantitative techniques like SDS-PAGE. Researchers at Fraunhofer institute (Germany) have successfully developed a semi-industrial extraction process for

separation of γ-conglutin (type F) [131]. However, the type F fraction is contaminated with different protein impurities in range of 14-45KDa. Since, γ-conglutin constitutes only 3-4% of total lupin proteins [38] developing an efficient purification process that can selectively capture γ-conglutin and provide high throughput with a minimal number of steps to produce high purity food grade γ-conglutin is required. High purity γ-conglutin can then serve as 'glucose controlling bioactive' in nutraceutical and biopharmaceutical applications.

The anti-diabetic mechanism of action of γ-conglutin has been discussed in section 2.3.2.1. Most of these mechanistic studies were performed in animal derived liver, muscle and fat cells. However, the validation of these studies in cells derived from humans (healthy and diabetic) has not yet been reported. Also, the majority of the anti-diabetic mechanisms of γ-conglutin was focused on its insulin-mimetic property. Other hypoglycaemic effects of γ-conglutin like insulinotropic action in pancreatic β cells and α-glucosidase and dipeptidyl peptidase 4 enzyme inhibitory effects should also be explored and validated. This can open a different area for exploring γ-conglutin's diverse mechanism of action in diabetes.

Chapter 3

Extraction, purification, and enzymatic hydrolysis of lupin proteins

A process patent application is being filed on the 'purification process of γ-conglutin' as described in this chapter.

Part of the information in this chapter (hydrolysis of extract; section 3.5.4) is published in 'Tapadia, M., Carlessi, R., Johnson, S., Utikar, R., & Newsholme, P. (2018). Lupin seed hydrolysate promotes G-protein-coupled receptor, intracellular Ca^{2+} and enhanced glycolytic metabolism-mediated insulin secretion from BRIN-BD11 pancreatic beta cells. Molecular and Cellular Endocrinology'.

3.1 INTRODUCTION

Lupin seed conglutins have wide applications as ingredients in food industries (e.g. emulsifiers, foaming agent, meat extenders) and as functional foods in the treatment of different metabolic dysfunctions [49, 50]. The hypoglycaemic actions of lupin have been specifically attributed to γ-conglutin which comprises 3-4% of lupin seed proteins [38]. As discussed in chapter 2, based on physiochemical properties of γ-conglutin (section 2.4) different ways for extraction and purification of γ-conglutin from lupin seed extract have been reported (section 2.5). Conventionally, alkaline extraction followed by acidic precipitation of proteins along with combination of different chromatographic techniques such as anion exchange chromatography followed by cation exchange chromatography and metal or insulin affinity chromatography are being employed for purification of γ-conglutin [38, 100, 121]. However, pure γ-conglutin is still not available commercially because the reported approaches involve a number of steps, increasing the overall process cost and time. In the literature, the purity of γ-conglutin used for exploring anti-diabetic mechanism of action is either not reported or calculated based on semi-quantitative techniques such as gel electrophoresis.

An in-house optimised process for selective extraction and purification of γ-conglutin from *L. angustifolius* defatted seed flour with a minimum number of steps was

previously reported [39]. In this thesis, the established in-house purification process is further improved with an objective to make process faster and achieve at least 95% pure γ-conglutin. Different protein identification and quantification techniques are used to characterize γ-conglutin in the purified chromatographic fraction. Later, the total extracted proteins and purified γ-conglutin are both subjected to *in-vitro* gastrointestinal digestion condition to hydrolyse the proteins into peptides and amino acids and their potential anti-diabetic action are evaluated in further chapters.

3.2 CHEMICALS AND REAGENTS

Hexane, sodium acetate, Tris base, hydrochloride acid (HCl), sodium hydroxide (NaOH), sodium phosphate monobasic and dibasic, sodium chloride (NaCl), pepsin from porcine gastric mucose (3200-4500 units/mg), pancreatin amylase and protease (USP), trypsin from bovine pancreas (10,000 units/mg), bovine serum albumin (BSA), carbonic anhydrase b, cytochrome C, aprotinin, angiotensin, encephalin, trifluoroacetic acid (TFA), formic acid, acetonitrile, β-mercaptoethanol, glycine, SDS, methanol, tween 20, o-phthaldehyde, and disodium tetraborate decahydrate were purchased from Sigma-Aldrich Pty. Ltd. (Castle Hill, NSW, Australia). Polyclonal goat anti-rabbit immunoglobulins/Horseradish peroxidase was ordered from Dako (Glostrup, Denmark). Pierce bicinchoninic acid assay method assay kit and Pierce quantitative colorimetric peptide assay kit were purchased form Thermo Fisher Scientific (San Jose, CA, USA) and D-glucose assay kit glucose oxidase/peroxidase format from Megazyme (Wicklow, Ireland). 4X Laemmli sample buffer, broad range marker, 'Any kDa' polyacrylamide electrophoresis gel, and Clarity Western enhanced chemiluminescent substrate were ordered from Bio-Rad Laboratories (Hercules, California, USA).

3.3 PROCESS METHODS

3.3.1 Lupin flour preparation

Mature seeds of *L. angustifolius*, (Coromup variety) were provided by Department of Primary Industries and Regional Development: Agriculture and Food Western Australia (South Perth, WA, Australia). The seeds were cleaned and the hulls were

removed by passing them through a dehuller (Graintec Scientific, Queensland, Australia). This was followed by vacuum induced separation of hull (Kimseed vacuum separator, Western Australia, Australia) and any remaining hulls were separated manually from the kernels (cotyledons). The kernels were milled (Cyclotec sample mill, Foss, Denmark) into flour and passed 100% through a 300µm sieve. Since kernel flour of *L. angustifoliu*s (Coromup) contains 7-8% (w/w) of fat [134], defatting was carried out in order to remove the fats, free fatty acids, and pigments which interfere with protein extraction process [135]. Thus, lupin flour was defatted three times with n-hexane (1:10 flour: hexane (w/v)) for an hour at room temperature followed by centrifugation at 4500xg for 5minutes. The supernatant was decanted and the kernel flour residue was air dried. This defatted kernel flour was then used as starting material for extraction of proteins and further purification of γ-conglutin.

3.3.2 Extraction of proteins from defatted flour

A previously optimised extraction process to achieve ~15% γ-conglutin enriched extract (w/w of kernel total proteins) developed in our laboratory was performed [39]. In brief, the defatted kernel flour was extracted in 10mM sodium acetate buffer, pH 4.0 (extraction buffer) in 1:30 (w/v) flour: buffer ratio on a magnetic stirrer (1000xg) for 35minutes at room temperature. The extract was then centrifuged at 4700xg for 20minutes and vacuum filtered through 0.45µm polyvinylidene fluoride (PVDF) disc filters (Pall Corporation, New York, USA).

3.3.3 Preparation of load for purification of γ-conglutin

In order to enrich γ-conglutin in the extract, pH of the extract was shifted to the isoelectric points of the impurities, majorly α and β conglutins (pH(I) 5 to 7), to induce their precipitation [38]. Therefore the pH of the extract (4.40) was adjusted to 6.5 with 1M Tris base followed by centrifugation at 12,000xg for 20minutes [39]. The supernatant was vacuum filtered through 0.45 µm PVDF disc filters. This solution was used as a load for chromatographic purification of γ-conglutin.

3.3.4 Cation exchange chromatography

At pH 6.5, γ-conglutin is below its pH(I) (7-8) and is thus positively charged. To purify a positively charged protein by using ion exchange chromatographic technique (principle explained in chapter 2; 2.4.3), it can be adsorbed (captured) on the negatively charged column matrix. Later, the adsorbed protein can be easily eluted from the matrix by increasing the ionic concentration of the buffer system. Cation exchange chromatographic process for purification of γ-conglutin from the extract (load) was optimised in our laboratory [39]. In this chapter, the established in-house method was further modified and developed to improve purity of eluted γ-conglutin fraction. HiScreen and HiTrap columns (Table 3.1) prepacked with Capto S cation exchange resins (GE Healthcare, Illinois, USA) were used for purification of γ-conglutin from the extract (load) produced in section 3.3.3.

Table 3.1 Details of pre-packed columns used for purification of γ-conglutin

	HiTrap Capto S	HiScreen Capto S
Column Dimension	7 X 25mm	7.7 X 100mm
Column volume	0.96ml	4.66ml
Max. pressure (over column during operation)	70psi (5bar)	44psi (3bar)

Sodium phosphate buffer (10mM) was used as an equilibration buffer (buffer A) and sodium chloride (0.5M) in buffer A was elution buffer (buffer B) (Table 3.2). After eluting the proteins, the column was cleaned and regenerated using NaCl (1M) and NaOH (1M). The salts in the purified γ-conglutin fractions were removed by using HiPrep 26/10 desalting column containing Sephadex G-25 resin (GE Healthcare, Illinois, USA). The desalting fractions were sterile filtered and stored in a freezer at -20°C.

Table 3.2 Details of the buffer used in γ-conglutin purification process

Buffers	Composition	pH	Conductivity (mS/cm)	Column volumes
Equilibration buffer	10mM Sodium phosphate	6.50	0.8-1.0	5
Elution buffer	0.5M NaCl in equilibration buffer	6.50	50-51	As per methods
Regeneration buffer	1M NaCl	6.95	84-86	5
	1M NaOH	14	188-190	5
Desalting buffer	10mM Sodium phosphate	6.50	0.8-1.0	5

3.3.5 Enzymatic hydrolysis of extract and γ-conglutin

The extract proteins and purified γ-conglutin were subjected to proteolytic gastro-intestinal digestion condition and the hydrolysate was further explored for their anti-diabetic properties in chapter 4 and 5. The extract and γ-conglutin protein were enzymatically hydrolysed using the enzymes, pepsin from porcine gastric mucosa (3200–4500U/mg) (1 mg/ml) and pancreatin amylase and protease (USP standard) (1 mg/ml), in two stages to mimic gastrointestinal digestion conditions. First, the protein solutions were hydrolysed with pepsin at pH 2 for 4 hours followed by hydrolysis with pancreatin at pH 7.5 for another 4 hours. The extract was adjusted to pH 2 and pH 7.5 by 1M HCl and 1M NaOH respectively. The enzymes were inactivated by heating the hydrolysate at 100°C for 10 min. Alternatively, the enzymes and the high molecular weight proteins were separated from the hydrolysate by ultrafiltration using 3kDa molecular weight cut off (MWCO) capsule membranes (Pall Corporation, New York, USA). The extract and γ-conglutin hydrolysates were sterile filtered and stored at -20°C.

Figure 3.1 displays an overview of the processes discussed in this chapter.
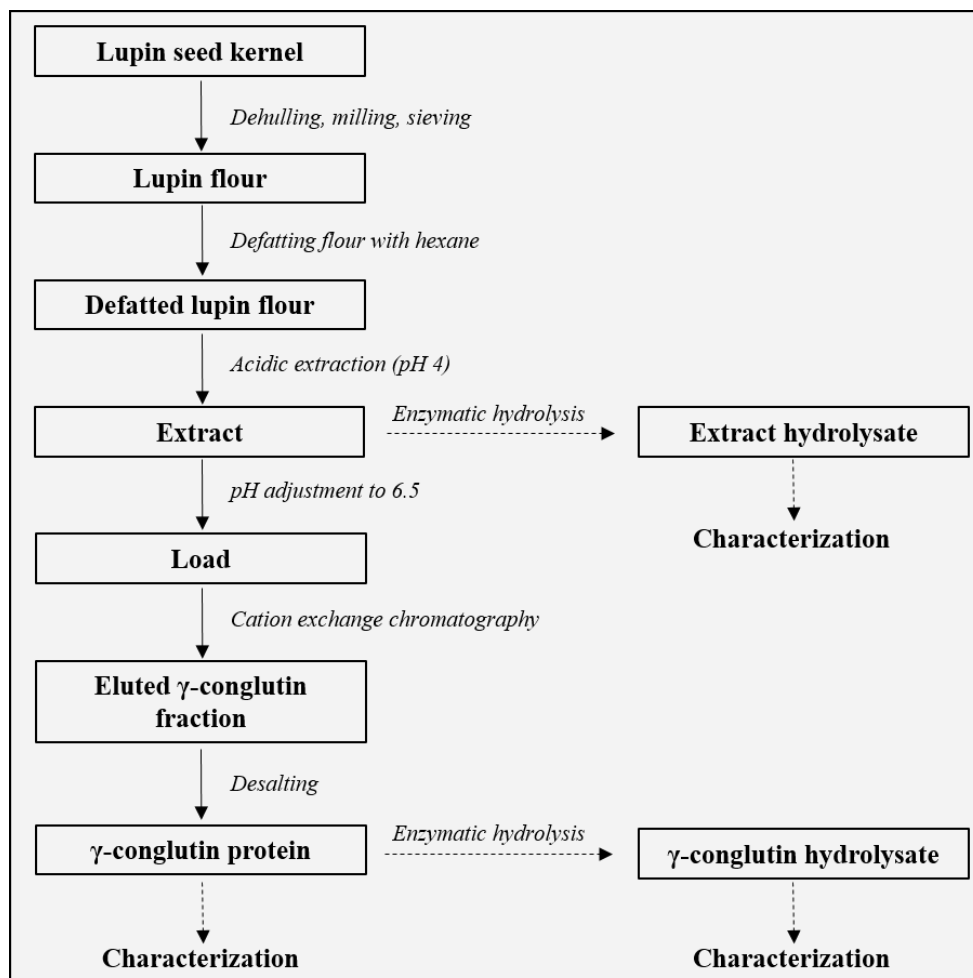
Figure 3.1 Schematic flow of different processes discussed in the chapter

3.4 ANALYTICAL METHODS

3.4.1 Protein, peptide and D-glucose quantification

Proteins, peptides, and D-glucose in the extract and the hydrolysate were quantified using Pierce bicinchoninic acid assay (BCA) method assay kit, Pierce quantitative colorimetric peptide assay kit, and D-glucose assay kit glucose oxidase/peroxidase format respectively according to the protocol provided by the manufacturer. Protein concentration was also determined by measuring the absorbance of purified protein fractions at 280nm and calculating its concentration from the standard curve (Absorbance Vs BSA protein concentration).

3.4.2 RP-HPLC

RP-HPLC is an analytical technique to separate, identify and quantify the desired component from the mixture. γ-conglutin protein from different chromatographic fractions (load, flowthrough, wash, and elution) were quantified by RP-HPLC method [136]. This method was also used to determine purity (%) of γ-conglutin in chromatographic elution fractions. In brief, Agilent Technologies 1200 series HPLC system (Agilent Technologies, CA, USA) equipped with a quaternary pump module, degasser, autosampler, thermostat column compartment and diode array detector was used for analysis. Chromatographic analysis was carried out on Zorbax 300SB C-18 column with 4.6 X 250mm dimension, 5μm particle size and 300Å pore size (Agilent technologies, CA, USA). For analysis, two different solvent gradient mobile phase consisting of 0.1% TFA in water v/v (phase A) and 0.1% TFA in acetonitrile v/v (phase B) were used. Both the mobile phases were degassed in a sonication bath for 5minutes. The method gradient used for the analysis of γ-conglutin is as presented in Table 3.3. The time take by γ-conglutin to elute from the column (retention time) was 29.53minutes.

Table 3.3 RP-HPLC method gradient for analysis of γ-conglutin

Time (mins)	% phase A	% phase B
0	100	0
16	100	0
26	50	50
36	0	100
41	0	100
45	100	0
50	100	0

The injection volume for all the samples was kept constant i.e. 50μl and the flowrate was maintained at 0.8ml/min throughout the run. After every 3-4 runs a blank (water) injection run was performed to check the presence of any ghost peaks or sample carry over from previous runs. The proteins were detected at 280nm.

3.4.3 SDS-PAGE

SDS-PAGE is an electrophoresis technique that separates proteins based on their mass. Molecular weight profile of proteins in different process steps of extraction, purification, and hydrolysis were analysed by SDS-PAGE method. This technique was also used for determining the purity of purified γ-conglutin fractions. Samples were diluted with 4X Laemmli sample buffer (non-reducing condition). To prepare reducing samples, β-mercaptoethanol was added to the samples diluted with sample buffer and heated at 99°C for 10minutes. Protein concentration and load volume of samples were adjusted in order to load fixed amount of proteins (3-5µg/well) per well in 'Any kDa' polyacrylamide gels (optimal resolution of 10-100kDa proteins). Broad range marker consisting of protein markers as Myosin (200KDa), β-galactosidase (116.25KDa), phosphorylase b (97.4KDa), bovine serum albumin (66.2KDa), ovalbumin (45KDa), carbonic anhydrase (31KDa), soybean trypsin inhibitor (31KDa), lysozyme (14.4KDa) and aprotinin (6.5KDa) was loaded in each gel. The electrophoresis was performed using tris-glycine-SDS electrophoresis buffer (2.5mM Tris, 19.2mM glycine, 0.01% SDS) in Mini-Protean tetra cell electrophoresis assembly (Biorad Laboratories Inc., CA, USA) at 100V.

After electrophoresis run, proteins were fixed and stained using silver staining protocol for visualisation of the protein bands [137]. The stained gels were scanned and analysed using Molecular Imager® Gel Doc™ XR System v5.2.1 (Bio-Rad Laboratories, CA, USA) tool. Image Lab 4 software was used to analyse the molecular weights of unknown bands using the standard curve of protein markers (Molecular weight Vs relative front; R^2=0.95). Band intensity (%) of each oligomeric band of γ-conglutin in the lane was calculated by densitometry analysis in the software.

3.4.4 Western blot analysis

Western blot analysis is a protein immunoblot technique used to detect the level or concentration of a specific protein in sample or cell/tissue lysates. A specific antibody (raised against a peptide of the target protein) is incubated with a mixture of proteins containing the target protein. This antibody binds tightly to the specific target protein even after washing away other proteins in the mixture. The conjugation of antibody

with the target protein is then detected by chemiluminescence substrate. Western blot technique was used to confirm the identity of γ-conglutin in the purified fraction.

Reduced and non-reduced protein bands in samples of extract and γ-conglutin were separated by SDS-PAGE as mentioned in section 3.4.3. The unstained protein gel and nitrocellulose membrane were equilibrated with transfer buffer (25mM Tris base, 192mM glycine, 20% (v/v) methanol; pH 8.3) for 15 to 20minutes. Gel and membrane sandwich was carefully placed together between the buffer soaked thick filter papers in gel holder cassette. The cassette was placed in the Mini Trans-Blot cell tank (Bio-Rad Laboratories, CA, USA) filled with transfer buffer and the gel proteins were transferred to nitrocellulose membrane at 250mA constant current for 90minutes in cold room. After the protein transfer step, the membrane was blocked with 3% milk for 60minutes and incubated overnight at 4°C with the γ-conglutin primary antibody (1:1000 dilution in Tris-buffered saline with 0.05% Tween 20 (TBST) containing 5% BSA). γ-conglutin antibody was raised against a synthetic peptide of γ-conglutin (heavy subunit - 30KDa) in the rabbit. The primary antibody of γ-conglutin was a kind gift from Prof. Karam Singh (Director of Centre for Crop and Disease Management, Curtin University, Western Australia). SNAP i.d. quick immunoblot vacuum system (Millipore, MA, USA) was used for washing and incubating membranes in horseradish peroxidase (HRP) conjugated secondary antibody for 60minutes. Clarity™ Western enhanced chemiluminescence (ECL) substrate was used to detect target bands. Bands were then visualized and quantified based on densitometry analysis using Molecular Imager® Gel Doc™ XR System v5.2.1 (Bio-Rad Laboratories, Hercules, CA, USA).

3.4.5 Mass spectrometry

Mass spectrometry (MS) analysis of proteins is an analytical technique that measures mass to charge ratio (m/z) of peptide ions to identify and quantify peptides corresponding to a specific protein. The protein samples are hydrolysed into peptides which are then ionised by the ion source. The electric and magnetic field of mass analysers deflects the path of individual ionised peptides based on their mass to charge ratio which is later detected by an ion detector. The MS spectra of the peptides are then matched with the established protein database that predicts the identity of the protein based on m/z values of peptides [138].

Purified desalted fractions and gel bands of γ-conglutin were detected and analysed by mass spectrometry. The samples were digested with trypsin and extracted according to the standard sample preparation method for liquid chromatography mass spectrometry i.e. LC-MS/MS analysis [139]. Peptides were analysed by electrospray ionisation (ESI) mass spectrometry using the Shimadzu Prominence nano HPLC system (Shimadzu Corp., Kyoto, Japan) coupled to a 5600 Triple TOF mass spectrometer (Sciex, Victoria, Australia). The tryptic peptides were loaded on to an Agilent Zorbax 300SB-C18 (4.6 X 250mm dimension; 3.5μm particle size, 300Å pore size) (Agilent Technologies, California, USA). The peptides were separated with a linear gradient of water (0.1% formic acid) and acetonitrile (0.1% formic acid). A temperature of 350°C and 2050 voltage was applied between the needle and the source in ESI mass spectrometer. The settings for MS and MS/MS analysis were as described in Table 3.4.

Table 3.4 Settings of MS and MS/MS analysis for protein identification

	Acquisition scan rate	Spectra collection rate
MS analysis	5 spectra/s	200 ms/spectra
MS/MS analysis	1 spectra/s	1000 ms/spectra

Spectra were analysed for protein identification using Mascot sequence matching software (Matrix Science) in MSPnr100 database with Viridiplantae (green plants) taxonomy.

3.4.6 Size exclusion chromatography

Size exclusion chromatography (SEC) is an analytical chromatographic technique to separate proteins/peptides in solution based on their size filtration through a gel. Small molecules diffuse into the pores of the resin matrix and thus their flow through the column is retarded while large molecules, traveling through column's void volume are eluted out faster.

SEC was performed to analyse the peptide molecular weight profile of the extract and γ-conglutin hydrolysate using Agilent Technologies 1200 series HPLC system (Agilent Technologies, CA, USA). A Bio SEC-3 column (Agilent Technologies Inc., Santa Clara, CA, USA) with 4.6 X 300mm dimension, 100Å pore size, 3μm particle size, and 100-100,000Da molecular weight range was used for the analysis. Sodium

phosphate (150mM) buffer (pH 6.5) was used as the isocratic mobile phase. The flow rate was maintained at 0.3ml/min throughout the run time of 50minutes. The eluting peptides were monitored at 214nm. Proteins and Peptides (albumin, 66.5kDa; carbonic anhydrase, 29kDa; cytochrome C, 12.4kDa; aprotinin, 6.5kDa; angiotensin, 1.1kDa and; and enkephalin, 0.57kDa) were used as standards for column calibration (Figure 3.2). The estimated molecular weight distribution of sample peaks was determined from the standard curve equation of proteins and peptides (retention time Vs log of molecular weight of standards in Da; $R^2 = 0.956$).
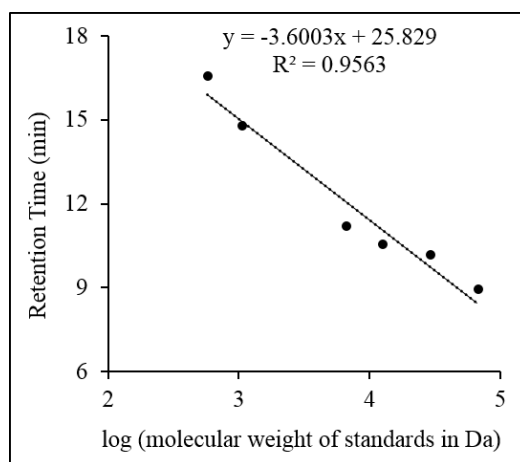
Figure 3.2 Calibration of size exclusion column using standards: albumin (66.5kD), carbonic anhydrase (29 kD), cytochrome C (12.4 kD), aprotinin (6.5 kD), angiotensin (1.1 kD), enkephalin (0.57 kD).

3.4.7 Degree of hydrolysis

Degree of hydrolysis (DH) is defined as the ratio of cleaved peptide bonds in a protein hydrolysate to the total peptide bonds present in the protein. DH of proteins in the enzymatic hydrolysis process was measured by o-phthalaldehyde (OPA) method [140] at time intervals of 30minutes. The OPA reagent consisted of disodium tetraborate decahydrate (0.1M), sodium dodecyl sulphate (1mg/ml), OPA (0.80mg/ml) and dithiothreitol (0.88mg/ml). In this assay, 300µl of the sample (Dilution factor 6X) was mixed with 3ml of OPA reagent. The primary amines (generated during hydrolysis of protein substrate) in sample react with OPA. After 5minutes of incubation, absorbance at 340nm was measured in UV visible spectrophotometer (Jasco V-670, Tokyo, Japan). The amino nitrogen content in the hydrolysate was calculated from the standard curve equation of 0-2mM L-serine (absorbance at 340nm Vs L-serine

concentration). The degree of hydrolysis was calculated according to the following equation [141]:

$$DH\ (\%) = \frac{(N_2 - N_1)\ X\ 100}{N_{pb}}$$

… Equation (3.1)

Where N_1 is amino nitrogen content of extract, N_2 is amino nitrogen content of hydrolysate at particular sample withdrawal time, and N_{pb} is nitrogen content in peptide bonds.

3.5 RESULTS AND DISCUSSION

Different methods for γ-conglutin extraction such as aqueous/alkaline extraction, salt assisted extraction, a combination of extraction and membrane filtration, and purification using gel filtration chromatography, a combination of cation and anion exchange chromatography, insulin and metal affinity chromatography have been reported in the literature [132]. These extraction and purification methods were found to give a γ-conglutin fraction that was still contaminated with other lupin conglutins (discussed in section 2.4.3; chapter 2) and thus the purity (%) of γ-conglutin was either low or not mentioned. With an aim of developing nutraceutical and pharmaceutical high purity grade γ-conglutin protein, an in-house lab scale process for purification of γ-conglutin was optimised by Mane S. [39]. Summary of this in-house γ-conglutin purification process is explained in section 3.5.1.

3.5.1 Summary of γ-conglutin purification methodology

The extraction of conglutins from defatted lupin flour was studied at different pH. The percentage of proteins extracted at acidic pH was less as compared to alkaline pH extraction [142]. However, extraction at acidic pH 4 was optimum as the intensity of the ratio of γ-conglutin to other conglutins was maximum due to the basic pH(I) (7-8) of γ-conglutin. The extraction process was replicated multiple (six) times and the protein concentration of extract was 1.7 ± 0.14 mg/ml. To achieve better separation of γ-conglutin from other conglutins the surface charge on the proteins was altered at a suitable pH where γ-conglutin is positively charged and other conglutins (impurities) were either neutral or negatively charged. This was attained by raising pH of the extract

(4.40) to different pH values from 5 to 7. Since γ-conglutin in this pH range was positively charged batch adsorption studies for selective adsorption of γ-conglutin on different cation exchange adsorbents were evaluated. It was observed that extract with pH 6.5 load resulted in the minimum loss of γ-conglutin in flowthrough (unbound) and wash fractions and maximum γ-conglutin was recovered in elution fractions. Also, Capto S resin had a better binding performance compared to other adsorbents Toyopearl®SP-550C, Toyopearl®SP-650M (Tosoh Biosciences, Tokyo, Japan), and SP-Sepharose FF (GE Healthcare, Illinois, USA). Thus, the extract at pH 6.5 was loaded on Capto S cation exchange column for purification of γ-conglutin. Different chromatographic process parameters like buffer pH and conductivity, method flow rate and elution gradient were optimised with an objective to maximise the yield and purity of eluted γ-conglutin in the purification process. Table 3.5 summarises different optimised parameters of the previously established in-house process.

Table 3.5 Process parameters of previously optimised in-house lab scale γ-conglutin extraction and purification processes [39]

Extraction process			
Extraction buffer	Sodium acetate (10mM)		
Extraction pH	4.00		
Flour: extraction buffer ratio (w/v)	1:30		
pH of extract	4.4 ± 0.1		
Conductivity of extract	2.2 ± 0.2mS/cm		
Chromatographic process			
Equilibration buffer (buffer A)	Sodium phosphate (10mM), pH 6.5		
Elution buffer (buffer B)	0.5M NaCl in equilibration buffer, pH 6.5		
Column	HiScreen Capto S		
Column volume (CV)	4.66ml		
Method flow rate	0.5ml/min		
Load (extract pH 6.5±0.1) volume	450ml (630mg proteins)		
Load concentration (mg/ml)	1.4 ± 0.1mg/ml		
Load conductivity	2.7 ± 0.2mS/cm		
Elution gradient steps:	Initial buffer B (%)	Final buffer B (%)	CV
Equilibration	0	0	2

Load (extract pH 6.5)	0	0	1
Column wash	0	0	5
Elution 1- linear	0	15	7
Elution 2- gradient	15	40	10
Elution 3- linear	40	40	5
Regeneration 1	100	100	2
Regeneration 2 – 1M NaOH	-	-	5
Total method time (hours)	8.4		

The chromatogram and SDS-PAGE of the fractions obtained with the above optimised method are as shown in Figure 3.3A and 3.3B respectively [39]. Load (extract at pH 6.5) in lane 2 of SDS-PAGE analysis showed the presence of γ-conglutin around 45KDa. A faint band of protein at 45KDa (less intense than load) was observed in flowthrough (lane 3). This band can either be γ-conglutin loss in flowthrough or correspond to any other protein equivalent to γ-conglutin molecular weight. The impurity proteins (proteins other than γ-conglutin) in wash (lane 4; box 4 in Figure 3.3A) and impurity peak fraction in elution 1 linear step between 0-15%B (lane 5; box 5 in Figure 3.3A) correspond either to Intermediate Molecular Weight (IMW) β-conglutin (MW – 25 to 46; pH(I) - 5.3 to 8.4) or basic α-conglutins (MW – 20 to 22; pH(I) – 6.7 to 8.6). Lane 6 (box 6 in figure 3.3A) represents fraction of proteins eluted in elution 2 gradient step between 15-40%B consisting majorly of γ-conglutin protein with IMW β-conglutin impurity bands.
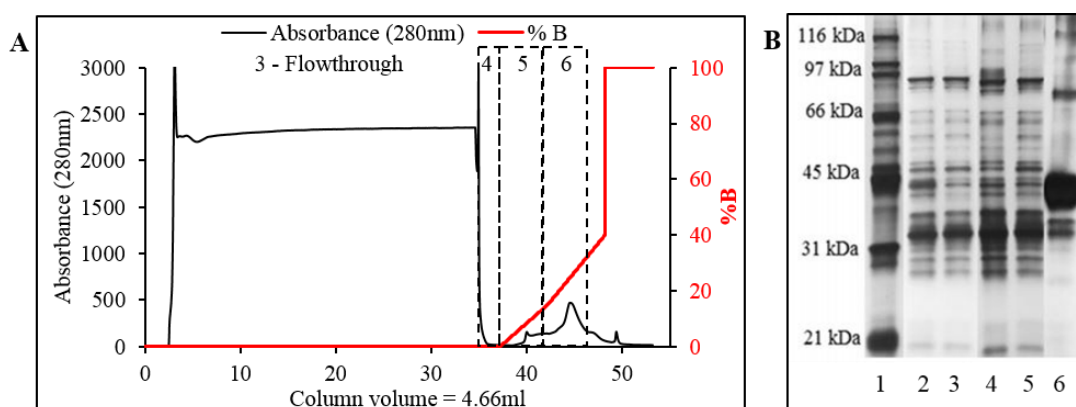
Figure 3.3 (A) γ-conglutin purification chromatogram of existing purification process and (B) SDS-PAGE profile of chromatographic fractions; Lane 1 – Marker; lane 2 – load (pH 6.5); lane 3 – flowthrough; lane 4 – wash; lane 5 – impurity peak in elution

1 linear step (0 – 15%B); lane 6 – γ-conglutin peak in elution 2 gradient step (15-40%B)

The above established in-house purification method by Mane (2018) consisted of only two major steps i.e. acidic extraction and cation exchange chromatography as compared to reported purification involving multiple process steps (section 2.5) [132]. However, the protein mass balance of the entire process and loss of protein (%) in each step was not reported. The amount of extract loaded on the column was below the maximum binding capacity of resin. In order to make the γ-conglutin purification process faster, the amount of extract (mg) loaded on the column can be increased. The protein content in purified γ-conglutin fraction was found to be ~95% w/w based on nitrogen elemental analysis [39]. However, γ-conglutin purity in eluted fraction (between 15-40%B) was not reported using quantitative analytical tool like RP-HPLC. In the purified γ-conglutin fraction (lane 6; Figure 3.3A), β-conglutin IMW impurities between 30-40KDa were observed. Thus, the eluted γ-conglutin was contaminated with IMW β-conglutin impurities. Therefore, the previously established in-house purification process was further developed to achieve pure γ-conglutin (purity ≥95%) as explained in following sections.

3.5.2 γ-conglutin purification process development

Interpretation of biophysical/structural characterization and bioactivity studies of a purified protein is based on several assumptions: protein purity and homogeneity, its precise quantification and solubility in its native active state [143]. For food and pharmaceutical purposes purity assessment is most critical, especially for the biologically active proteins [144]. As discussed earlier, different anti-diabetic properties have been ascribed to γ-conglutin protein and only a few reports have mentioned the protein purity based on SDS-PAGE analysis [40, 41, 100, 101]. However, SDS-PAGE analysis is a semi-quantitative technique whereas RP-HPLC analysis is sensitive, specific, precise and reproducible quantitative analytical technique often used in pharmaceutical industrial and analytical sectors. As a result, reporting γ-conglutin purity based on HPLC analysis is more accurate and reliable. As discussed in section 3.5.1, γ-conglutin obtained from the previously optimised in-house γ-conglutin purification method (developed by Mane, 2018) was contaminated with impurities (proteins and small molecules other than γ-conglutin). As a result, in

the current thesis γ-conglutin purity based on RP-HPLC analysis was reported after every modification made to the existing method.

Generally, the downstream purification process comprises up to 70-80% of the entire bioprocess cost production. This has caused the producers to shift their focus from improving the upstream process to improving downstream production. With this perspective, the established in-house γ-conglutin purification method was further developed in this thesis to make the process faster. This was achieved by increasing the extract load volume (% binding capacity) and decreasing the process run time (by increasing method flowrate). All the modifications for further purification process optimization were performed on Capto S HiTrap column (column volume = 0.96ml) and later linearly scaled-up to HiScreen column (column volume = 4.66ml).

HiTrap Capto S column was continuously loaded with pH 6.5 extract at two flowrates 0.5ml/min (total process time = 36 hours) and 0.75ml/min (total process time = 24.22hours) and γ-conglutin in flowthrough was evaluated by RP-HPLC analysis. Since, the presence of γ-conglutin in flowthrough was below the limit of detection, it was difficult to calculate percent loss of γ-conglutin in flowthrough as compared to load (Figure 3.4A and 3.4B). However, the profile of γ-conglutin peaks in flowthrough operated at both the flow rates were similar. As a result, 0.75 ml/min was selected as loading flowrate to reduce the total run time. While loading extract, the column pressure increased with increase in load volume. It was observed that after loading approximately 1000ml extract (1.4 ± 0.03mg/ml), the column pressure reached its maximum operating pressure limit. As a result, the load volume of 1000ml (1824 mg proteins) was selected for further optimisation studies.
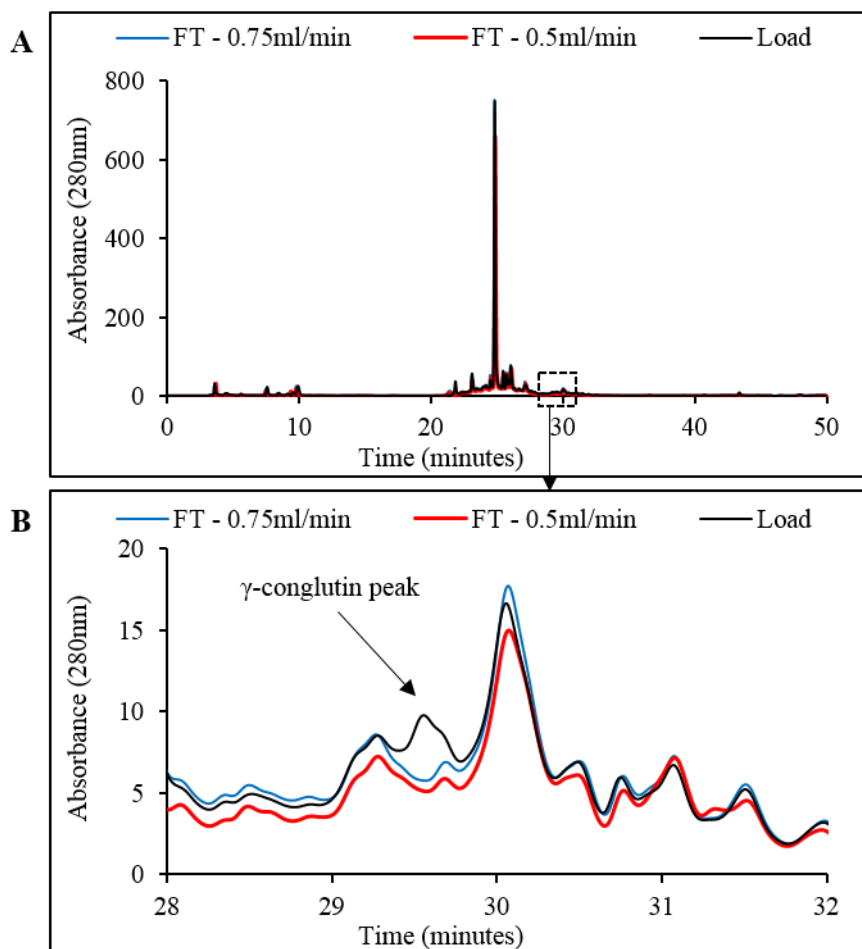
Figure 3.4 (A) RP-HPLC analysis of γ-conglutin in load and flowthrough (loading flow rate 0.5ml/min and 0.75ml/min) (B) zoomed chromatogram of the Figure 3.4A (from 28 to 32 mins).

At first, 1000ml of extract (pH 6.5) was loaded on the HiTrap Capto S column (column volume = 0.96ml) at 0.75ml/min and the previously established optimised elution gradient (Table 3.6) was used to elute γ-conglutin from the column [39].

Table 3.6 Chromatographic elution gradient for 'Modified method I' adapted from elution gradient of established in-house purification process [39]

	%B	CV
Elution 1- linear	0 -15	7
Elution 2- gradient	15-40	10
Elution 3- linear	40	5
Regeneration 1	100	2

The chromatogram of 'modified method I' is represented in Figure 3.5A. During elution (Figure 3.5B), an impurity hump at 24%B consisting of conglutins along with γ-conglutin was observed to be merged in the fronting region of γ-conglutin peak i.e. the resolution between the impurity peak and γ-conglutin peak was poor (dotted box 5

and 6; Figure 3.5B). Figure 3.5C shows the SDS-PAGE protein profile of load, flowthrough, wash, impurity peaks, and γ-conglutin peak of chromatogram in Figure 3.5B. It was observed that the hump eluting at 24%B (lane 5 and 6) majorly consisted of γ-conglutin and impurities that can be addressed as β-conglutin IMW peptides or basic units of α-conglutin (pH(I) range 5.2-8.4) [38] and small molecular weight peptides (22-7kDa) as explained in section 3.5.1. Because of the merged impurity peak (hump), the overall % purity of γ-conglutin was 73% based on RP-HPLC analysis (Figure 3.6).
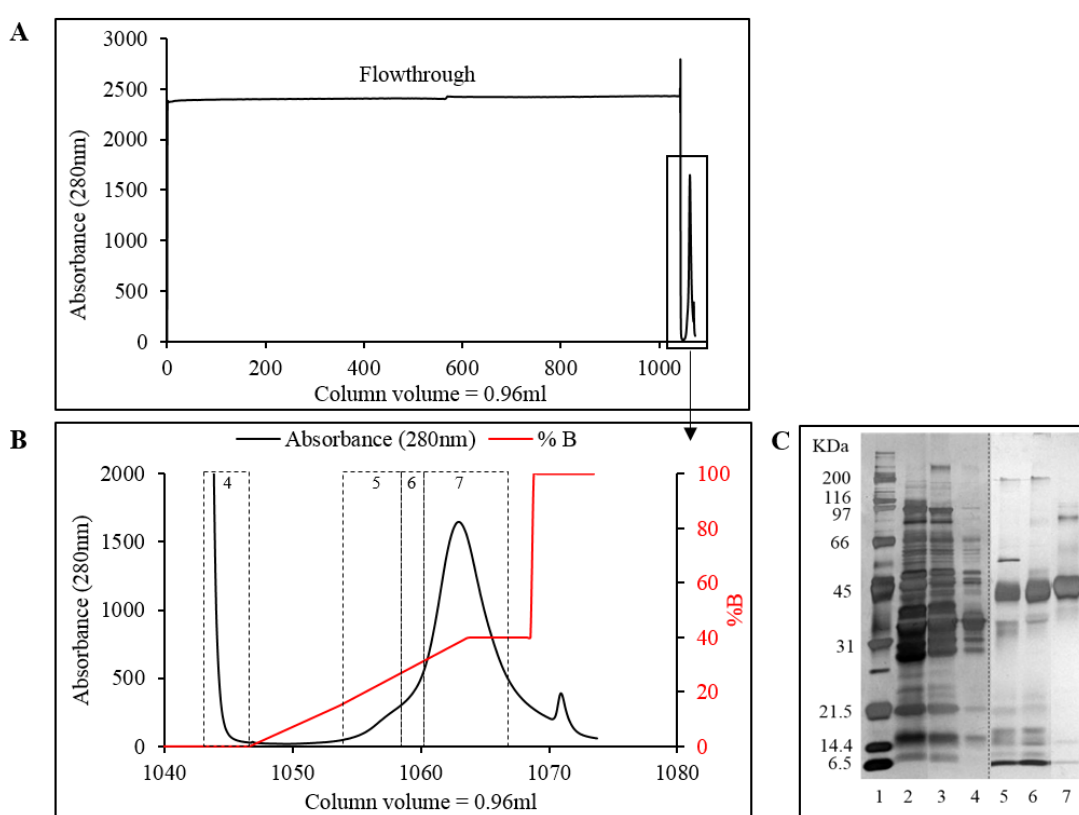
Figure 3.5 (A) chromatogram of 'modified method I' (B) Elution step of 'modified method I'. Box 4 – wash; box 5 and 6 - impurity peak; box 7 -γ-conglutin peak (C) SDS-PAGE protein profile of 'modified method I' fractions. Lane 1 – marker; lane 2 – extract pH 6.5 (load); lane 3 – Flowthrough (unbound); lane 4 – wash; lane 5 and 6 – merged impurity peak; lane 7 - γ-conglutin peak.
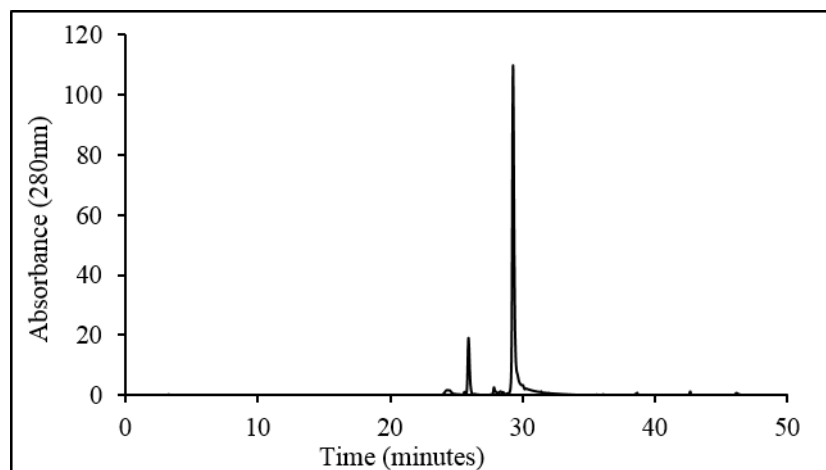
Figure 3.6 RP-HPLC analysis of γ-conglutin peak (dotted box 7 of Figure 3.3B) obtained from 'modified method I'.

The bound proteins to the resin are eluted by controlled changes in ionic concentration. Long and shallow gradient (% buffer B) gives maximum separation between the eluted peaks. Thus, in order to separate the impurity peak (consisting of other conglutin proteins) from the main γ-conglutin peak, the method was further modified by splitting elution 2 - gradient step (15 to 40%B – 10CV) into 2 steps as reported in Table 3.7 ('modified method II'). All the other steps were the same as 'modified method I'.

Table 3.7 Chromatographic elution gradient for 'Modified method II'

	%B	CV
Elution 1- linear	0 -15	7
Elution 2A- gradient	*15-32*	*11*
Elution 2B- gradient	*32-40*	*3*
Elution 3- linear	40	5
Regeneration 1	100	2

The elution chromatogram obtained from the 'modified method II' is shown in Figure 3.7. The dotted box indicates the collected γ-conglutin fraction for RP-HPLC analysis. The purity of γ-conglutin fraction was increased to 79%. However, the impurity peak consisting of other conglutins and γ-conglutin peak were still not completely resolved.
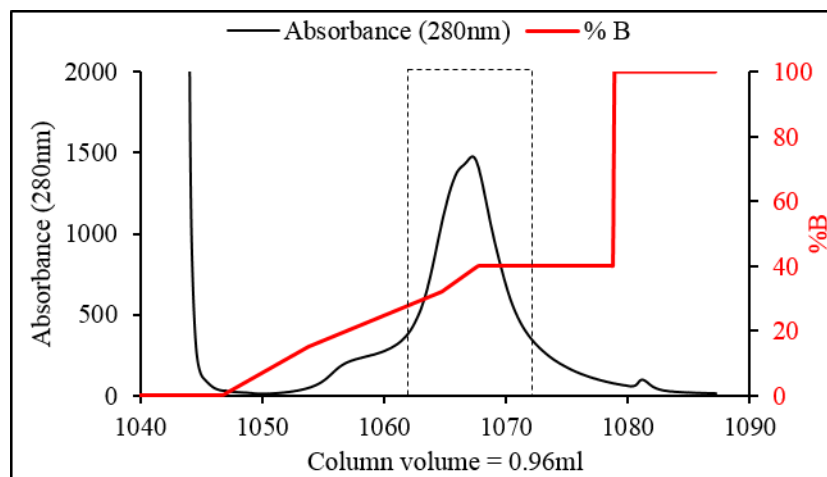
Figure 3.7 Elution chromatogram of 'modified method II'

Since the elution of impurity peak started at 15%B an isocratic step of 15%B (*elution 2A-linear*) was inserted before the elution *2A-gradient step* to separate former impurity peak from the main γ-conglutin peak. Similarly, an isocratic step of 30%B (elution 2B linear) was introduced to elute pure γ-conglutin and avoid its merging with subsequent peak impurities (Table 3.8).

Table 3.8 Chromatographic elution gradient for 'Modified method III'

	%B	CV
Elution 1- linear	0 -15	5
Elution 2A- linear	*15*	*15*
Elution 2A- gradient	*15-30*	*18*
Elution 2B- linear	*30*	*12*
Elution 3- linear	40	10
Regeneration 1	100	5

The elution chromatogram obtained from 'modified method III' is shown in Figure 3.8. The impurity peak separated from γ-conglutin peak at the isocratic step of 15%B. The % purity of γ-conglutin achieved using 'modified method III' was 89%. Isocratic condition at 15%B was responsible for tailing of the impurity peak.
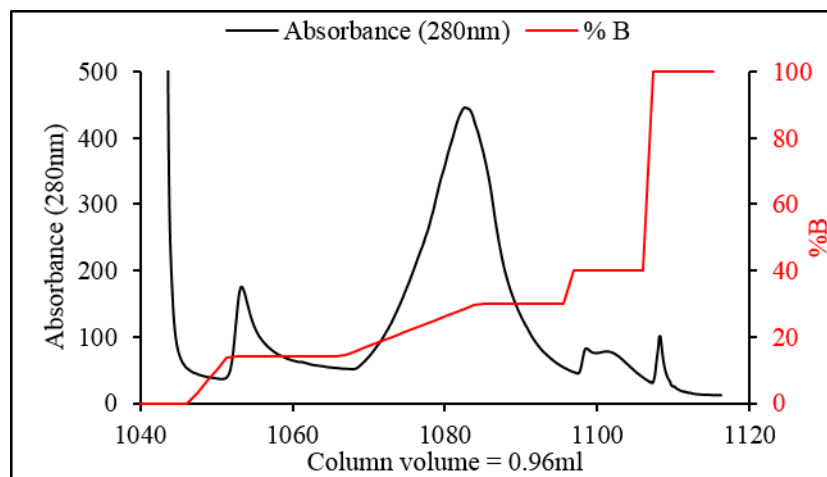
Figure 3.8 Elution chromatogram of 'modified method III'.

Resolution (Rs) of peaks is a measure of how well the peaks are separated from each other in the chromatographic process. Rs is defined as the ratio of the difference between peak retention times to the average of peak widths [145]. Rs can also be calculated by using half-height equation 3.2.

$$Rs = \frac{2[V_{R2} - V_{R1}]}{1.7\,[W_{0.5,1} + W_{0.5,2}]}$$
… (Equation 3.2)

where V_{R1} and V_{R2} are retention volumes of two peaks and $W_{0.5,1}$ and $W_{0.5,2}$ are peak widths measured at half height. The half-height formula for measuring resolution is used when the baselines of two peaks are non-resolved or merged and it is difficult to measure the peak base width. Rs value greater than 1 ensures the separation of two peaks to a degree at which their height and area can be calculated [145]. Resolution between impurity peak and γ-conglutin peak was calculated to be 2.43.

In gradient condition, at every point, a stronger ionic concentration mobile phase elutes molecule through the column faster than weaker ionic concentration mobile phase, unlike the isocratic condition where the ionic concentration is constant throughout the step. Thus, steeper ionic gradient results in the concentrated peak with reduced tailing effect as compared to the isocratic condition. [146]. In method development, the peak symmetry is an indication of a well-behaved system and provides ease in quantitation. Peak asymmetry can be represented by Asymmetry factor (As) as shown in equation 3.3.

$$As = \frac{b}{a}$$
… (Equation 3.3)

56

where a and b are the distances from the peak midpoint to the leading edge and trailing edge respectively measured at 10% of the peak height [145]. The As (0.91) of γ-conglutin peak was within the acceptable range of 0.9-1.2. The purity (%) of γ-conglutin obtained with this method was 87%. As the modified method 3 resolved impurity and target peak and resulted in satisfactory purity of γ-conglutin (≥85%), it was scaled up from Capto S HiTrap (CV=0.96ml) to Capto S HiScreen (CV=4.66ml).

Column performance is dependent on the column design and operating conditions. A successful scale-up of chromatographic purification process maintains the productivity and quality of the product. Different kinetic and dynamic parameters (e.g. particle size, pore size, ligand chemistry, gradient condition, flowrate) and system parameters (e.g. load volume, mobile phase composition, column volume) should be optimised in a cost-effective way during lab process development [147]. Residence time of the target protein with resin matrix in the column critically controls its separation from other proteins [148]. The process parameters are linearly scaled up according to the column bed height by keeping residence time in terms of 'flowrate in units of column volumes/time' and 'load volume/column volume' constant [149]. Increasing column bed height also increases the number of theoretical plates (HETP – height equivalent to theoretical plate) in the column, thus, improving separation of the target protein [150]. Considering all the above key points, the purification method was further developed (scaled-up) on a prepacked Capto S HiScreen column with 10cm bed height, 0.77cm diameter and 4.66ml column volume (Table 3.9). The flow rate was changed to 3.63 ml/min and the load volume of extract (1.4 ±0.3) was increased to 4790ml (6720mg proteins).

Table 3.9 Modified method III linearly scaled-up from Capto S HiTrap to Capto S HiScreen by maintaining constant residence time

Parameters	Capto S HiTrap	Capto S HiScreen
Height (cm)	2.50	10.00
Diameter (cm)	0.70	0.77
Area (cm^2)	0.38	0.47
Column volume (ml)	0.96	4.66
Process flowrate (ml/min)	0.75	3.63
Linear velocity (cm/min)	1.95	7.79
Residence time (min)	**1.28**	**1.28**
Loading time (hours)	22	22
Extract (load) volume (L)	0.99	4.79

It was observed that after loading 4000ml of extract, the back pressure on the column increased beyond column operating pressure limits and, thus, load volume was reduced to 4000ml (5612mg proteins). Each run was followed by consecutive column regeneration steps (1M NaCl and 1M NaOH). As shown in Figure 3.9A and 3.9B, the elution pattern of γ-conglutin was observed to be similar as Capto S HiTrap chromatographic run (Figure 3.8 A and B). Figure 3.9C shows the SDS-PAGE protein profile of feed, flowthrough, wash, impurity peak and γ-conglutin peak of chromatogram in Figure 3.9A and B. Flowthrough (lane 3) and wash (lane 4) fractions showed a faint band at 48KDa which indicates either minimal loss of γ-conglutin in flowthrough as explained earlier (Figure 3.4) or loss of other protein equivalent to γ-conglutin's molecular weight. Impurity peak (lane 5) showed the presence of IMW β-conglutin (MW – 25 to 46; pH(I) - 5.3 to 8.4) or basic α-conglutins (MW – 20 to 22; pH(I) – 6.7 to 8.6) along with γ-conglutin protein. γ-conglutin peak (lane 6, 7, and 8) exhibited two bands around 45KDa and 90KDa. γ-conglutin exists in a monomeric-dimeric-tetrameric state between slightly acidic to neutral pH [117]. Due to pH modifications (pH 4 to 6.5) involved in the load preparation stage (section 3.3.3), γ-conglutin shows its existence in monomeric (45KDa) and dimeric (48KDa) forms. However, these bands need to be characterised further in detail (section 3.5.3). Later, γ-conglutin fractions (dotted box 6, 7 and 8; Figure 3.9B) were pooled together.
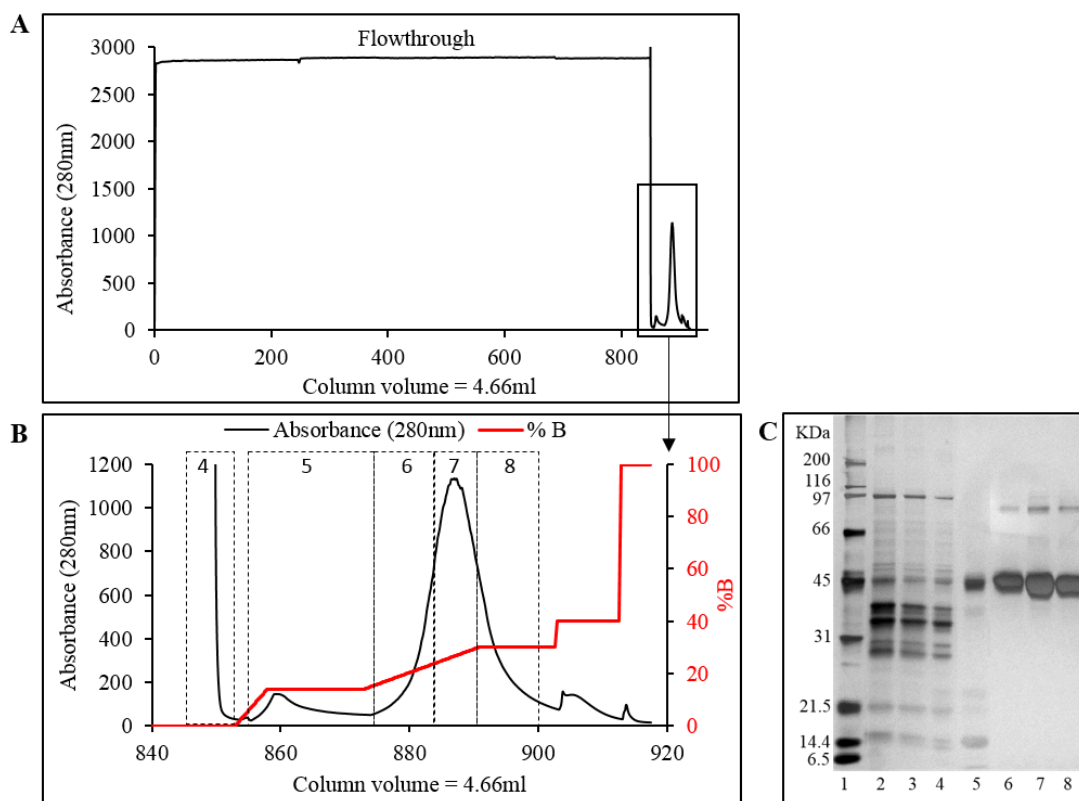
Figure 3.9 (A) complete chromatogram of 'modified method III' on Capto S HiScreen column (B) elution chromatogram of 'modified method III' on Capto S HiScreen. Box 4 – wash; box 5 - impurity peak; box 6, 7 and 8 -γ-conglutin peak (C) SDS-PAGE protein profile of 'modified method III' on Capto S HiScreen. Lane 1 – marker; lane 2 – extract pH 6.5 (load); lane 3 – Flowthrough (unbound); lane 4 – wash; lane 5 – impurity peak; lane 6, 7, 8 - γ-conglutin peak.

Column efficiency is directly proportional to 'height equivalent to theoretical plate (HETP)' which increases with an increase in column height. As a result, γ-conglutin purity increased from 87% to 94% (Figure 3.10) when the process was scaled up from CaptoS HiTrap (height = 2.5cm) to HiScreen (height = 10cm). The asymmetry factor of γ-conglutin peak and the Rs factor between the two peaks (impurity and γ-conglutin peak) were 1.12 and 2.32 respectively. The optimised process for purification of γ-conglutin from crude extract on HiScreen column was performed three times. The purity of γ-conglutin reported by HPLC analysis was $91.5 \pm 1.2\%$. The process mass balance i.e. mass of protein loaded on the column (extract) and mass of protein fractions in the flowthrough, wash, elution, and regeneration steps was found to be $98.5 \pm 0.9\%$.
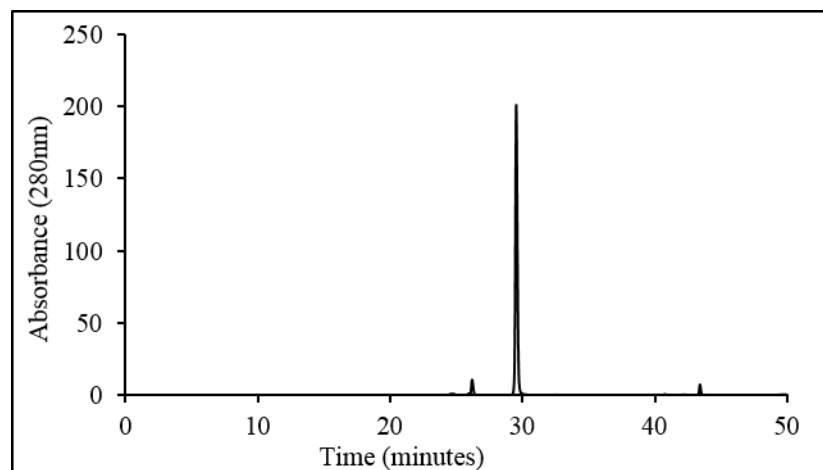
Figure 3.10 RP-HPLC analysis of γ-conglutin pooled fraction (dotted box 6,7and 8) of the chromatogram in Figure 3.9B.

γ-conglutin pooled fraction consisted of salts (sodium phosphate and sodium chloride) which were removed further using HiPrep desalting column. Figure 3.11 shows γ-conglutin chromatogram obtained from the desalting column. After elution of γ-conglutin, a rise in conductivity to 4.4mS/cm corresponding to elution of salts from the column was observed. Multiple purification process runs on Capto S HiScreen (CV = 4.66ml) coupled with desalting step were performed to produce γ-conglutin protein for further enzymatic hydrolysis and anti-diabetic bioactivity studies.
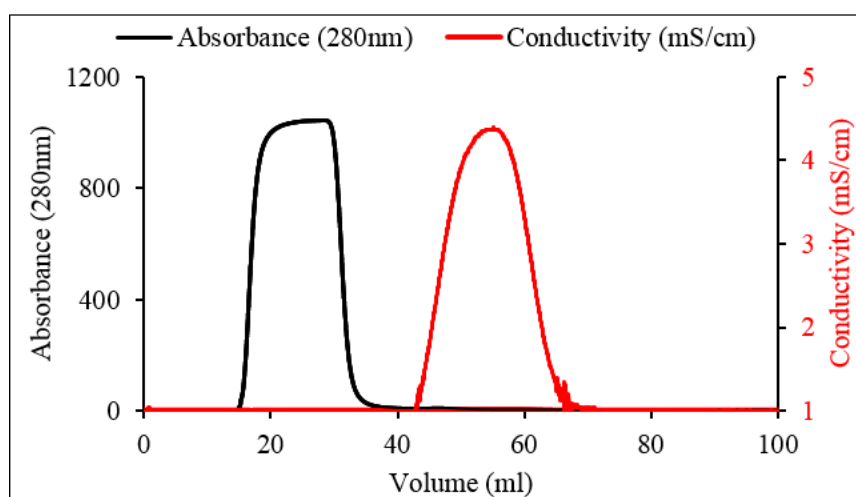
Figure 3.11 Chromatogram of γ-conglutin eluted from desalting column

3.5.3 Characterisation of purified γ-conglutin protein

Accurate identification, quantification, and characterization of a protein purified from a natural source or cell cultures is an essential step in process development. Various protein identification and characterization techniques enable a quality control check

throughout the process for production of high-quality protein products. Different techniques discussed in following sections were used for qualitative and quantitative assessment of γ-conglutin protein.

3.5.3.1 SDS-PAGE

Being a simple, least expensive and sensitive technique, SDS-PAGE is often the first choice for purity assessment. It was used to study protein profile in the extract (pH 4) and load (extract at pH 6.5), and to estimate the purity of pooled γ-conglutin fraction (Figure 3.12A). Different molecular weight proteins (10-100KDa) were present in the extract (lane 2) and load (lane 3) along with γ-conglutin. These proteins can be intermediate (25-46kDa) and low (17-20kDa) molecular weight β-conglutins having pH(I) in range of 5.3-8.4 or basic subunits of α-conglutin (20-22kDa) with pH(I) range of 6.7-8.6 [38]. Densitometric analysis of reduced and non-reduced γ-conglutin lanes was performed to measure the intensity of the protein bands in its lane (Figure 3.12B).
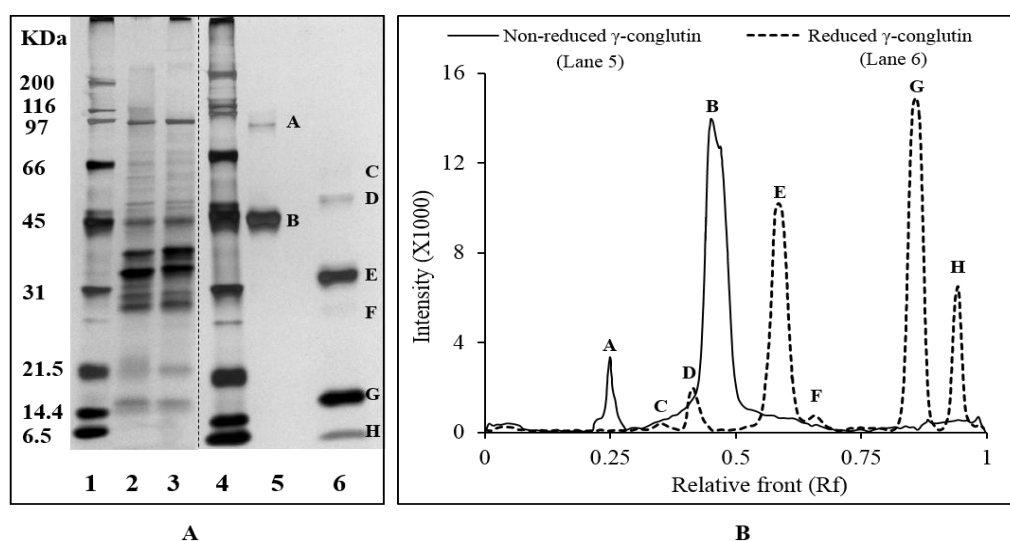
Figure 3.12 (A) SDS-PAGE profile of extract at pH 4 (lane 2), extract at pH 6.5 i.e. load (lane 3), non-reduced (lane 5) and reduced (lane 6) γ-conglutin; (B) SDS-PAGE densitogram of non-reduced and reduced γ-conglutin.

Molecular weight and % band intensity of the bands were calculated as shown in Table 3.10. γ-conglutin is known to exhibit pH-dependent oligomeric conformational modifications i.e. γ-conglutin changes from tetrameric to dimeric to monomeric forms between neutral (≥pH 6.5) to acidic pH (pH 3.5) [73]. Due to pH modifications in extraction and purification steps, γ-conglutin exists in two forms: dimer at 91KDa (band A) and monomer at 45KDa (band B) in the lane 5 (Figure 3.12A) of purified γ-

conglutin (non-reduced). Except for the two bands at 91KDa (9% band intensity) and 45KDa (91% band intensity), no other bands were visible in lane 5 of pure γ-conglutin indicating ~100% γ-conglutin purity. SDS-PAGE is a semi-quantitative analytical technique. The reported purity might be an overestimate due to (a) inability of the tool to detect low abundant bands (b) unequal staining of all the proteins (c) co-migration of the impurity proteins having a molecular weight equivalent to γ-conglutin molecular weight. As a result, γ-conglutin purity should be confirmed with another quantitative analytical tool.

The presence of γ-conglutin dimer was confirmed by analysing the reduced γ-conglutin gel profile (Figure 3.12A; lane 6 - bands C to H). The disulphide bonds in γ-conglutin gets cleaved when the protein is heated at 99°C for 10 minutes in presence of β-mercaptoethanol sample buffer. Under this reducing condition, γ-conglutin protein breaks down into polypeptides. The non-reduced γ-conglutin dimer band A and monomer band B (lane 5) were cleaved into polypeptides - heavy subunit (band E; 33KDa) and light subunit (band G; 18KDa). The high temperature stressed condition induced aggregation of uncleaved γ-conglutin or incomplete degradation of γ-conglutin dimers (bands C and D) [151]. Also, at high temperature, γ-conglutin protein degraded into peptides (bands F and H).

Table 3.10 SDS-PAGE densitometric analysis of non-reduced and reduced γ-conglutin

Lane	Band	Molecular weight (KDa)	% band intensity	Band properties
Non-reduced γ-conglutin (Lane 5)	A	91	9.0	γ-conglutin dimer
	B	45	91.0	γ-conglutin monomer
Reduced γ-conglutin (Lane 6)	C	60	1.0	γ-conglutin aggregate or incomplete reduction of dimer
	D	50	4.6	
	E	33.2	35.8	Cleaved γ-conglutin (heavy)
	F	28.8	2.1	γ-conglutin degraded peptide
	G	18	43.9	Cleaved γ-conglutin (light)
	H	8.3	12.6	γ-conglutin degraded peptide

3.5.3.2 Western blot

To further confirm γ-conglutin identity and purity, western blot was performed. It is an important characterization technique in biopharmaceutical process development, from early pretreatment and process optimization stage to the final purified product development stage. Different amounts (µg) of non-reduced (-) and reduced (+) extract and pure γ-conglutin proteins were loaded in the well (Figure 3.13A). After SDS-PAGE, proteins were transferred on the membrane and were stained with γ-conglutin antibody having specificity to a heavy subunit of γ-conglutin (around 30kDa).

Monomeric (45KDa) and dimeric (91KDa) bands of γ-conglutin were visible in the non-reduced extract (Figure 3.13A - lane 2 and 4). In reduced extract (Figure 3.14A; lane 3 and 5) heavy subunit band of γ-conglutin (33KDa) and γ-conglutin aggregate band (50KDa) were observed. Apart from the γ-conglutin bands in the extract, the antibody showed non-specific binding to a protein at 37KDa which was not explored in detail.
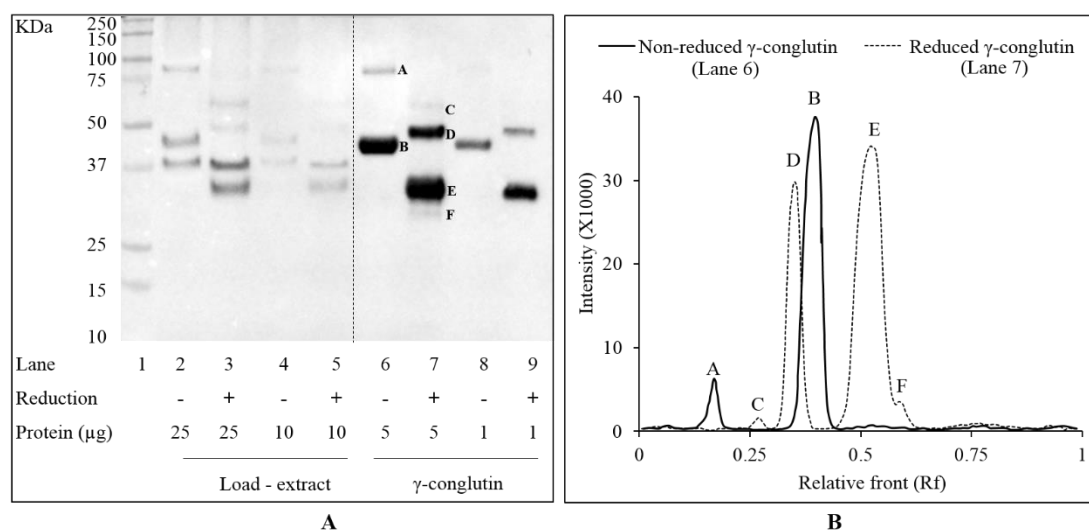
Figure 3.13 (A) Western blot of different amounts (µg) of non-reduced (-) and reduced (+) extract and pure γ-conglutin proteins (B) western blot densitogram of non-reduced and reduced γ-conglutin

Molecular weight and band intensity (%) of protein bands in non-reduced and reduced γ-conglutin samples were calculated by Image lab 4 software (Figure 3.13B; Table 3.11). The non-reduced γ-conglutin showed the presence of band A - dimeric (8.6% band intensity) and band B - monomeric (91.4% band intensity) forms in lanes 6 and 8 (Figure 3.13A). The band intensities of these two forms were similar to the non-

reduced γ-conglutin SDS-PAGE bands profile (lane 5; Table 3.10). Thus, the selective immunodetection of γ-conglutin by its antibody confirmed the presence of γ-conglutin. As γ-conglutin antibody had specificity to heavy subunit of the protein, an intense band at 33KDa (band E) was observed in the reduced γ-conglutin samples (Lane 7 and 9). The molecular weight, band intensities, and properties of other bands in these lanes are as described in Table 3.11.

Table 3.11 Western blot densitometric analysis of non-reduced and reduced
γ-conglutin

Lane	Band	Molecular weight (KDa)	% band intensity	Band properties
Non-reduced γ-conglutin (Lane 6)	A	91.8	8.6	γ-conglutin dimer
	B	45.2	91.4	γ-conglutin monomer
Reduced γ-conglutin (Lane 7)	C	58.3	1.7	γ-conglutin aggregate or incomplete reduction of dimer
	D	48.5	31.1	
	E	33.1	64.0	Cleaved γ-conglutin (heavy)
	F	29.9	3.1	γ-conglutin degraded peptide

3.5.3.3 RP-HPLC

RP-HPLC is an easy, linear, efficient and reproducible analytical technique for identification and quantification of compounds in the mixture. RP-HPLC is a common tool used for purity evaluation and impurity profiling of pharmaceutical drugs. γ-conglutin peak was analysed, as discussed in section 3.5.2., using a developed reverse phase HPLC method for γ-conglutin quantification [136]. Purified γ-conglutin chromatographic fractions were pooled, desalted, and sterile filtered and the final protein product was analysed. γ-conglutin HPLC chromatogram (Figure 3.14) showed presence of two peaks – an impurity peak at 26.19 minutes and γ-conglutin peak at 29.53 minutes. Using Agilent OpenLAB CDS Chemstation software (Agilent Technologies, CA, USA) for peak auto-integration, the percent area under the curve (purity) of the γ-conglutin peak eluting at 29.53 minutes was found to be 95.2%.
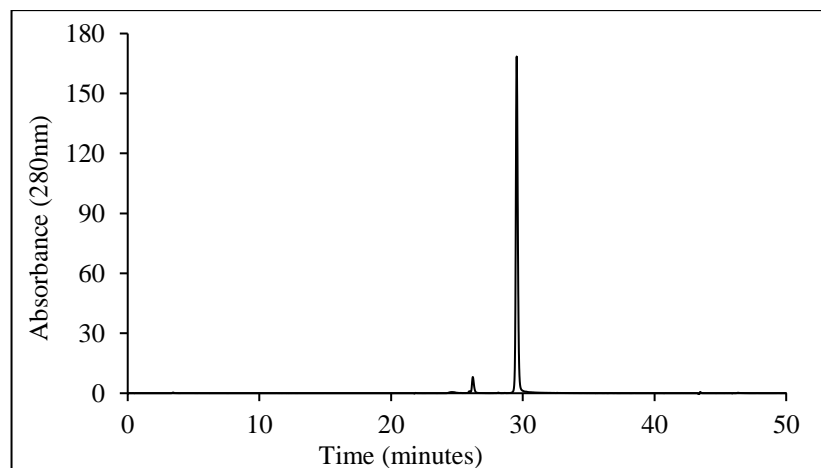
Figure 3.14 RP-HPLC analysis of pooled and desalted γ-conglutin fraction obtained from the chromatographic purification process.

3.5.3.4 Mass spectrometry

MS is an established primary method for protein identification from complex biological origin samples [152]. Purified fractions and SDS-PAGE gel bands of γ-conglutin were analysed by mass spectrometry (LC-MS/MS) to substantiate its identity as γ-conglutin. The samples were prepared and digested with trypsin enzyme as mentioned in section 3.4.5. The MS/MS spectra of peptides were analysed using Mascot sequence matching software (Matrix Science) with MSPnr100 database. After completion of the search, a summary of all the hit proteins with their accession number was obtained (Table 3.11). For each protein match, the overall protein score was calculated. 'Protein score' is the sum of the highest ion scores associated with each distinct peptide sequence (excluding the score of duplicate peptide sequence). A higher protein score indicates a more significant (confident) match. Protein scores greater than 67 (threshold score) are considered to be significant ($p<0.05$) and are reported in Table 3.12. These proteins are ranked according to their protein score. 'Coverage' is the percentage of detected peptides that match with the protein sequence available in the database. The 'matches' represent the number of MS/MS spectra matched to the protein. The number of peptide sequences generated from the spectra that matched with the database is indicated by 'sequences' in the table. The number in parentheses is the counts obtained above the specific threshold (significant matches/sequences). A confident identification should have minimum two significant matches/sequences [153].

From Table 3.12 is was observed that γ-conglutin protein from *L. angustifolius* (accession number - Q42369) hit with the highest score of 2137. This high score lowered down the probability of the observed match to be a random event [154]. VGFNSNSLK peptide is a signature tryptic peptide of γ-conglutin and is used as an internal standard for isotope labeled quantification of γ-conglutin [155, 156]. This unique signature peptide was identified in the peptide sequences of γ-conglutin (Q42369) and this further increased the confidence of the protein to be identified as γ-conglutin from *L. angustifolius* (accession number - Q42369). In Q42369, 12 peptide sequences matched with γ-conglutin protein database contributing to 35% coverage of the protein sequence as observed in Figure 3.15. The second highest score (OIW19056.1) and other protein scores (OIW08851.1, OIV97544.1, B9RG92, OIW00888.1) in the Table 3.12 did not have a significant number of peptide sequences required for identification of the protein [157]. Also, the molecular weight and pH(I) of the proteins (except Q42369) listed in Table 3.12 did not match either with γ-conglutin's molecular weight (48KDa) or its pH(I) (7-8) mentioned in the literature [38].

1	MARNMAHILH	ILVISLSYSF	LFVSSSSQDS	QSLYHNSQPT	SSKPNLLVLP
51	VQEDASTGLH	WANIHK**RTPL**	**MQVPLLLDLN**	**GK**HLWVTCSQ	HYSSSTYQAP
101	FCHSTQCSRA	NTHQCFTCTD	STTTRPGCHN	NTCGLLSSNP	VTQESGLGEL
151	AQDVLAIHST	HGSKLGPMVK	VPQFLFSCAP	SFLAQK**GLPN**	**NVQGALGLGQ**
201	**APISLQNQLF**	**SHFGLKR**QFS	VCLSR**YSTSN**	**GAILFGDIND**	**PNNNNYIHNS**
251	**LDVLHDLVYT**	**PLTISKQGEY**	**FIQVNAIR**VN	**KHLVIPTK**NP	FISPSSTSYH
301	GSGEIGGALI	TTTHPYTVLS	HSIFEVFTQV	FANNMPKQAQ	VKAVGPFGLC
351	YDSR**KISGGA**	**PSVDLILDKN**	**DAVWR**ISSEN	FMVQAQDGVS	CLGFVDGGVH
401	AR**AGIALGAH**	**HLEENLVVFD**	**LER**SR**VGFNS**	**NSLK**SYGKTC	SNLFDLNNP

Figure 3.15 Protein view displaying 35% γ-conglutin peptide sequence coverage to Q42369 (matched peptide sequences are in bold).

Similarly, the MS/MS spectra of SDS-PAGE gel bands A (dimer) and B (monomer) from the non-reduced γ-conglutin sample (lane 5; section 3.5.3.1) were analysed to identify proteins of interest using Mascot sequence matching software (Matrix Science) with MSPnr100 database (Table 3.13). The highest score was observed to match with γ-conglutin protein from *L. angustifolius* (Q42369) along with the presence of signature peptide VGFNSNSLK in the sequence list.

All the above MS/MS analysis results confirmed the identity of purified protein as γ-conglutin from *L. angustifolius* (Q42369).

Table 3.12 Summary of all the hit proteins generated by MS/MS ion search with matching peptide sequences obtained from tandem mass spectrometric analysis of purified γ-conglutin fraction. VGFNSNSLK peptide (indicated in red) is a signature tryptic peptide of γ-conglutin

Rank order	Accession	Score	Mol. Wt. (Da)	pH(I)	Coverage (%)	Matches	Sequences	Peptides sequence
1	**Q42369**	**2137**	**48885**	**7.66**	**35**	**88 (65)**	**12 (10)**	**HLVIPTK** **VGFNSNSLK** **ISGGAPSVDLILDK** **QGEYFIQVNAIR** **KISGGAPSVDLILDK** **TPLMQVPLLLDLNGK** **RTPLMQVPLLLDLNGK** **ISGGAPSVDLILDKNDAVWR** **AGIALGAHHLEENLVVFDLER** **YSTSNGAILFGDINDPNNNNYIHNSLDVLHDLVYTPLTISK**
2	OIW19056.1	699	11712	9.38	17	19 (18)	1 (1)	AAAANTPGLNPSNAGSLPGK
3	OIW13331.1	209	12957	9.49	25	6 (5)	3 (2)	YGAGGNYY ETAANIGASAK MNQAELDKLAAR
4	OIW13848.1	201	11872	9.07	50	10 (10)	5 (5)	LVLVASSK KLTSFELA GESQVVSGTNYR EIADFAVTEHNK NYQAVVYEKPWLHFK
5	OIW15434.1	195	46671	9.14	22	8 (7)	7 (6)	SIVPIASGR VLYDVPNSR LSEPAYVAVR QIIQSPTYIVR SSLYYVNLFAIR TTGTSTPPQGLLGLGR IVNIPPPALAFNPTTGAGTIFDSGTVFTR
6	OIW08851.1	127	13967	5.37	11	2 (2)	1 (1)	AVDVTGPDGANVQGSR

7	A0A061FK97	122	12375	9.34	46	7 (2)	5 (2)	ADLIAYLK NMAVNWEEK QGPNLNGLFGR TLYDYLLNPK QSGTTPGYSYSAANK LSGTTPGYSYSAANK
8	OIV97544.1	97	24667	8.79	7	1 (1)	1 (1)	DQYGNPIQLTDQYGNPVK
9	OIV98539.1	97	45201	6.72	17	6 (5)	6 (5)	VAVVLLNR MYVLKPIA ETADALVSTGLSK TFASWGIDYLK NSITANWDDIDIPTK TTGDINDSWESMITR
10	OIV89537.1	77	13479	9	24	2 (2)	2 (2)	VFASGNDQIR AGDLLIFNYDSTSHNVVAVDR
11	B9RG92	74	46284	9.46	2	1 (1)	1 (1)	SSLYYVNLMAIR
12	OIW00888.1	73	11670	9.26	10	1 (1)	1 (1)	ALVAAAQSTADK
13	OIV96297.1	72	60824	9.27	8	3 (2)	3 (2)	QYLGQQFYLR DQIGSFYYFPSLGFHK IPVPFPDPAGDYTILIGDWYK
14	OIW10115.1	68	19175	9.16	33	4 (2)	3 (2)	GPLGLVEQPPSR QLNLGLPVATVYFNSQK VTLTGNMDNLYTLVMTDPDAPSPSEPSHR

Table 3.13 Summary of all the hit proteins generated by MS/MS ion search with matching peptide sequences obtained from tandem mass spectrometric analysis of non-reduced γ-conglutin SDS-PAGE gel bands.

	Rank order	Accession	Score	Mol. Wt. (Da)	pH(I)	Coverage (%)	Matches	Sequences	Peptides sequence
Gel band A (Dimer)	**1**	**Q42369**	**88**	**48885**	**7.66**	**35**	**7 (6)**	**4 (3)**	**QFSVCLSR** **VGFNSNSLK** **AVGPFGLCYDSR** **QGEYFIQVNAIR**
	2	XP_014632490.1	57	23039	8.91	6	1 (1)	1 (1)	YPEWVVNIVSVPK
	3	A0A0Q3RAB4	28	101116	8.12	1	1 (1)	1 (1)	YGAGGNYY ETAANIGASAK MNQAELDKLAAR
Gel band B (monomer)	**1**	**Q42369**	**208**	**48885**	**7.66**	**23**	**14 (10)**	**13 (9)**	**HLVIPTK** **QFSVCLSR** **VGFNSNSLK** **SRVGFNSNSLK** **AVGPFGLCYDSR** **ISGGAPSVDLILDK** **VGFNSNSLKSYGK** **AVGPFGLCYDSRK** **QGEYFIQVNAIR** **KISGGAPSVDLILDK** **TPLMQVPLLLDLNGK** **VPQFLFSCAPSFLAQK** **ISGGAPSVDLILDKNDAVWR**
	2	XP_009385446.1	81	98155	5.63	2	2 (1)	2 (1)	VGFGVTIKK NMSSGATKDLAVR
	3	OIV90725.1	75	46437	9.16	2	1 (1)	1 (1)	DLSSSTPQYITK
	4	XP_014632490.1	67	23039	8.91	6	1 (1)	1 (1)	YPEWVVNIVSVPK

3.5.4 Proteolytic hydrolysis of extract and γ-conglutin protein

In order to evaluate the potential of lupin extract proteins and purified γ-conglutin as oral anti-diabetic agents, they were, initially, subjected to *in-vitro* gastrointestinal proteolytic hydrolysis condition and later the hydrolysates were used to carry out different bioactivity studies (chapter 4 and 5). For enzymatic hydrolysis, pepsin and pancreatin enzymes were added to the substrates - extract and γ-conglutin in consecutive stages. Pepsin is an endopeptidase that breaks the peptide bonds at non-terminal amino acids within the protein molecule resulting in the generation of relatively large peptides. It has maximum activity at acidic pH 1-3. Pancreatin, produced by exocrine cells of the pancreas, is a combination of digestive enzymes containing endopeptidase and exopeptidase that cleave the peptides into oligo, tri and dipeptides, and amino acids at neutral to slightly alkaline pH [158].

The protein concentrations of the extract and γ-conglutin were 2.19 ± 0.2 mg/ml and 4.8 ± 0.61 mg/ml respectively and were suitable substrates for hydrolysis. The DH for these substrates was determined by calculating free amino acids generated by pepsin and pancreatin enzymes during hydrolysis using a spectroscopic method with OPA reagent (Figure 3.16). Initially, a high rate of reaction was observed with pepsin in the first 90 minutes for extract and 30 minutes for γ-conglutin, thereafter, the proteolytic rate got stabilised. Being an endopeptidase pepsin cannot break down proteins into monomers (amino acids) resulting in low DH of 5.6% for extract and 3.4% for γ-conglutin. With further addition of pancreatin enzyme, the DH increased with time reaching to its plateau state after 450mins. Pancreatin is a mixture of trypsin, α-chymotrypsin, elastase, carboxypeptidase A and B. Trypsin has high specificity for lysine and arginine peptide bonds (except when they are bound to c-terminal proline) and chymotrypsin has specificity for tryptophan, tyrosine, leucine and phenylalanine bound to N-terminal [159, 160] leading to high DH. The extract contains a mixture of proteins (different conglutins) providing different substrate sites for proteolytic action of enzymes resulting in higher DH (22%) compared to γ-conglutin (18%).
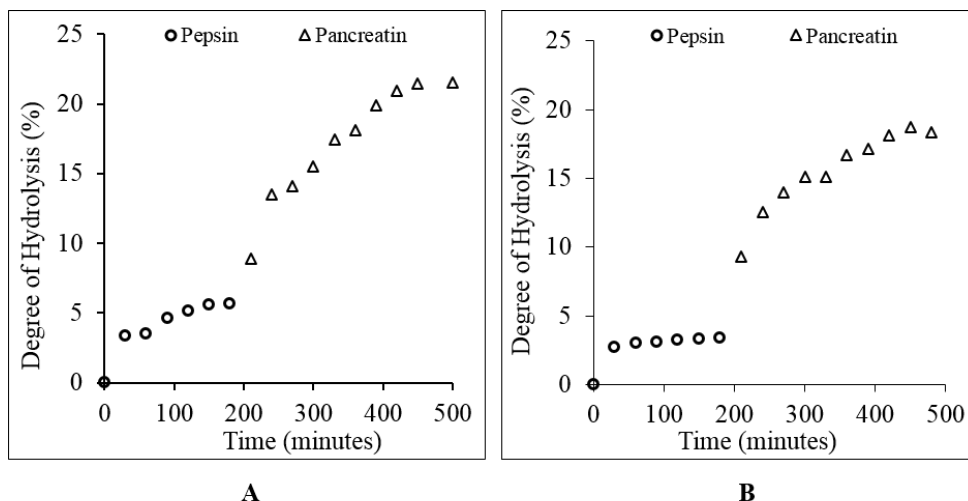
Figure 3.16 Degree of hydrolysis of extract (A) and γ-conglutin (B) by pepsin and pancreatin enzyme after every 30 minutes time interval from the starting point.

SDS-PAGE profile of the hydrolysate after every 60 minutes is shown in Figure 3.17. Enzymatic hydrolysis resulted in partial/complete degradation of high molecular weight proteins giving rise to low molecular weight proteins/peptides. It was observed that pepsin majorly hydrolysed the proteins into polypeptides with molecular weight ≤22KDa for extract and ≤30kDa for γ-conglutin, while pancreatin hydrolysed large peptides into small peptides (≤6.5KDa) except a peptide around 15KDa.
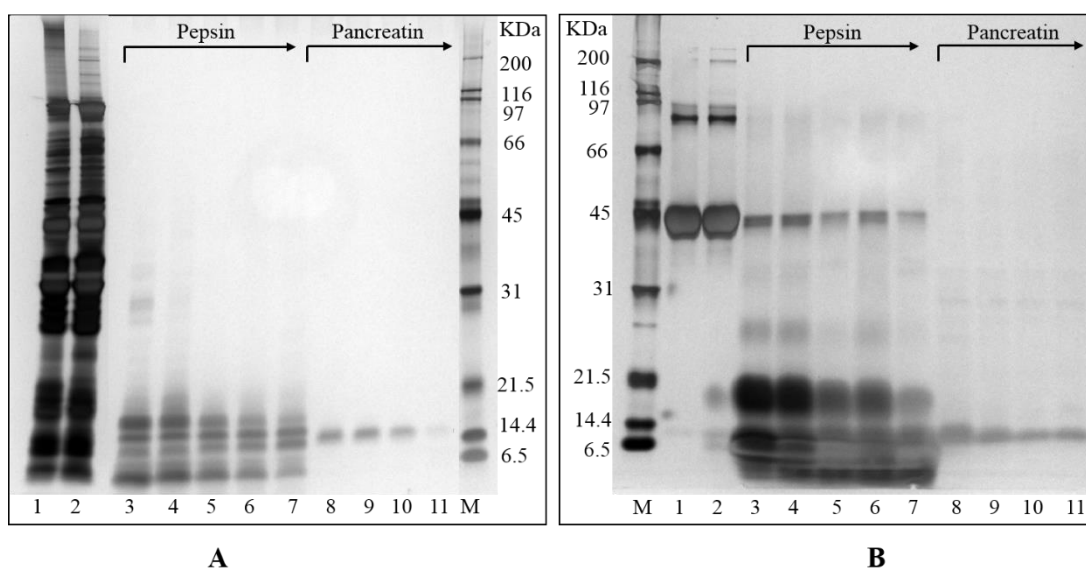
Figure 3.17 SDS-PAGE of extract (A) and γ-conglutin (B) hydrolysate at different time intervals. Extract/γ-conglutin (lane 1); extract/γ-conglutin at pH 2 before addition of pepsin (lane 2); hydrolysate collected after 30, 60, 120, 180, 240 mins of pepsin addition (lane 3, 4, 5, 6, 7 respectively); hydrolysate collected after 60, 120, 180, 240 mins of pancreatin addition (lane 8, 9, 10, 11 respectively)

To understand the detailed molecular weight size distribution of peptides ≤6.5KDa, SEC of both the substrates (extract and γ-conglutin) and final hydrolysates was performed. The substrate proteins were eluted at low retention time and the biomolecules in hydrolysate were eluted at higher retention times (Figure 3.18). The molecular weight distribution of hydrolysates (Table 3.14) revealed the presence of a mixture of peptides in the range of 12.7-0.6KDa peptides in extract and 8.4 to 0.6KDa peptides in γ-conglutin. Characterisation of these peptides is not in the scope of this research work as it would be a major project in itself.
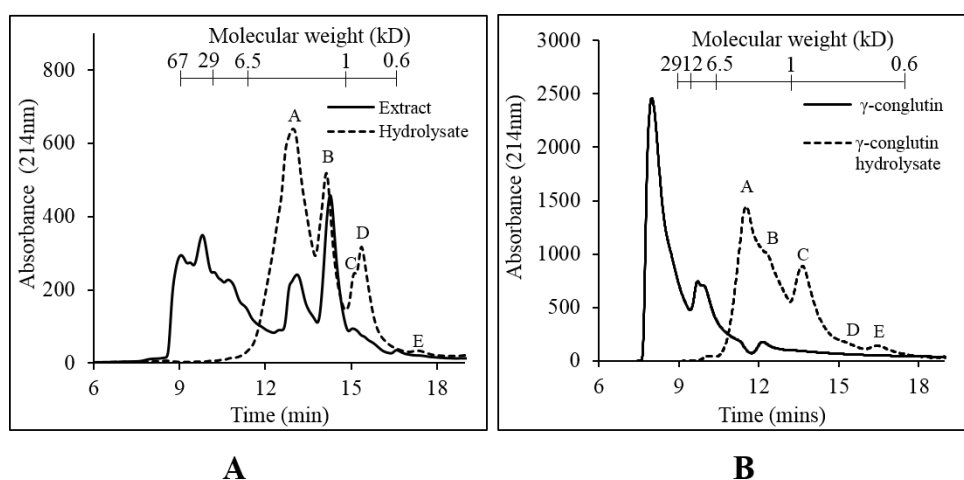
Figure 3.18 Size exclusion chromatogram of protein and hydrolysates of extract (A) and γ-conglutin (B)

Table 3.14 Molecular weight size distribution of extract and γ-conglutin hydrolysates

Sample peaks	Extract hydrolysate		γ-conglutin hydrolysate	
	Molecular weight range (KDa)	% AUC	Molecular weight range (KDa)	% AUC
A	12.7-2.3	55.90	8.4-3.6	41.52
B	2.3-1.2	23.06	3.6-2.2	23.86
C	1.2-0.9	4.81	2.2-1.0	26.01
D	0.9-0.6	13.43	1.0-0.6	4.42
E	<0.6	2.78	<0.6	4.18

In general, protein hydrolysates exhibit increased bioavailability as compared to their intact protein counterparts [161]. As a result, these bioactive compounds from natural sources are attracting interest for the development of nutraceuticals and functional

foods [162], however, investigation of the molecular mechanisms responsible for the bioactivity of these hydrolysates has been lacking up to this point.

3.6 CONCLUSION

This chapter summarises the extraction, purification, and characterisation of lupin protein, γ-conglutin. The extraction and purification of γ-conglutin from lupin proteins was previously optimised in our laboratory [39]. The protein content in purified γ-conglutin fraction was found to be ~95% (based on nitrogen element analysis). The main objective of this chapter was to increase the purity of γ-conglutin for studying its anti-diabetic action. In order to make the process faster and to improve the purity of eluted γ-conglutin the process was further developed by increasing the load volume on the column and modifying the elution gradient method. The identity of γ-conglutin in eluted fraction was confirmed by western blot and mass spectrometry analysis. The purity of eluted γ-conglutin fraction was found to be ~100% based on semi-quantitative SDS-PAGE analysis and ~95% based on RP-HPLC analysis. However, the process needs to be further developed to prevent loss of γ-conglutin in flowthrough and impurity fractions. This will improve the overall process yield.

To evaluate the anti-diabetic potential of extract proteins and γ-conglutin as an oral anti-diabetic agent, the proteins were digested by gastrointestinal proteolytic enzymes, pepsin and pancreatin. After hydrolysis, the extract and γ-conglutin hydrolysate consisted of peptides in the range of 12.7-0.6KDa and 8.4-0.6KDa respectively. The extract and γ-conglutin hydrolysates were evaluated for their anti-diabetic mechanism in different cell lines as explained further in chapter 4 and 5.

Chapter 4

Lupin seed hydrolysate promotes G-protein-coupled receptor, intracellular Ca^{2+} and enhanced glycolytic metabolism-mediated insulin secretion from BRIN-BD11 pancreatic β cells.

4.1 INTRODUCTION

Various studies have demonstrated the hypoglycaemic action of lupin seed preparations (bread, beverages) and lupin proteins (extract, isolates) when administered orally in animals and humans as discussed in chapter 2 [32-35, 90, 100, 101]. These constituents of lupin seeds (proteins, alkaloids, fibers) either stimulate insulin production from pancreatic β cells (insulinotropic action) or act like insulin to promote the entry of glucose in the peripheral tissues (insulin-mimetic action).

The current literature (chapter 2; section 2.3.2), majorly, attribute the hypoglycaemic action of lupin seed bioactives, particularly lupin proteins, to insulin-mimetic effects observed in fat, liver and muscle cells. Only a few studies demonstrate the insulinotropic action of lupin. In β cells, a white lupin seed extract, in the presence of glucose, promoted an increase in intracellular Ca^{2+} and a decrease in K$^+$ permeability resulting in a glucose-dependent insulinotropic effect [36]. Similarly, lupanine, an alkaloid extracted from *L. albus*, was reported to increase *Ins-1* gene expression (the gene encoding insulin) and potentiate glucose-stimulated insulin release by inhibition K-ATP channels [94]. These studies were focused on the underlying ionic mechanisms involved in inhibition of K-ATP channel and Ca^{2+} release from intracellular stores in islets and β cells. However, the effect of lupin extracts on energy metabolism, G-protein coupled receptor (GPCR) signal transduction and activation of secondary messenger systems in β cells have up to this point, not been studied. As a result, the

focus of this investigation was to study the acute effects of hydrolysed lupin extract on insulin secretion and the signalling pathways related to this effect in BRIN-BD11 β cells.

The extracts of *L. angustifolius* seeds were hydrolysed by digestive enzymes *in-vitro* to mimic oral gastrointestinal proteolytic digestive condition (chapter 3; section 3.5.4). In the present chapter, the hydrolysed lupin extract (lupin hydrolysate) was examined for its insulinotropic action in BRIN-BD11 pancreatic β cells. Also, the effect of hydrolysate on cellular glucose uptake and metabolism was studied. Further, different signalling pathways like K-ATP depolarisation and/or cyclic adenosine monophosphate (cAMP) - protein kinase A (PKA) and/or $G\alpha_q$ - phospholipase C (PLC) - protein kinase C (PKC) responsible for insulinotropic action of lupin hydrolysate were investigated and a summarised mechanism was presented.

4.2 CHEMICALS AND REAGENTS

All chemicals were obtained from Sigma Aldrich (Castle hill, NSW, Australia), unless indicated otherwise. BIM-46187, YM-254890, U-73122, and Go-6983 were obtained from Cayman Chemical (Ann Arbor, MI, USA). 'Any kDa' TGX precast polyacrylamide gels, Laemmli sample buffer (2X), Broad Range Marker protein standards and Clarity™ Western ECL substrate were purchased from Bio-Rad Laboratories Inc. (Hercules, CA, USA). Fluo-4, AM from Molecular probes (Eugene, Oregon, USA). Seahorse XF calibrant solution was acquired from Agilent Technologies Inc. (Santa Clara, CA, USA). Polyclonal goat anti-rabbit immunoglobulins/HRP from Dako (Glostrup, Denmark) and protease/phosphatase inhibitor cocktail (100X), cAMP regulatory element binding (48H2) rabbit mAb and phospho- cAMP regulatory element binding (Ser 133) (87G3) rabbit mAb were obtained from Cell Signaling Technology (Danvers, MA, USA).

4.3 EXPERIMENTAL METHODS

4.3.1 Preparation of lupin protein extract

Mature seeds of *L. angustifolius* (Coromup variety) were dehulled, milled, sieved and defatted according to the protocol described in section 3.3.1 and 3.3.2 (chapter 3). An efficient extraction process was previously optimized in the lab to achieve ~15% γ-conglutin enriched extract (w/w of kernel total proteins) [39]. In brief, the lupin proteins from defatted kernel flour was extracted in 10mM sodium acetate buffer, pH 4.0 (extraction buffer) in 1:30 (w/v) flour: buffer ratio on a magnetic stirrer (1000xg) for 30 minutes at room temperature. The extract was centrifuged at 4700xg for 20 minutes and the supernatant was later subjected to enzymatic hydrolysis.

4.3.2 Enzymatic hydrolysis of extract

In order to mimic gastrointestinal proteolytic digestion condition, lupin extract was hydrolysed using pepsin and pancreatic enzymes as described in section 3.3.5 (chapter 3). Hydrolysate generated from the hydrolysis of lupin extract is referred as 'lupin hydrolysate' in the text. The enzymes were inactivated by heating the hydrolysate at 100°C for 10 min. Alternatively, the enzymes and the high molecular weight proteins were separated from hydrolysate by ultrafiltration using 3kDa MWCO capsule membranes (Minimate Tangential Flow Filtration, Pall Corporation, East Hills, NY, USA).

4.3.3 Pancreatic β cell lines and culture conditions

BRIN-BD11 cells were cultured in RPMI-1640 medium (11.1mM glucose) supplemented with Foetal bovine serum (FBS) (10%), penicillin (100U/ml), streptomycin (0.1mg/ml), pH 7.4 in T75 sterile tissue culture flasks and incubated at 37°C in a humidified atmosphere of 5% CO_2 and 95% air. The cells were subcultured once in 3-4 days and the media was changed after 2-3 days. All the experiments using BRIN-BD11 were performed with passages 20-32.

INS-1E cells were a kind gift from Prof. Marco Falasca (School of Pharmacy and Biomedical Sciences, Curtin University, Western Australia). INS-1E cells were

cultured in RPMI-1640 medium (11.1mM glucose) supplemented with FBS (15%), penicillin (100U/ml), streptomycin (0.1mg/ml), sodium pyruvate (1mM), β-mercaptoethanol (50μM), HEPES (10mM) pH 7.4 in T75 sterile tissue culture flasks and incubated at 37°C in a humidified atmosphere of 5% CO_2 and 95% air. The cells were subcultured once in 3-4 days and the media was changed after every 48 hours. Cells with passage 11 to 15 were used for the experiments.

4.3.4 Cell viability assay

Cell viability assays can measure the metabolism, proliferation, and viability or death of cells. Cell viability of BRIN-BD11 cells in the presence and absence of hydrolysate was conducted according to Mosmann [163] which determines the activity of mitochondrial dehydrogenase enzymes. About 10,000 cells/well were seeded in a 96 well plate with the above media and incubated at 37°C overnight. Next day, the cells were incubated in the same conditions for 3, 6, 12 and 24 hours in presence and absence of hydrolysate (500 μg/ml, 200 μg/ml and 100 μg/ml) in media. Following the indicated incubation times, 20μl of MTT (3-(4,5-dimethylthiazol-2-yl)-2,5-diphenyl tetrazolium bromide) solution (5mg/ml; 20μl per 200μl medium) was added to all the wells and cells were incubated for additional 4 hours. MTT (yellow coloured) compound was taken up by cell and reduced to insoluble formazan crystals (purple coloured product) by mitochondrial succinate dehydrogenase enzyme in the cells. Then, the media from each well was removed and dimethylsulfoxide (DMSO) was added to dissolve the formazan crystals. The plate was shaken thoroughly and absorbance was measured at 570 nm using the Ensight Multimode plate reader (Perkin Elmer, Massachusetts, USA).

4.3.5 Acute insulin secretion *in-vitro*

BRIN-BD11 and INS-1E cells were seeded at a concentration of 20,000 cells/well in 96 well plates for overnight attachment prior to acute insulin secretion studies. Next day, cells were washed with Krebs Ringer bicarbonate buffer (KRBB) and pre-incubated with KRBB for 40 mins at 37°C. To ensure maximum inhibitory effect, inhibitors were incubated with the cells in pre-incubation step [164]. Cells were then incubated for 20 mins at 37°C with 100μl KRBB containing 1.1 - 20 mM glucose in the presence and absence of hydrolysate/stimulators/inhibitors. Insulin secretion in the

supernatant was quantified (μg/L) using ultrasensitive rat insulin enzyme-linked immunosorbent assay (ELISA) kit (Mercodia, Sweden). All the insulin secretion primary outcomes were first normalized to the total cell protein content (quantified by BCA analysis; section 3.4.1) and these values were then pooled from independent experiments and reported as fold change in insulin secretion with respect to 16.7mM glucose (control).

4.3.6 Provoking and defining the level of lipotoxicity in BRIN-BD11 cells

Palmitate, a saturated free fatty acid solution was prepared by dissolving palmitate in 0.1M NaOH for 30 mins at 70°C to achieve 100mM concentration. Palmitate (100mM) was conjugated with fatty acid-free BSA (10% w/v in water) by robust stirring for 4 hours at 60°C to produce 5mM BSA conjugated palmitate stock solution. The stock solution was filter sterilized and diluted in culture medium to achieve a final concentration of 100μM and 200μM. The control solution was prepared under the same condition (without palmitate) by adding 0.1M NaOH to fatty acid-free BSA solution. In order to establish lipotoxic condition, BRIN-BD11 cells (15,000 cells/well) were treated with BSA conjugated palmitate (100μM and 200μM) for 24 hours at 37°C in a humidified atmosphere of 5% CO_2 and 95% air. Similarly, the cells were treated with control solution (without palmitate). Next day, acute insulin secretion assay *in-vitro* (described in section 4.3.5) was performed.

4.3.7 Extracellular flux analysis

Extracellular flux analysis is a fluxomic technique to measure the rate of production and consumption of metabolites occurring in a cellular system. The XFe96 analyzer (Seahorse Biosciences, Massachusetts, USA) was used according to manufacturer's protocol to measure Extracellular Acidification Rate (ECAR) and Oxygen Consumption Rate (OCR) in the cells. On the previous day of analysis, BRIN-BD11 cells were seeded at a concentration of 20,000 cells/well in Seahorse 96 well assay plate (Agilent Technologies Inc., Santa Clara, CA, USA) and the cartridge was hydrated with Seahorse XF calibrant solution at 37°C in CO_2 free incubator for 24 hours. Next day, the assay plate was washed thrice with Dulbecco's modified Eagle's medium (DMEM; pH 7.4) containing sodium pyruvate (1mM), alanyl-glutamine

(2mM) with glucose (2.5mM) for mitochondrial stress test and without glucose for glycolytic stress test using XF Prep station (Seahorse Biosciences, Massachusetts, USA) and incubated in DMEM for 30minutes. The final concentration of the mitochondrial and glycolytic stress reagents (oligomycin (2µM), carbonilcyanide p-triflouromethoxyphenylhydrazone (FCCP) (0.3µM), rotenone (1µM), antimycin A (1µM), 2-deoxyglucose (100mM) were preloaded in assay plate delivery ports. The concentrations of these stress reagents were previously optimised in the lab for achieving optimal responses in BRIN-BD11 cells [165, 166]. The injection strategy for measuring glycolytic stress was (1) glucose, (2) hydrolysate/vehicle, (3) oligomycin, (4) 2-deoxyglucose and the strategy for mitochondrial stress was (1) hydrolysate/vehicle, (2) oligomycin, (3) FCCP, (4) rotenone and antimycin A. Following calibration of XF cartridge, the assay plate was inserted in XF^{e}96 analyzer and both ECAR and OCR were measured after every 4 minutes. Later, the measurements were normalised with total cell protein content in each well by BCA protein assay method (section 3.4.1; chapter 3). This normalisation was performed to eliminate cell number variation in data analysis. The data were analysed using software Wave Desktop 2.3.0. and following formulae were used for calculation of glycolysis and glycolytic capacity (mpH/min/mg/ml) [166].

Glycolysis = MAX (first measure after glucose injection through measurement prior to oligomycin injection) - measurement prior to glucose injection   …equation (4.1)

Glycolytic Capacity = MAX (first measurement after oligomycin injection through measurement prior to 2-deoxyglucose injection) - measurement prior to glucose injection   …equation (4.2)

4.3.8 Glucose uptake assay

2-NBDG (2-(N-(7-nitrobenz-2-oxa-1,3-diazol-4-yl) amino)-2-deoxyglucose) is a fluorescent glucose analog that allows a direct and sensitive measurement of glucose uptake or consumption in cells using flow cytometry technique. The glucose uptake in BRIN-BD11 cells procedure was according to Carlessi et al. [164]. On the day prior to analysis, 100,000 cells were seeded per well in 24 well plates. Next day, the cell plates were washed and replaced by glucose-free - DMEM media containing 20µM of

2-NBDG with and without hydrolysate. The control wells were treated in a similar manner but in the absence of 2-NBDG. The plate was incubated at 37°C for 30 minutes. Later, the cells were recovered by trypsinization, centrifuged and resuspended in cold phosphate buffer saline (PBS) containing 1µg/ml propidium iodide (PI) used for dead cell detection. The cell suspensions were maintained at cold temperature throughout the analysis. For each measurement 10,000 live cells events were recorded in FACS LSR Fortessa flow cytometer (BD Biosciences, Heidelberg, Germany). Forward scatter (FSC), side scatter (SSC) and 2-NBDG median fluorescence intensities were analysed using FlowLogic FCS analysis software (Inivai Technologies, Melbourne, Australia) after gating for singlet and PI negative (live) cells.

4.3.9 Western blot analysis of cAMP response element-binding protein (CREB) and phospho-CREB proteins

The BRIN-BD11 β cells were incubated in RPMI-1640 media in the presence and absence of hydrolysate (200µg/ml), forskolin (10µM) and H89 (5µM) for 20 minutes. The cells were lysed in radioimmunoprecipitation buffer (RIPA) containing 1% protease and phosphatase inhibitors cocktail followed by sonication and the total cell protein content was quantified using BCA assay method (section 3.4.1). Cell protein extracts were separated by SDS-PAGE and electrotransferred on nitrocellulose membrane (section 3.4.3 and 3.4.4; chapter 3). Later, membranes were blocked with 3% BSA for 60 minutes and incubated overnight at 4°C with the primary antibodies CREB (48H2) Rabbit mAb and phospho-CREB (Ser 133) (87G3) Rabbit mAb (1:1000 dilution in TBST containing 5% BSA). The membranes were washed and incubated in HRP conjugated secondary antibody for 60 minutes. The target bands were detected as discussed in section 3.4.4.

4.3.10 Measurement of intracellular Ca^{2+} fluctuations

Fluo-4 indicator exhibits large fluorescent intensities on binding to Ca^{2+} ions without any spectral shift. Fluo-4AM, a non-fluorescent acetoxy methyl ester, is cleaved intracellularly by cell esterase to give fluorescent Fluo-4 probe that measures intracellular Ca^{2+} concentration [167]. BRIN-BD11 cells (20,000 cells/well) were subcultured in black clear-bottom tissue culture grade 96 well plate. Cells were incubated at 37°C in a humidified atmosphere of 5% CO_2 and 95% air. Next day, media

was removed and the cells were washed with KRBB containing 1.1mM glucose. The cells were incubated in KRBB containing glucose (1.1mM) and Fluo-4AM (5μM) for 40 minutes at 37°C (dye loading step). The cells were washed twice with KRBB and incubated in KRBB with 1.1 mM glucose for 10 minutes. In this step, esterases inside the cells cleave the intracellular Fluo-4AM molecules into Fluo-4 (de-esterification step). Next, the cells were inserted into a temperature-controlled (37°C) multimode plate reader (Ensight, Perkin Elmer). The basal fluorescence from each well was recorded for 60 seconds by using appropriate wavelength settings (excitation at 494nm and emission at 516nm). Later, stimuli (hydrolysate / alanine (16.7mM) / KCl) were added and fluorescence was recorded each 8 seconds intervals for 400 seconds.

4.3.11 Statistical Analysis

All statistical analyses were performed using GraphPad Prism v.6.0 software. All variables were reported as mean ± standard deviation (SD). The datasets that satisfied normality following a Kolmogorov-Smirnov test were further analysed for statistical significance using t-test (when comparing two groups) and analysis of variance - ANOVA (when comparing three or more groups) with a Dunnett post-hoc test. The datasets that failed the normality test were analysed using the non-parametric Mann-Whitney test (when comparing two groups) and Kruskal Wallis test (when comparing three or more groups). P≤0.05 was considered statistically significant.

4.4 RESULTS AND DISCUSSIONS

The insulinomimetic action of biomolecules obtained from lupin seeds (proteins, peptides, alkaloids) has been studied in detail in various cell lines and animal models (discussed in chapter 2; section 2.3), but their insulinotropic properties remain largely unexplored. Several human studies using intestinal perfusion techniques have reported that protein hydrolysates consisting of short peptides and amino acids facilitate faster intestinal protein digestion and absorption rates as compared to intact proteins [168-171]. Potent insulinotropic effects were observed in pancreatic β cells when exposed to hydrolysates containing di-tri peptides and free amino acids [172-174]. Also, hydrolysates containing low molecular mass peptides derived from milk have been reported to induce insulin secretion and improve glucose homeostasis [175, 176].

Thus, at first, the primary objective was to develop an oral nutraceutical agent from a natural source for the treatment of type 2 diabetes. Accordingly, lupin seed extracts were hydrolysed in an *in-vitro* gastrointestinal proteolytic hydrolysis environment by using amylase, as well as pepsin and pancreatin protease enzymes (chapter 3; section 3.5.4). The studies in this chapter are focussed on the mechanisms of insulinotropic action of the bioactives present in the hydrolysate obtained from lupin seed extract.

4.4.1 Heat resistant lupin hydrolysate contents promoted insulin secretion without affecting cell viability.

4.4.1.1 Cell viability and insulin secretion

The insulinotropic action of the lupin hydrolysate in BRIN-BD11 rat insulin secreting β cells was substantiated. BRIN-BD11 is a derived cell line produced by electrofusion of a primary culture of rat pancreatic beta cells with rat insulinoma RINm5F β cells [177]. McClenaghan et al. have highlighted the importance of the BRIN-BD11 (β cells) cell model as a tool for discovery and characterisation of new and improved drugs in the management of diabetes [178]. This β cell model was used to explore the insulinotropic action of lupin hydrolysate. Cell viability of BRIN-BD11 β cells in the presence of the lupin hydrolysate was evaluated to determine if the hydrolysate resulted in any release of insulin by cell death. Cell viability remained unaltered in the presence of hydrolysate. The addition of hydrolysate to β cells only significantly ($p \leq 0.01$) impacted cell viability at the highest concentration of 500µg/ml after the longest incubation of 24 hours (88% cell viability) (Figure 4.1A) while at other concentrations and time durations no difference was observed compared to control. The acute exposure (20 minutes) of the cells to different concentrations of lupin hydrolysate in the presence of 16.7mM glucose demonstrated a dose-dependent stimulatory effect on insulin release (Figure 4.1B). Insulin secretory response of hydrolysate at 500µg/ml and 200µg/ml was observed to be greater than a combination of L-alanine (10mM) and 16.7mM glucose, a widely acknowledged potent and robust insulin secretagogue [179]. This revealed that lupin hydrolysate, even at lower concentration (200µg/ml), possessed strong insulinotropic properties. Also, prior exposure of cells to hydrolysate (200µg/ml) for 24 hours did not diminish the subsequent cellular response to L-alanine (10mM) (Figure 4.1C) providing evidence

that insulin secretory action of the hydrolysate was not due to adverse cellular effects. Thus, the lupin hydrolysate concentration of 200µg/ml was used for the remainder of the studies.
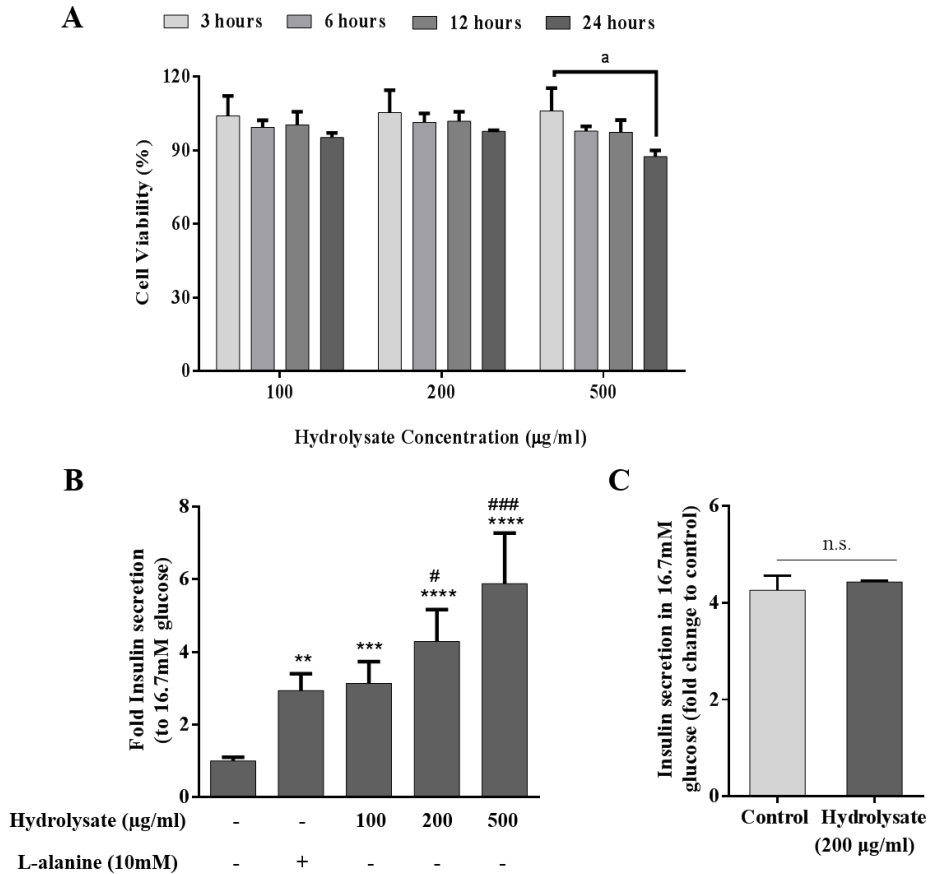
Figure 4.1 Cell viability and hydrolysate stimulated insulin secretion. (A) BRIN-BD11 cell viability at different hydrolysate concentrations after 3, 6, 12 and 24 hours. (B) Dose-dependent effect of the hydrolysate in (16.7mM glucose) on acute (20 minutes) insulin secretion from BRIN-BD11 cells. The response was compared with control (16.7mM glucose) and positive control (10mM L-alanine in 16.7mM glucose). Insulin secretion is reported as values normalised with control i.e. 16.7mM glucose. '+' and '-' indicates the presence and absence of hydrolysate/L-alanine in 16.7mM glucose. (C) Insulin secretion response of hydrolysate treated BRIN-BD11 cells to L-alanine (10mM) in 16.7mM glucose (Cells were initially treated with hydrolysate (200µg/ml in media) for 24 hours followed by incubation with L-alanine (10mM) in 16.7mM glucose). Values are mean ± standard deviation of three independent experiments; 'a' denotes significant difference ($p{\leq}0.01$) between cell viability on exposure to 500µg/ml hydrolysate for 24 hours and 3 hours. ****$p \leq0.0001$, ***$p \leq0.001$ and **$p \leq0.01$ are significantly different as compared to control. #$p \leq0.05$ and ###$p \leq0.001$ are significantly different compared to L-alanine (positive control).

4.4.1.2 Enzyme inactivation step after lupin hydrolysis

The effect of different enzyme (hydrolysate associated) inactivation methods on the insulinotropic action of lupin hydrolysate was performed. At the end of the lupin extract hydrolysis process, the enzymes were inactivated by either (a) heating the hydrolysate at 100°C for 10min or (b) removing the enzymes from the hydrolysate by ultrafiltration using 3kDa MWCO membrane. No significant difference was observed in acute insulin secretion using either of the enzyme deactivation/removal methods (Figure 4.2). The hydrolysate biomolecule(s) responsible for the enhancement of *in-vitro* insulin release were not destroyed by heat inactivation of the digestive enzymes. Moreover, molecules below 3kDa were found to be both biologically active and, importantly, possess a similar level of insulinotropic action compared to the unfiltered hydrolysate. This indicated that a combination of short peptides (≤ 30 amino acid residues), amino acids and other biomolecules might be responsible for the insulin release. Similar results have been obtained for whey protein hydrolysate in β cells, where peptides exhibited better insulinotropic activity as compared to proteins [175]. Further studies focused on the fractionation of hydrolysate into its constituents and characterization of the specific molecule(s) responsible for the insulinotropic actions are in progress. Hereafter, the heat inactivation method was adopted for enzyme inactivation at the end of the hydrolysis process.
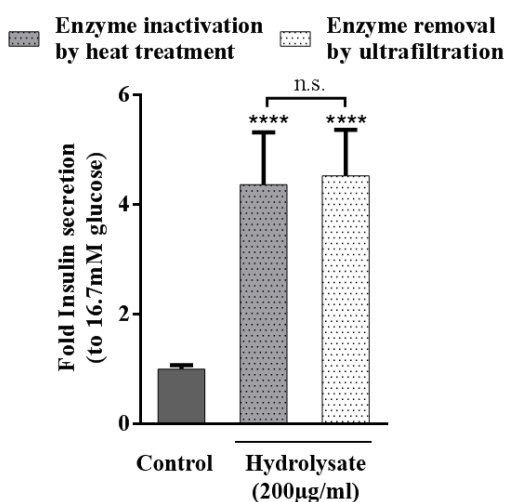
*Figure 4.2 Effect of enzyme inactivation by heat treatment and enzyme removal by ultrafiltration on insulinotropic action of hydrolysate in 16.7mM glucose. Insulin secretion is reported as values normalised with 16.7mM glucose (control). Values are mean ± standard deviation of three independent experiments; ****p ≤0.0001 is significantly different as compared to control (16.7mM glucose).*

4.4.1.3 Insulin secretory effect of lupin hydrolysate on palmitate stressed β cells

Diabetic patients are found to be present with high levels of circulating free fatty acids and lipotoxicity is a widely recognised inducer of β cell dysfunction [180]. Hence, the ability of the lupin hydrolysate to stimulate insulin secretion from BRIN-BD11 cells after a lipotoxic insult was determined. Lipotoxicity in BRIN-BD11 cells was established by incubating the cells with BSA conjugated palmitate (100μM and 200μM) for 24 hours. A significant difference ($p \leq 0.05$) in glucose-induced insulin secretion between control and palmitate-treated cells was observed, which evidenced the establishment of the lipotoxic insult (Figure 4.3A and 4.3B). Alanine (positive control) and hydrolysate, both, induced significantly higher insulin secretion as compared to glucose (16.7mM) alone in cells treated with 100μM or 200μM palmitate for 24 hours ($p \leq 0.0001$ and $p \leq 0.001$, respectively). Thus, lupin hydrolysate was able to improve insulin secretion function in a palmitate-induced lipotoxic β cell condition. This highlighted the fact that the hydrolysate may have the potential to exhibit its insulinotropic property even under a typical physiological environment frequently observed in type 2 diabetes patients.
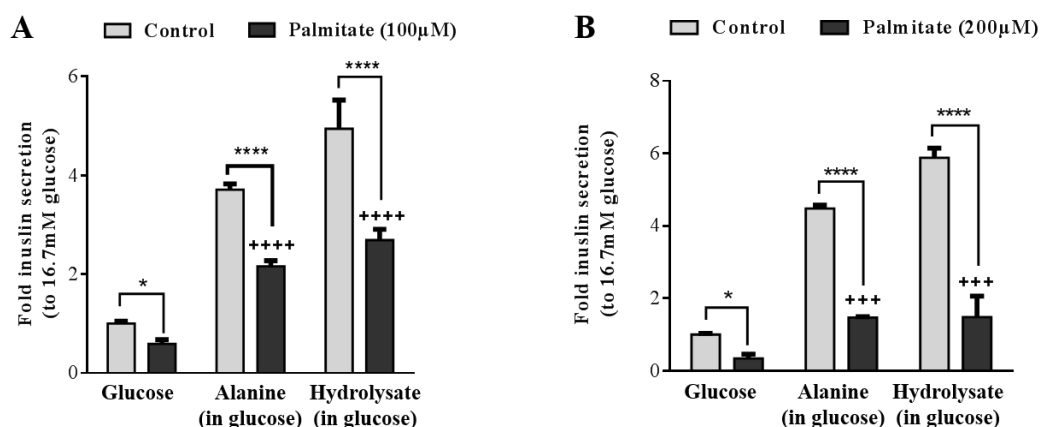
Figure 4.3 Effect of hydrolysate on insulin secretory response of palmitate stressed β cells. Acute (20 minutes) insulin secretion by 16.7mM glucose alone; 200μg/ml hydrolysate in 16.7mM glucose; and 10mM alanine in 16.7mM glucose on cells pre-incubated with palmitate (100μM and 200μM) or vehicle control for 24 hours. Insulin secretion is reported as values normalised with glucose (16.7mM) of control. Values are mean ± standard deviation of three independent experiments; ****p ≤0.0001 and *p ≤0.05 are significantly different as compared to control. ++++p ≤0.0001 and +++p ≤0.001 are significantly different as compared to insulin secretion in 16.7mM glucose palmitate pre-treated cells.

4.4.2 Insulin secretion by lupin hydrolysate was glucose-permissive and involved enhanced glucose metabolism.

4.4.2.1 Effects of glucose on hydrolysate-induced insulin secretion

Glucose-stimulated insulin secretion (GSIS) is impaired in type 2 diabetes [181]. Furthermore, modern antidiabetic agents such as incretin-mimetics promote insulin secretion in a glucose-dependent manner, consequently mitigating hypoglycaemic episodes during therapy [182]. INS-1E insulin secreting β cells are well differentiated clones of radiation induced rat insulinoma INS-1 cell lines [183]. Both BRIN-BD11 and INS-1E insulin secreting β cell lines are responsive to glucose [177,183]. As a result, studies were conducted to establish if the insulinotropic action of lupin hydrolysate was glucose dependent and/or permissive in these cell lines. Hydrolysate-induced insulin secretion was studied at 7 different glucose concentrations – 0, 1.1, 2.5, 5, 10, 16.7, 20mM in the presence and absence of hydrolysate (200μg/ml) in both BRIN-BD11 (Figure 4.4A) and INS-1E (Figure 4.4B) β cells. An increasing trend in insulin secretion with an increase in glucose concentrations was observed and hydrolysate exhibited maximal stimulatory effect at 16.7mM glucose compared to lower glucose concentrations in BRIN-BD11 cells. Hydrolysate also induced its insulin-releasing action in INS-1E cells at higher glucose concentrations (10-20mM). Since, the response of hydrolysate stimulated insulin secretion was higher in BRIN-BD11 cells compared to INS-1E cells, this cell model was used for further mechanistic studies. The present study indicated that the insulinotropic effect of hydrolysate is glucose permissive as glucose at increasing concentrations enhanced the insulin secretory action of hydrolysate in two independent β cell lines, BRIN-BD11 and INS-1E. As the hydrolysate also exhibited insulinotropic action at fasting physiological glucose concentrations (<5mM) in BRIN-BD11 cells, we concluded that, at least in this cell model, hydrolysate activity is not strictly glucose dependent, therefore there is a need for further *in-vivo* studies to assess the risk of occurrence of hypoglycaemic episodes upon hydrolysate administration. One of the limitations of this study was the direct determination of coupling factors generated upon exposure to the lupin hydrolysate was not accomplished. This would be a major project in itself. However,

the reported increase in glucose utilization was identified by an increase in glucose uptake and glycolytic flux in our cell model as explained in further section 4.4.2.2.
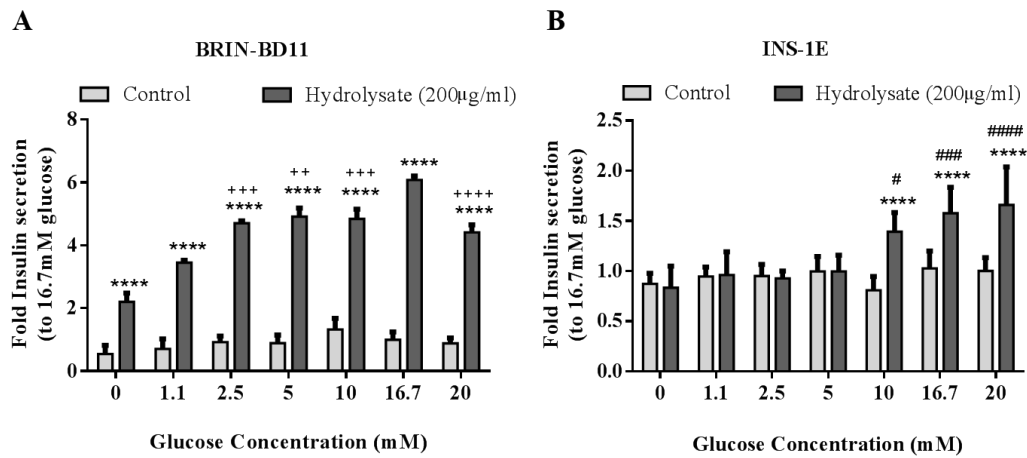
*Figure 4.4 Effect of glucose concentrations on hydrolysate (200μg/ml) induced insulin secretion. Acute (20minutes) levels of hydrolysate induced insulin secretion at 7 different glucose concentrations- 0, 1.1, 2.5, 5, 10, 16.7, 20mM in (A) BRIN-BD11 cells and (B) INS-1E cells. Insulin secretion is reported as the value normalised with the response obtained from control at 16.7mM glucose. Values are mean ± standard deviation of three or more independent experiments; ++++p ≤0.0001, +++p ≤0.001 and ++p≤0.01 are significantly different compared to hydrolysate at 16.7mM glucose in BRIN-BD11 cells; ####p ≤0.0001, ###p ≤0.001 and #p≤0.05 are significantly different compared to hydrolysate at 5mM glucose in INS-1E cells. ****p ≤0.0001 and ***p ≤0.001 are significantly different as compared to respective control.*

4.4.2.2 Glycolytic flux, mitochondrial respiration and glucose uptake in β cells

Since the lupin hydrolysate promoted maximum insulin secretion in the presence of glucose (16.7mM), effect of hydrolysate on glucose metabolism in β cells was investigated further. Glycolytic flux and mitochondrial respiration were assessed by measuring ECAR and OCR in β cells using the Seahorse XF^{e}96 flux analyser. Specific glycolytic and/or mitochondrial inhibitors were injected (as described in section 4.3.7) in the presence and absence of the hydrolysate. OCR was reported in units of pmol/minute and ECAR was reported in mpH/minute.

As observed in Figure 4.5A, at first, basal i.e. non-glucose derived ECAR in the cells was recorded. After the first injection of glucose, the ECAR value increased due to the breakdown of glucose to pyruvate by the glycolytic pathway, and further fermentation to lactic acid, which is promptly released by cells, increasing protons in the media and consequently contributing to a measurable enhancement in ECAR. Later, lupin

hydrolysate injection to the cells caused a substantial increase in ECAR values compared to the cells receiving vehicle injection. Addition of oligomycin A, a mitochondrial ATP synthase inhibitor, caused glycolytic machinery to function at its maximum capacity. Later, injection of 2-deoxyglucose, a glycolytic inhibitor [184], lowered down the ECAR values. The rate of glycolysis and glycolytic capacity values (calculated from equation (1) and (2) mentioned in section 4.3.7) were normalised with their respective vehicle values and the percentages were reported (Figure 4.5B and 4.5C). In spite of the prior 16.7mM glucose injection, lupin hydrolysate was still able to further increase glycolytic rates by approximately 21% ($p \leq 0.0001$) with no significant changes in glycolytic capacity. This suggests that the hydrolysate is capable of inducing an increase in the glycolytic flux and ultimate generation of coupling factors.

While monitoring OCR values (Figure 4.5D), at first, basal respiration corresponding to resting energetics of the cells were measured. Next, lupin hydrolysate was injected. No significant changes in OCR values were observed as compared to the cells receiving vehicle injection. This result suggests that excess pyruvate produced by enhanced glycolytic flux in response to hydrolysate exposure is entirely converted to lactate, since no measurable changes in mitochondrial respiration could be detected. Chao et al. demonstrated that primary rat islets do not express monocarboxylate transporter (MCT) isoforms on their plasma membrane and exhibited low lactate dehydrogenase activity, whereas, high levels of MCT1 were expressed in RINm5F cells (derived β cells) [185]. Thus, in islets, glycolysis is closely coupled to mitochondrial oxidation. Being a derived cell line, BRIN-BD11 cells likely express MCTs on their surface. Thus, it is hypothesized that lactate formed due to excess metabolism of glucose in the presence of hydrolysate was released through MCT in BRIN-BD11 cells, resulting in increased ECAR values. It is noteworthy to mention that previous studies demonstrated that BRIN-BD11 cells secreted lactate to the tissue culture media, and ECAR was a good surrogate for lactate secretion [186]. The fact that BRIN-BD11 cells present this metabolic leakage in the form of secreted lactate, in contrast to primary islets, also explained the absence of any changes in OCR in spite of increased glycolytic flux in this β cell model. Oligomycin injection lowered down the OCR values due to its action of inhibiting mitochondrial ATP synthase [183]. However, some respiration (OCR) still persisted in presence of oligomycin due to

proton leak across the mitochondrial membrane. Injection of FCCP (mitochondrial uncoupler) [187] stimulated the maximal respiration in the cells. This pattern mimics the energetic crisis arising in the cells when they have to rapidly oxidise their substrates in situations of metabolic stress. Finally, rotenone and antimycin A were injected simultaneously to the cells to determine non-mitochondrial oxygen consumption rates. Non-mitochondrial oxygen consumption is accomplished by certain cellular enzymes such as plasma membrane nicotinamide adenine dinucleotide phosphate reduced (NADPH) oxidase, cytochrome P450 and others [188].

Impaired glucose sensing ability of β cells due to a deficiency in expression of glucose transporters and/or reduction in glucose uptake can lead to β cell dysfunction which ultimately diminishes insulin secretion response [189, 190]. Thus, the next approach was to study glucose uptake rate in β cells using non-hydrolysable fluorescently labeled glucose analog 2-NBDG in a flow cytometer. In lupin hydrolysate treated cells, a significant increment of approximately 13% (p≤0.001) in 2-NBDG uptake rate was observed as compared to the vehicle control (Figure 4.5E). For the same acute treatment, no changes in cell size and complexity estimated by FSC and SSC analysis respectively were observed (Figure 4.5F). It has previously been reported that under normal physiological conditions, β cells do not store or metabolise glycogen [191]. In islets, glucose taken up by β cells is mainly directly metabolised by the glycolytic pathway and only 1-7% of the glucose flux is diverted to glycogen synthesis [191]. As the rate of glucose metabolism is directly proportional to the amount of insulin secreted [192], we believe that even small increases in glucose uptake (13%) and glycolytic flux (21%) promoted by lupin hydrolysate can lead to an increase in metabolic coupling factors (such as ATP/ADP) [193] thus, enhancing insulin secretion in β cells.
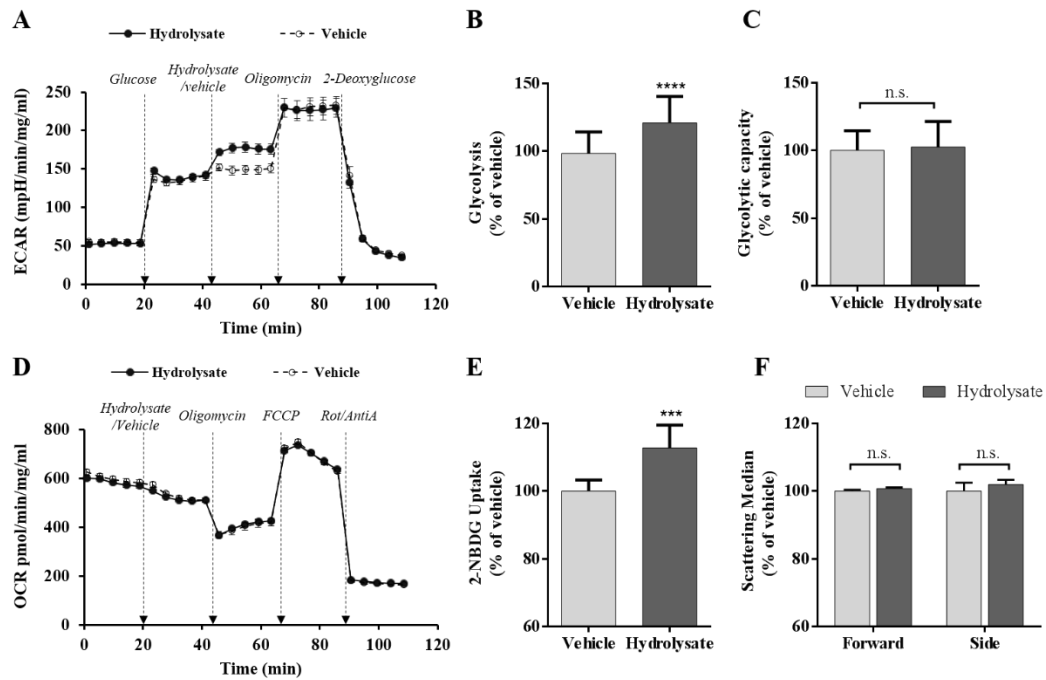
Figure 4.5 Effects of hydrolysate (200μg/ml) on cellular glycolytic flux, mitochondrial respiration and glucose uptake in BRIN-BD11. (A) Extracellular acidification rate (ECAR) values were monitored in BRIN-BD11 cells after sequential injections (indicated by dotted arrows) of glucose (16.7mM), hydrolysate (200μg/ml) or vehicle, oligomycin and 2-deoxyglucose. (B and C) Glycolysis and glycolytic capacity were calculated as discussed in methods. (D) Oxygen consumption rate (OCR) values were monitored with time after sequential injections (indicated by dotted arrows) of hydrolysate (200μg/ml) or vehicle, oligomycin, carbonylcyanide p-triflouromethoxyphenylhydrazone (FCCP) and rotenone (Rot) with antimycin A (Anti-A). (E) 2-(N-(7-nitrobenz-2-oxa-1,3-diazol-4-yl) amino)-2-deoxyglucose (2-NBDG) uptake in β cells in presence of hydrolysate (200μg/ml) and vehicle. (F) Forward and side scatter were analysed for the same treatments to evaluate changes in cellular size and complexity respectively. Values are mean ± standard deviation of three or more independent experiments. ****p ≤0.0001 and ***p ≤0.001 are significantly different as compared to respective control/vehicle.

To summarize, this dataset suggested that hydrolysate induced insulin secretion in a manner that is glucose permissive, however not entirely glucose-dependent, since insulin secretion was also observed at lower glucose concentrations, although at a lesser extent. Additionally, it promoted glucose metabolism by strikingly enhancing glucose uptake and glycolytic flux in β cells.

4.4.3 Lupin hydrolysate caused plasma membrane depolarization

Pancreatic β cells secrete insulin in 'glucose-dependent/stimulated insulin secretion' manner as explained in section 2.3 (chapter 2). In brief, the rise in blood glucose level leads to increased glucose uptake in pancreatic β cell. The intracellular glucose gets

metabolised increasing the level of ATP and other metabolies. Increase in the ATP:ADP ratio subsequently results in closure of K-ATP channels and membrane depolarisation which later triggers the opening of calcium channels, the upsurge of intracellular calcium ions and insulin exocytosis [84]. The classical K-ATP dependent insulin secretion, occurring in the initial phase of insulin release, is also accompanied by amplification processes mediated by glucose metabolic coupling factors (citrate, glyceraldehyde, NADH/NAD$^+$, adenine nucleotides, glutamate, 2-ketoisocaproate, malonyl CoA) [192, 193] and activation of secondary messengers like cAMP, inositol triphosphate (IP3), diacyl glycerol (DAG) and effectors like PKA and PKC enhancing insulin release [194]. However, insulin secretory mechanisms involving these regulatory and metabolic coupling factors are not completely established.

The insulinotropic action of lupin hydrolysate through K-ATP dependent membrane depolarisation pathway was investigated. First, the cells were incubated with an inhibitory concentration of K-ATP channel opener diazoxide (250µM) and maximum membrane depolarisation concentration of KCl (30mM) in the presence and absence of hydrolysate in 16.7mM glucose. Diazoxide opens K-ATP channels and acts as a blocker of membrane depolarisation [195]. As observed in Figure 4.6A, diazoxide strongly inhibited the insulin secretory action of hydrolysate, indicating that the hydrolysate likely operated through the canonical secretory pathway involving the closure of K-ATP channels and resulting in β cell membrane depolarisation [196, 197]. In addition, it has been reported that significant increases in glucose-mediated insulin secretion are observed even when K-ATP channels are kept open by diazoxide and membranes completely depolarised by a high concentration of K$^+$ ions [198]. A similar effect has also been observed in animals with knocked out sulphonyl urea receptor (a subunit in the K-ATP channel) in β cells, thus, supporting a key mechanism whereby glucose signalling occurs via a 'K-ATP independent pathway(s)' [194, 199, 200]. KCl, on the other hand, maximally depolarizes the cell membrane, resulting in potent insulin secretion even in the absence of metabolic stimulation. KCl depolarised cells treated with hydrolysate exhibited a significant increase in insulin secretion (Figure 4.6B; p≤0.01) compared to cells treated only with KCl. This suggested that hydrolysate was also capable of influencing the insulin secretion by interacting with other cellular components that lie distal to the K-ATP channel and are independent of membrane depolarisation pathway. Similar insulin secretion findings were also reported from the

natural bioactives in *Ocimum Sanctum* leaf extract [201] and *Asparagus racemosus* root extract [202].

*Figure 4.6 Effect of hydrolysate (200µg/ml) on acute (20 minutes) insulin secretion from BRIN-BD11 cells in presence and absence of K-ATP membrane depolarisation stimulators and inhibitors (A) diazoxide (250µM) – ATP sensitive K^+ (K-ATP) channel opener (B) KCl (30mM) - membrane depolarizing agent. The control refers to 16.7mM glucose. '+' and '-' indicates the presence and absence of hydrolysate/stimulator/inhibitor in 16.7mM glucose. The values are normalised with 16.7mM glucose and are mean ± standard deviation of three or more independent experiments; n.s. = non-significant; ***p ≤0.001, **p ≤0.01 and *p ≤0.05.*

4.4.4 Insulinotropic action of lupin hydrolysate was not mediated via cAMP/PKA pathway.

As lupin hydrolysate exhibited potent insulin release similar to incretin hormones such as GLP-1 [182], further studies were conducted to determine if any peptide and/or other biomolecules in the lupin hydrolysate activated the cAMP/PKA pathway (the canonical signalling module mediating GLP-1 action) [203]. GLP-1, an incretin hormone secreted from L-cells of the intestine, induces insulin secretion in the presence of glucose after binding to its receptor, a $G\alpha_s$ protein coupled receptor (GLP-1R) [204, 205]. Binding of GLP-1 activates the $G\alpha_s$ subunit of GLP-1R, which subsequently elicits adenylate cyclase (AC) activity and increases cAMP levels in β cells [182]. A prominent second messenger in insulin secretion signalling pathways, cAMP, mediates its action through its effectors PKA and EPAC2 (exchange protein directly activated by cAMP 2) that trigger insulin secretion via different mechanisms [198, 206, 207]. This includes activation of the K-ATP channel, deactivation of voltage-dependent K^+ channel (K_v), elevation in intracellular Ca^{2+} levels, thus, increasing the number of insulin secretory vesicles in the readily reserve pool in β cell [208-213].

Forskolin, an AC activator, promotes a rise in cellular cAMP levels by accelerating the conversion of ATP into cAMP [214]. Significant differences in the response of cells treated with forskolin (10µM) in the presence and absence of hydrolysate (Figure 4.7A; p≤0.01) were observed. This indicated that the hydrolysate-induced insulin secretion also involved stimulation of different signalling pathways activated by secondary messengers other than cAMP. Further, the involvement of PKA in the insulinotropic mechanism of hydrolysate was also verified. Since its discovery, PKA inhibitor - H89 [215] has been extensively used to evaluate the role of PKA in different cellular mechanisms of hepatocytes [216], smooth muscle [217], heart muscle [218], osteoblasts [219], neuronal tissue [220] and many more [221, 222]. The insulinotropic action of hydrolysate was not diminished in the presence of H89 (5µM), suggesting that PKA activity was not necessary for the insulinotropic actions of the hydrolysate (Figure 4.7B; p≤0.001). In the cAMP/PKA signalling pathway, the downstream protein CREB is mainly phosphorylated by PKA at a particular site (serine133), which further binds to cAMP response elements (CRE) in the DNA to regulate transcription of target genes involved in various cellular processes including proliferation, survival and insulin secretion [223]. Immunoblot analysis further revealed that the hydrolysate was not able to induce phosphorylation of CREB at serine 133 (Figure 4.7C), whereas the positive control, forskolin, promptly elicited extensive phosphorylation at this regulatory site. The latest validated that hydrolysate treatment did not activate PKA in β cells. Altogether, these results suggested that cAMP/PKA pathway, a well-known signalling axis in insulin secretion, is not involved in hydrolysate-induced insulin secretion.

Since hydrolysate-stimulated insulin secretion was glucose permissive, its operation through a well-known glucose-dependent insulin secretion potentiator - GLP-1 receptor, was also examined. Cells were exposed to GLP-1 analog, exendin-4, and hydrolysate in the presence and absence of the GLP-1R antagonist, exendin 9-39. As expected, exendin 9-39 (1µM) inhibited the stimulatory effect of the exendin-4 (0.01µM) (p≤0.001) but had no effect on the insulinotropic action of hydrolysate (Figure 4.7D). Moreover, it has been shown that the prolonged stimulation of GLP-1R (18 hours) with exendin 4 reprogrammed cellular bioenergetics, promoted GSIS and increased insulin secretion in β cells [164]. However, when β cells were exposed to hydrolysate for 24 hours, no significant increase in insulin secretion was observed,

compared to the vehicle control (Figure 4.7E) Thus, it can be concluded that the bioactive molecules in the hydrolysate do not activate GLP-1R in β cells.

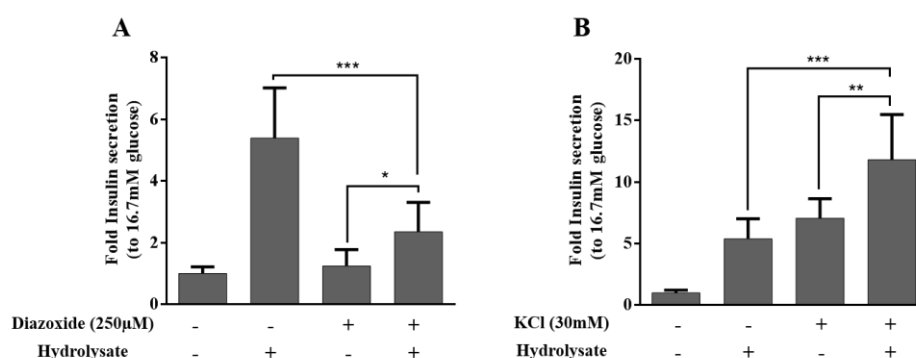*Figure 4.7 Effect of hydrolysate (200μg/ml) on acute (20 minutes) insulin secretion from BRIN-BD11 cells in presence and absence of GLP-1/cAMP/PKA pathway stimulators and inhibitors (A) forskolin (10μM) – adenylate cyclase (AC) stimulator (B) H89 (5μM) – protein kinase A (PKA) inhibitor (D) Exendin 9-39 (1μM) – glucagon-like protein 1 receptor (GLP-1R) inhibitor and Exendin 4 (0.01μM) - GLP-1R agonist. The control refers to 16.7mM glucose. '+' and '-' indicates the presence and absence of hydrolysate/stimulator/inhibitor in 16.7mM glucose. The values are normalised with 16.7mM glucose and are mean ± standard deviation of three or more independent experiments; n.s. = non-significant; ****p≤0.0001, ***p ≤0.001, **p ≤0.01 and *p ≤0.05. (C) Immunoblots of phosphorylated cAMP regulatory element binding (CREB) protein and total CREB proteins in cell extract and ratio of their band*

intensity (phosphorylated CREB/total CREB) in presence and absence of hydrolysate (200μg/ml), forskolin (10μM) and H89 (5μM). Immunoblot protein bands shown are representative of 2 independent experiments. (E) Insulin secretory response of BRIN-BD11 cells to hydrolysate and control (media) incubated for 24 hours. Values are mean ± standard deviation of two independent experiments each performed in duplicates; n.s.= non-significant.

4.4.5 Lupin hydrolysate activated Gα$_q$ protein signal transduction, PLC/PKC pathway and increased intracellular Ca^{2+} levels.

In β cells, GPCR signalling through Gα$_s$ and Gα$_q$ subunit isoforms stimulate insulin secretion and Gα$_i$ inhibits insulin release [224]. Different neurotransmitters and neuropeptides such as acetylcholine [225], cholecystokinin [226], arginine vasopressin [227], and endothelin [228] play an important role in regulation of insulin secretion from pancreatic β cells [229, 230]. These neurotransmitters and neuropeptides mediate their action through the Gα$_q$ family of heterotrimeric G proteins which are ubiquitously expressed on the surface of the β cell. The next step was to examine the role of Gα$_q$ protein-coupled receptor in insulinotropic action of lupin hydrolysate. YM-254890 and BIM-46187, inhibitors of heterotrimeric Gα$_q$ proteins, prevent the activation of Gα$_q$ subunit by blocking the guanosine diphosphate (GDP) / guanosine triphosphate (GTP) exchange reaction at the subunit. During the process of GDP/GTP exchange, YM-254890 inhibits GDP release from Gα$_q$ protein and BIM-46187 inhibits GTP entry by trapping Gα$_q$ in empty pocket conformation [231, 232]. BIM46187 (10μM) and YM-254890 (1μM) significantly diminished the insulin secretory response of the hydrolysate (Figure 4.8A and 4.8B; p≤0.0001), thus highlighting the association of a Gα$_q$ mediated signal transduction pathway in the insulinotropic action of the hydrolysate.

A variety of Gα$_q$ protein-coupled receptors potentiate insulin secretion via generation of secondary messengers and effectors. Gα$_q$ protein activates the membrane-associated enzyme PLC. PLC, upon activation, cleaves phosphatidylinositol 4,5 biphosphate (PIP2) into IP3 and DAG which together act as secondary messengers in the regulation of insulin secretion [233]. IP3 diffuses through the cytoplasm and binds to IP$_3$ regulated Ca^{2+} channels on the surface of endoplasmic reticulum, triggering the release of intracellular Ca^{2+} ions whereas DAG in the plasma membrane activates PKC [233]. The involvement of various PKC isoforms in the phosphorylation of downstream protein substrates and in regulation of PLC generated intracellular Ca^{2+} ions has been

reported to be important for insulin secretion [234-237]. Since, $G\alpha_q$ protein activates PLC enzyme, hydrolysate induced insulin secretion was examined in presence of PLC inhibitor U-73122 [238]. The insulin secretion evoked by hydrolysate was inhibited by U-73122 at 20µM, while at 40µM complete inhibition was observed (Figure 4.8C). This further confirmed activation of PLC by the hydrolysate via the $G\alpha_q$ pathway. Moreover, a decrease in hydrolysate induced insulin secretion by a PKC inhibitor, Go-6983 (50µM) [239], was also noticed (Figure 4.8D). From the above results, it was evident that activation of PLC-PKC pathway was one of the responsible mechanisms for insulinotropic action of hydrolysate.

Ultimately, we measured changes in intracellular Ca^{2+} occurring downstream of the proposed $G\alpha_q$/PLC/PKC pathway activated by lupin hydrolysate in β cells. Intracellular Ca^{2+} fluctuations were measured using the fluorescent probe Fluo-4AM in response to acute addition of hydrolysate or other known insulin secretagogues (alanine and KCl) as positive controls. A sharp increase in fluorescence was detected after addition of the hydrolysate or secretagogues, which was significantly higher than the response to glucose 16.7mM (control) alone (Figure 4.8E). Moreover, this increase in response to the hydrolysate was equivalent and slightly superior to the response by alanine, a widely recognised positive stimulant of insulin secretion. KCl induced the most potent intracellular calcium response, as extracellular K^+ ions caused maximum depolarisation of the β cell membrane, leading to an influx of extracellular Ca^{2+} and, consequently, Ca^{2+}-induced Ca^{2+} release from intracellular stores. Figure 4.8F described the quantification of stimuli dependent release of intracellular Ca^{2+} (over 400 seconds) represented as the area under the curves (normalised with respect to glucose 16.7 mM alone - control). Both hydrolysate and KCl significantly (p≤0.01 and p≤0.0001, respectively) induced Fluo-4AM fluorescence more potently than glucose (16.7mM) alone.

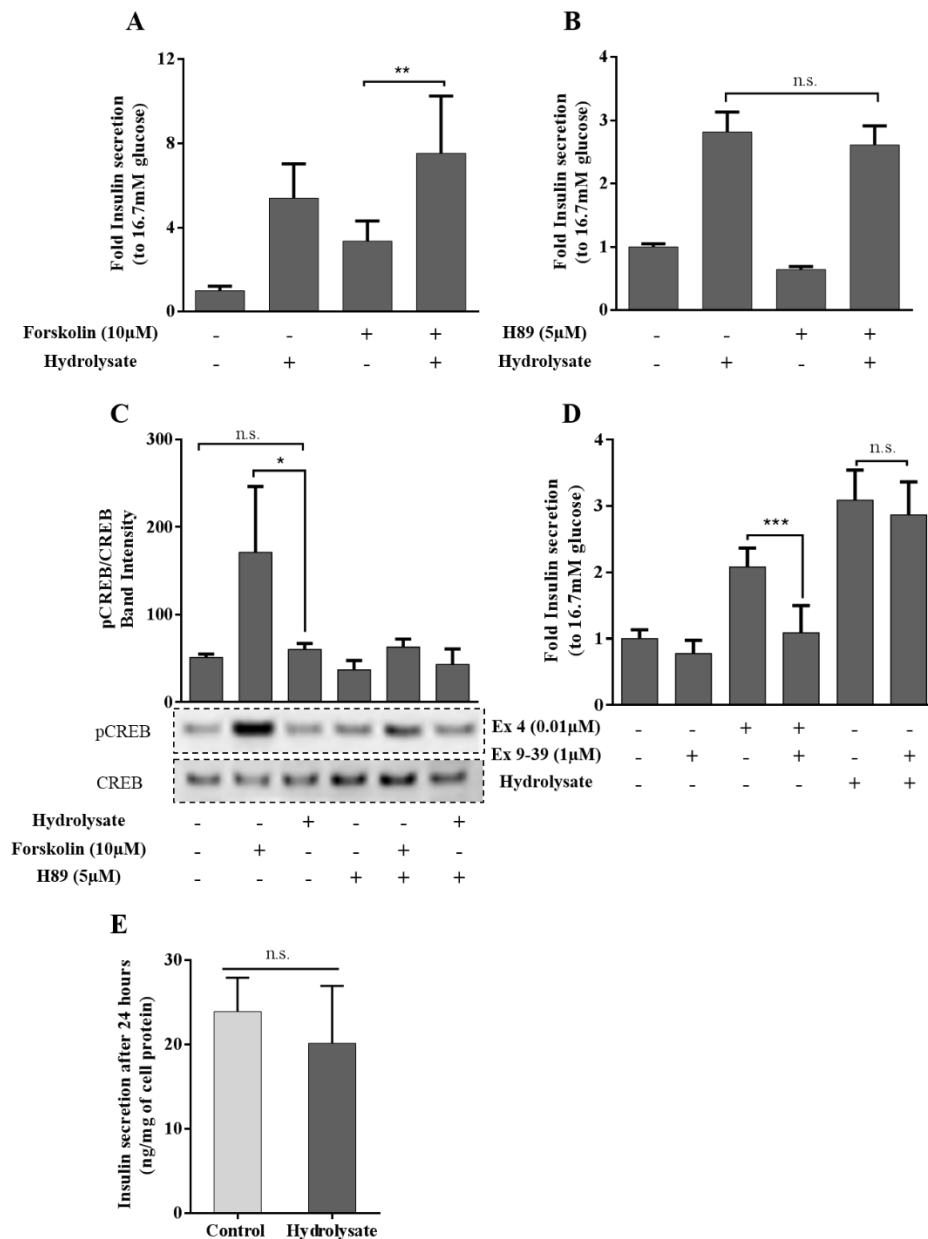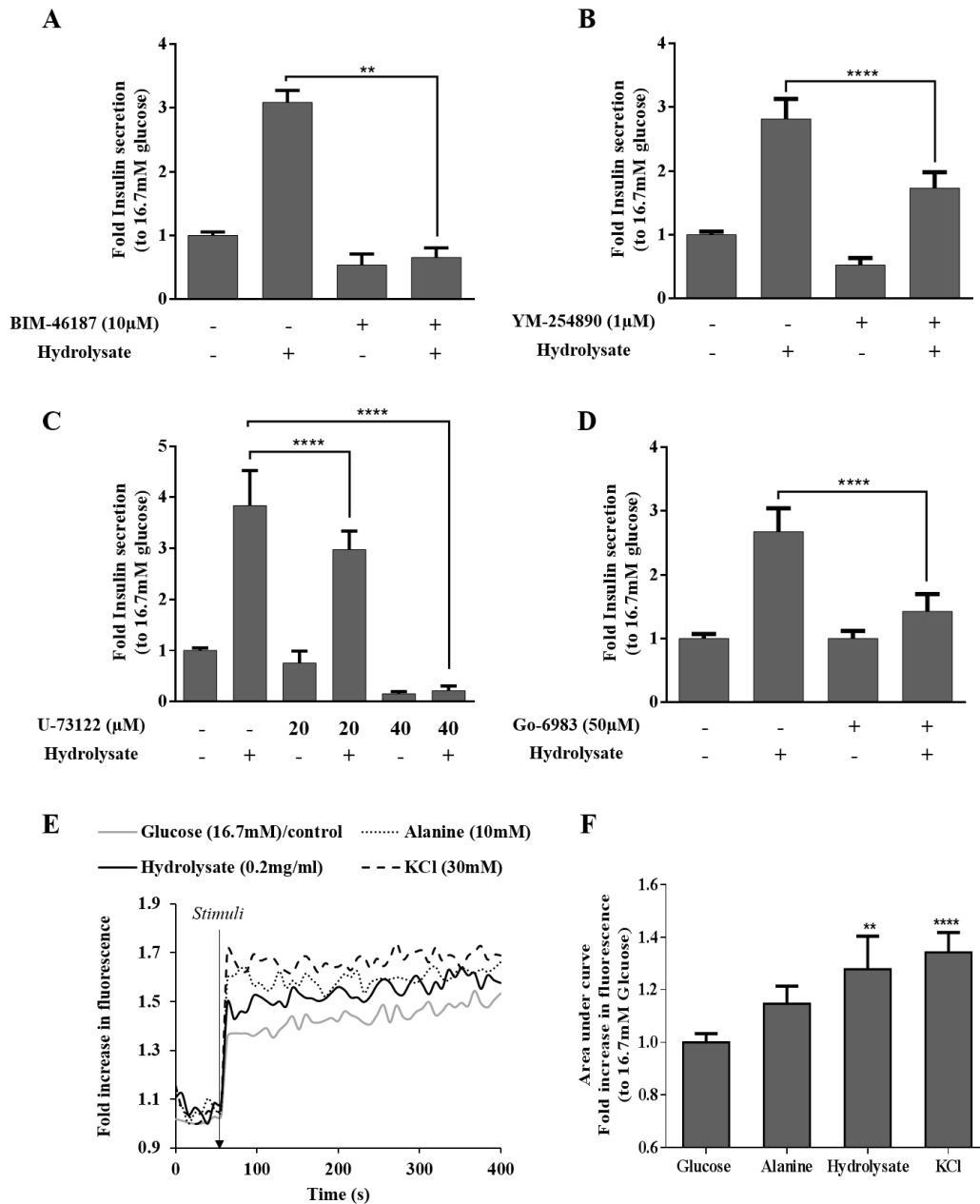*Figure 4.8 Effect of hydrolysate (200µg/ml) on acute (20minutes) insulin secretion from BRIN-BD11 cells in the presence of Gαq/PLC/PKC pathway inhibitors and on intracellular Ca2+ levels. Insulin secretion following exposure to (A) BIM-46187 (10µM) - Gαq inhibitor, (B) YM-254890 (1µM) - Gαq inhibitor, (C) U-73122 – PLC inhibitor, (D) Go-6983 (50µM) – PKC inhibitor. (E) Representative recordings exhibiting an increase in fluorescence upon stimulation of Fluo-4AM loaded cells with 16.7mM glucose alone or 16.7mM glucose + different stimuli as indicated. Fluorescence signals were normalized to basal 1.1mM glucose conditions before addition of stimuli. (F) Quantification of total intracellular Ca^{2+} during 400s represented as area under curves (normalised to 16.7mM glucose control). All values are mean ± SD of three or more independent experiments; n.s. = non-significant; ****p≤0.0001, ***p≤0.001 and **p≤0.01 are significantly different as compared to control (glucose 16.7mM).*

Overall, these studies indicated that the stimulatory action of the lupin hydrolysate operated through a $G\alpha_q$ mediated signal transduction which mostly required signalling via the PLC-PKC pathway and increased downstream intracellular Ca^{2+} levels, ultimately promoting insulin exocytosis. Various $G\alpha_q$ protein receptors – GPR40, GPR43, GPR54, GPR120 (short chain and long chain fatty acid receptors), M3 (muscarinic receptor), CCKAR (cholecystokinin receptor), HTR2B (serotonin receptor) expressed by islet β cells are known to stimulate insulin secretion [240-242]. All the above results are limited to two different well established pancreatic β cell models, BRIN-BD11 and INS-1E, used for cell signalling studies. As a result, the outcomes in this chapter further needs to be validated on rodent or human origin pancreatic β cells. Future research aiming at identifying specific bioactive peptides from the hydrolysate, as well as binding to $G\alpha_q$ protein receptors in β cells, will further enable deeper mechanistic insight into the observed hydrolysate stimulated insulin secretion.

4.5 CONCLUSION

Based on our results reported herein, insulinotropic mechanism of action of lupin hydrolysate in β cells was proposed (Figure 6). It is concluded that the insulinotropic action of lupin hydrolysate was glucose permissive and activated $G\alpha_q$ subunit of GPCR that stimulated signalling through the PLC/PKC pathway and not the cAMP/PKA pathway (A); involved increase in glucose uptake leading to enhanced glycolytic flux (B); promoted closure of K-ATP channels triggering cell membrane depolarisation, influx of extracellular Ca^{2+}, and insulin exocytosis (C). We demonstrated that the proposed pathways either directly or indirectly increased intracellular Ca^{2+}, widely reported to ultimately drive the fusion of insulin granules with the plasma membrane in β cells. The worldwide success of established GLP-1 therapeutics for diabetes treatment has brought to attention the possibility of targeting other GPCRs mediated through $G\alpha_s$ and $G\alpha_q$ in pancreatic β cells [243-245]. To date, the mechanisms previously identified as mediating the insulinotropic action of lupin seed extracts was focused only on the membrane depolarisation pathway [36, 37]. In the growing field of GPCR research, this study, for the first time, has opened the possibility of a new mechanism to explain the insulin secretory action of lupin hydrolysate via a GPCR

mediated signal transduction mechanism (Gα$_q$/PLC/PKC pathway). This strengthens the notion that lupin hydrolysates can improve glucose homeostasis in type 2 diabetic patients or glucose intolerant individuals, by increasing insulin secretion, thus leading to better glucose management and representing a new source of the potential oral therapeutic agent(s).
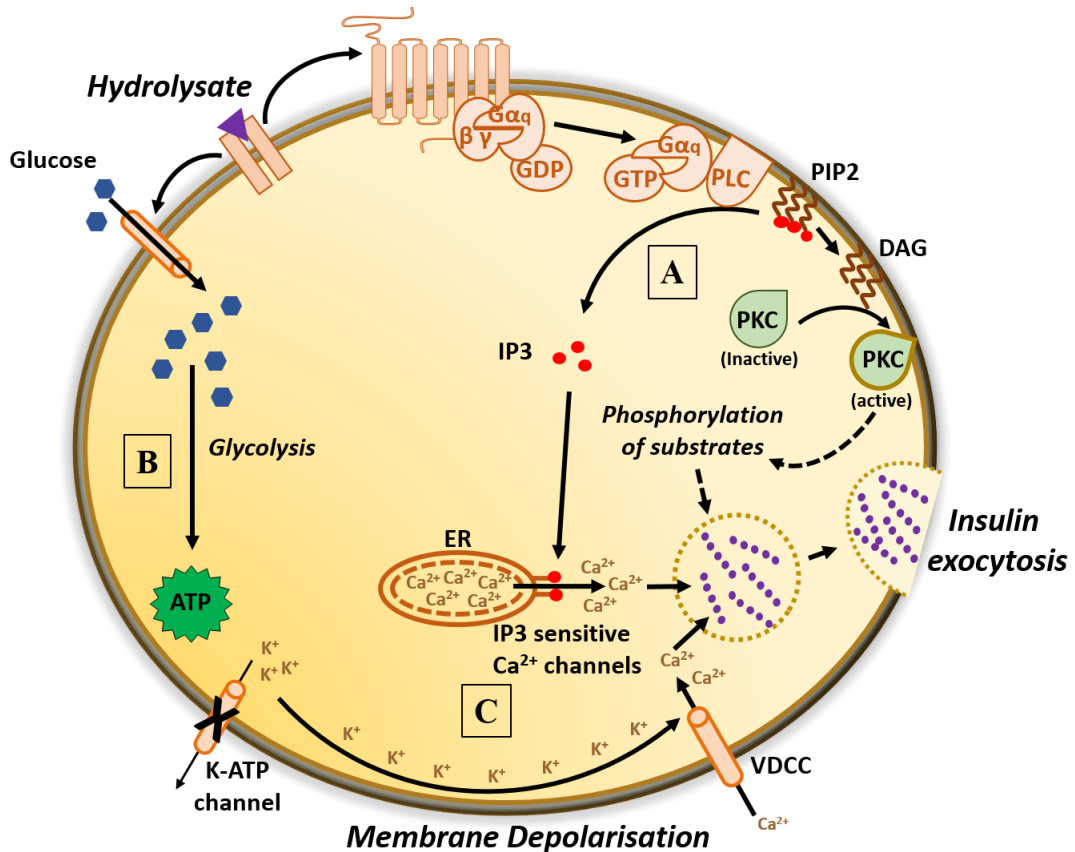
Figure 4.9 Hypothesized insulinotropic mechanism of action of lupin hydrolysate in BRIN-BD11 cell: (A) Hydrolysate activates Gα$_q$ subunit of G protein coupled receptor which further stimulates membrane associated phospholipase C (PLC) enzyme. PLC hydrolyses phosphatidylinositol 4,5-bisphosphate (PIP2) into secondary messengers inositol triphosphate (IP3) and diacyl glycerol (DAG). Further, DAG located in plasma membrane activates protein kinase C (PKC) resulting in translocation of PKC from the cytosol to the plasma membrane. PKC promotes phosphorylation of downstream proteins required for insulin exocytosis. IP3 diffuses through the cytosol and binds to IP3 sensitive Ca^{2+} channels on the surface of endoplasmic reticulum (ER) causing release of intracellular Ca^{2+} (B) Hydrolysate induces insulin secretion in glucose permissive manner with increase in glucose uptake and glycolytic rate and (C) promotes closure of ATP sensitive K$^+$ channel (K-ATP) triggering cell membrane depolarisation leading to influx of extracellular Ca^{2+} from voltage dependent Ca^{2+} channels (VDCC) and insulin exocytosis.

Chapter 5

In-vitro anti-diabetic mechanistic action of a lupin protein, γ-conglutin

Information in this chapter will be published in the paper:

Tapadia, M., Carlessi, R., Johnson, S., Utikar, R., & Newsholme, P. (2019). 'Anti-diabetic action of γ-conglutin peptides.' Possible Journal for submission: Food and Function. (To be submitted)

5.1 INTRODUCTION

Various clinical studies report γ-conglutin protein to be responsible for the glucose modulatory action of lupin seeds (section 2.3.2.1; chapter 2). γ-conglutin enriched preparations exhibited glucose-lowering effects in animal and humans [101]. Similarly, γ-conglutin enriched pasta significantly decreased serum glucose concentration upon glucose overload trials in rats [31]. Administration of this protein (1 week) to neonatal streptozotocin-induced type 2 diabetic rat models decreased glucose level and increased insulin level in serum and increased *Ins-1* gene expression and insulin content in the pancreatic β cell [102]. Also, in type 2 diabetic rat model, γ-conglutin modified gene expressions of enzymes *in-vivo* resulting in decreased hepatic glucose production [109]. All these animal studies indicate the beneficial effect of γ-conglutin on hyperglycaemia in diabetes.

The possible mechanisms responsible for hypoglycaemic action of γ-conglutin was reported in liver, muscle and fat cell models (section 2.3.2.1; chapter 2). In chapter 4, it was shown that lupin extract hydrolysate induced insulin secretion in pancreatic β cell models (BRIN-BD11 and INS-1E). Lupin hydrolysate stimulated insulin secretion via Gα$_q$ protein signal transduction (Gα$_q$/PLC/PKC pathway) in β cells [246]. However, it was not established if lupin γ-conglutin was typically responsible for the insulin secretion action. Moreover, no report has specified the insulin secretion property of γ-conglutin in literature and, thus, the first objectives of this chapter was to investigate its insulinotropic action in pancreatic β cells.

Similar to insulin, γ-conglutin was reported to activate intracellular kinases and adaptor proteins involved in insulin signaling cascade in an *in-vitro* mouse myoblast cell model (C2C12) [41]. γ-conglutin exhibited insulin-mimetic behaviour in this cell model by activating the primary upstream insulin receptor (IR) / IRS-1 / PI3K pathway eventually followed by translocation of GLUT-4 receptors to the cell membrane. In the same report, γ-conglutin was also observed to activate downstream effectors that regulate protein synthetic pathway and muscle-specific gene transcription similar to insulin [41]. However, this mechanism of action was investigated only in derived immortal C2C12 myoblasts without further validation in different muscle cell lines or primary human cells. As a result, the second objective of this chapter was to validate the reported insulin-mimetic property of γ-conglutin in primary human skeletal muscle myotubes isolated from a donor.

DPP4 enzyme is responsible for the degradation of metabolic hormones responsible for insulin secretion (incretins). Thus, DPP4 inhibitors increase the circulating levels of incretins in the blood which further increases insulin secretion from pancreatic β-cells [113]. Also, inhibition of α-glucosidase enzyme in intestinal gut prevents the degradation of starch and disaccharides into glucose monomers consequently preventing a rise in blood glucose levels [247]. Bioactive peptides obtained from dietary proteins have been reported to modulate insulin secretion and glucose metabolism through inhibition of these enzymes. Soy and lupin derived peptides inhibited the activity of DPP4 enzyme in an *in-vitro* screening bioassay [248]. Further, these peptides inhibited the enzyme in-situ human intestinal Caco-2 cells and ex-vivo human serum [114]. Thus, evaluation of enzyme inhibitory actions of γ-conglutin peptides by performing preliminary *in-vitro* bioassays against DPP4 and α-glucosidase was the next objective.

Overall, the present chapter focuses on investigating the antidiabetic action of peptides obtained from gastrointestinal digestion of pure γ-conglutin protein. The potential mechanism of action of γ-conglutin peptides on insulinotropic effects in pancreatic β cells (BRIN-BD11 and INS-1E), insulin-mimetic effects in primary muscle myotubes and enzyme (DPP4 and α-glucosidase) inhibitory effects were assessed and described below.

5.2 CHEMICALS AND REAGENTS

Sodium phosphate monobasic and dibasic, sodium carbonate, hydrochloric acid, sodium hydroxide, 2-(N-(7-nitrobenz-2-oxa-1,3-diazol-4-yl)amino)-2-deoxyglucose, DMEM, DMEM high glucose, DMEM Nutrient mixture F-12 Ham, glucose, poly-D-lysine, cycloheximide, phosphate buffer saline, p-nitrophenol-α-D-glucopyranoside, α-glucosidase, acarbose, insulin were obtained from Sigma Aldrich (Castle hill, NSW, Australia). Amplex®Red glucose/glucose oxidase assay kit, Quant-iT™ PicoGreen dsDNA assay kit, Click-iT® Plus O-propargyl-puromycin (OPP) protein synthesis assay kit, and Prolong® Antifade Diamond mountant were obtained from Molecular probes (Eugene, Oregon, USA). Dipeptidyl peptidase 4 inhibitor screening assay kit was obtained from Cayman Chemical (Ann Arbor, MI, USA). Polyclonal goat anti-rabbit immunoglobulins/HRP from Dako (Glostrup, Denmark) and protease/phosphatase inhibitor cocktail (100X), rabbit phosphorylated and total primary antibodies: protein kinase B (Ser 473), mammalian target of rapamycin, S6 ribosomal protein (Ser 235/236) protein, ribosomal protein S6 kinase β1 (Thr 389), 44/42 extracellular signal-regulated kinase, glycogen synthase kinase-3β, Glyceraldehyde-3-phosphate dehydrogenase were obtained from Cell Signaling Technology (Danvers, MA, USA). Skeletal muscle growth medium-2 (CC-3245) kit was ordered from Lonza (Basel, Switzerland).

5.3 EXPERIMENTAL METHODS

5.3.1 Cell culture

5.3.1.1 Pancreatic β cell lines

BRIN-BD11 and INS-1E cells were cultured as described in section 4.3.3 (chapter 4). These well characterised and robust cell line models were used for studying the insulinotropic property of γ-conglutin peptides.

5.3.1.2 Human skeletal muscle myotubes (HSMM)

Human skeletal muscle myoblasts (catalog #: CC-2580, isolated from the upper arm or leg muscle tissue of a healthy female donor) were purchased from Lonza (Basel,

Switzerland). The myoblasts were cultured in skeletal muscle growth medium-2 (CC-3245) containing the following growth supplements: human epidermal growth factor, FBS, L-glutamine, gentamicin/amphotericin-B, dexamethasone. The media was changed after 48 hours until 60-70% cell confluency was achieved. The differentiation process of myoblasts into myotubes was started by replacing the growth media with equal volume of differentiation media - DMEM F-12 medium containing horse serum (2%), penicillin (100U/ml), streptomycin (0.1mg/ml), pH 7.4 at 37°C in a humidified atmosphere of 5% CO_2 and 95% air. The differentiation media was changed after every 48 hours and the cells were cultured for 6 days until multinucleated (more than 3 nuclei) were observed (Figure 5.1). These human skeletal muscle myotubes (HSMM) model were used for investigating the insulin-mimetic property of γ-conglutin peptides.
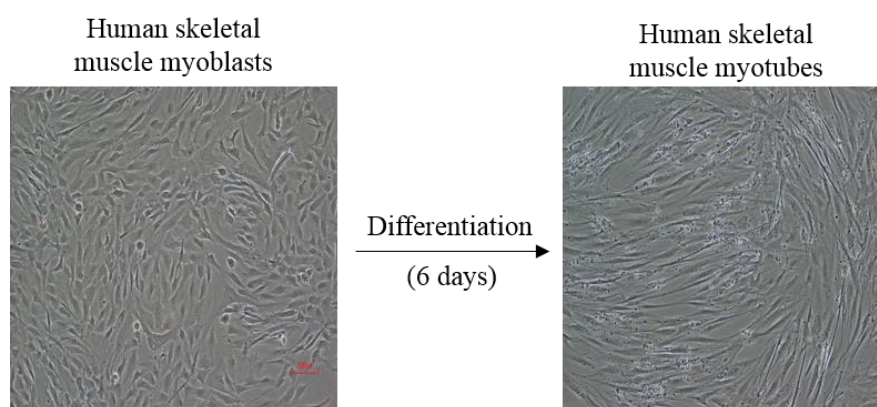
Figure 5.1 Images of human skeletal muscle myoblasts and myotubes under 10X microscope objective lens

5.3.2 Cell viability

The cell viability assay was performed as explained in section 4.3.4 (chapter 4).

5.3.3 Acute insulin secretion (*in-vitro*)

Acute (20minutes) insulin secretion from pancreatic β cells was carried out as explained in section 4.3.5 (chapter 4).

5.3.4 Western blot analysis

HSMM (differentiated) in T75 flasks were serum starved overnight. Next day, the cells were treated with insulin (100nM) and different concentrations of γ-conglutin peptides (2-200µg/ml) for 20 minutes. The cells were lysed in RIPA buffer containing 1% protease and phosphatase inhibitors cocktail followed by sonication and the total cell protein content was quantified using BCA assay method (section 3.4.1; chapter 3). Cell protein extracts were separated by SDS-PAGE and electrotransferred on nitrocellulose membrane (section 3.4.3 and 3.4.4; chapter 3). Later, the membranes were blocked with 3% BSA for 60 minutes and incubated overnight at 4°C with the following rabbit phosphorylated and total primary antibodies: Akt (Ser 473), mammalian target of rapamycin (mTOR), S6 ribosomal protein (Ser 235/236) protein, p70S6K (Thr 389), 44/42 mitogen-activated protein kinases (MAPK) also known as extracellular signal-regulated kinase 1 and 2 (ERK1/2), glycogen synthase kinase-3β (GSK3β). Glyceraldehyde-3-phosphate dehydrogenase (GAPDH) was used as a housekeeping protein and loading control for protein normalisation. All the primary antibodies were diluted 1000 times in TBST containing 5% BSA. The membranes were washed and incubated in HRP conjugated secondary antibody for 60 minutes. The target bands were detected as discussed in section 3.4.4.

5.3.5 Glucose uptake assay

Differentiated HSMM cells were seeded in 6 well plates (150,000 cells/well) were serum starved overnight. Next day, the cells were incubated with glucose-free DMEM media containing 20µM of 2-NBDG with and without treatments: insulin / γ-conglutin peptides (200µg/ml and 20µg/ml). Glucose uptake assay was performed as described in section 4.3.8 (chapter 4).

5.3.6 Glycogen measurement

The glycogen content in cells is analysed by hydrolysing cells in acid at high temperature. Under this condition, the glycogen chains breakdown into its glucose monomers [249]. The glycogen derived D-glucose units are then quantified by glucose oxidase assay. The glucose oxidase enzyme converts D-glucose to D-gluconolactone and hydrogen peroxide (H_2O_2). The latter product (H_2O_2) reacts with Amplex® Red

reagent in presence of HRP enzyme to generate red fluorescent oxidative product known as 'resorufin' which can be analysed with an excitation wavelength of 571nm and emission wavelength of 585nm.

After 6 days of differentiation in T75 flasks, HSMM were overnight serum starved. Next day, the cells were incubated in glucose-free DMEM media without glucose for 2 hours (glucose starvation step). After the glucose and serum starvation step, the cells were treated with insulin and γ-conglutin peptides (200µg/ml and 20µg/ml) in DMEM high glucose media for 2 hours. The cells were recovered by trypsinization, centrifuged in cold condition, resuspended in 1ml cold PBS containing 0.5% BSA and transferred to microcentrifuge tubes. An aliquot (50µl) of the cell suspension from each tube was removed and lysed with RIPA buffer for quantification of DNA content (Quant-iT™ PicoGreen™ ds DNA assay). The remainder cell suspensions were centrifuged and the cell pellets were resuspended in 2M HCl (100µl). The microcentrifuge tubes were carefully sealed with parafilm and heated at 99°C for an hour. Later, the acidic suspension was neutralised with 2M NaOH (100µl). The pH of the suspension was checked with pH indicator strips (Merck, Darmstadt, Germany) and if required the pH was adjusted to 7 using either acid (2M HCl) or base (2M NaOH). The cell suspension was centrifuged and glucose content in the supernatant of each sample tube was determined.

The supernatant of each sample tube was diluted 20X and glucose content was determined using Amplex® red glucose/glucose oxidase assay kit. The assay was performed in duplicates in 96-well solid black plate. Stock solution of Amplex®red (10mM), glucose oxidase (100U/ml), HRP (10U/ml) were prepared according to the manufacturer's protocol. The final (working solution) reaction mixture consisted of Amplex®Red reagent (100µM), glucose oxidase (2U/ml), HRP (0.2U/ml) in sodium phosphate (50mM) reaction buffer. In 96 well plate, 50µl of sample/glucose standards (50-3.13µM) were added and the reaction was initiated by addition of 50µl reaction mixture. After incubating the plate for 30minutes in dark, fluorescence signals were measured in multimode plate reader (Ensight, Perkin Elmer) using appropriate wavelength settings (Excitation wavelength: 530-560nm and emission wavelength: 590nm). The glucose concentration in samples was determined from the glucose standard curve equation.

5.3.7 Protein synthesis assay

Click-iT® Plus O-propargyl-puromycin (OPP) protein synthesis assay kit was used to detect nascent proteins in cultured cells. OPP is an aminonucleoside antibiotic that causes premature termination of newly synthesised polypeptide chains by forming an amide bond between C-terminal of the nascent polypeptide chain and the amino group of puromycin. OPP-polypeptide conjugate on addition of fluorescent azides undergoes copper catalysed azide-alkyne cycloaddition reaction. The fluorescent labeled OPP-polypeptide conjugate is visualised by fluorescence microscopy. The fluorescent signal emitted by the conjugate is proportional to the nascent protein synthesised and can be quantified relative to control/vehicle-treated cells.

Human skeletal muscle myoblast cells were seeded (150,000 cells/well) on glass coverslips coated with 0.5mg/ml poly-D-lysine in the skeletal muscle growth media. Once the cells were 70% confluent, the media was replaced with differentiation media. After 6 days of differentiation, HSMM were serum starved overnight. Next day, the cells were incubated in DMEM media containing Click-iT® OPP reagent (10µM) in the presence and absence (control) of treatments: insulin (100nM), γ-conglutin peptides (200µg/ml and 20µg/ml) and cycloheximide (10µM) for 30minutes. After incubation, the cells were washed with PBS and fixed with paraformaldehyde (4%) for 15minutes. The cells were permeabilised with Triton®X-100 (0.5%) for 15 minutes and washed with PBS again. The Click-iT® OPP reaction cocktail consisting of reaction buffer, copper protectant, Alexa Fluor® picolyl azide was prepared as recommended by the manufacturer and the cells were incubated in this reaction cocktail for 30minutes at room temperature protected from light. Later, the cells were washed with Click-iT® rinse buffer and were stained with HCS NuclearMask® Blue stain to measure DNA content. After 30minutes of incubation with the stain, the coverslips were washed several times with PBS, air dried and mounted in glycerol-based Prolong® Antifade Diamond mountant. The mounted samples were allowed to dry overnight at room temperature in dark.

The stained cell samples were imaged by confocal microscopy on Nikon A1+ microscope equipped with 450/50 and 595/50 filters and 20X objective (Nikon, Tokyo, Japan). Images were captured using NIS Elements image acquisition software (Nikon,

Tokyo, Japan) and analysed using ImageJ1 software [250]. Three independent experiments were performed with a similar set of treatments as mentioned before and 15 images per treatment (per mounted coverslip) were obtained. The AF594 red images of each treatment were converted to grey scale and the same global threshold values were set for analysing all the images. Lower and higher threshold values were set to exclude the black background and artifacts pixels (if any) respectively. 'Pixel integrated density per unit area (mean)' within the set threshold window was obtained. The image mean value of cells unlabelled with OPP (blank) was subtracted from the image mean value of treated/control cells labelled with OPP. Fold increase in mean values of treatments (OPP labeled cells treated with insulin/γ-conglutin peptides/cycloheximide) with respect to control (OPP labelled cells only) were reported.

5.3.8 DPP4 activity assay

DPP4 enzyme is a serine exopeptidase that cleaves X-alanine or X-proline dipeptides from N-terminal polypeptides. In this assay, fluorogenic substrate Gly-Pro-aminomethylcoumarin (AMC) is used to measure DPP4 activity. The enzyme cleaves the substrate into dipeptides and releases free AMC fluorogenic group which can be analysed using an excitation wavelength in the range of 350-360nm and an emission wavelength of 450-465nm.

DPP4 inhibitor screening assay kit was used to evaluate the enzyme inhibitory action of γ-conglutin protein and peptides. The assay was carried out in triplicates in half volume 96-well solid white plate. DPP4 enzyme and substrate Gly-Pro-AMC were diluted to the desired concentration as per the manufacturer's protocol. The reaction mixture was prepared by adding reagents in the wells in the following order: 30µl of Tris-HCl (20mM) assay buffer containing NaCl (100mM) and EDTA (1mM), 10µl of DPP4 enzyme, 10µl of the sample (γ-conglutin protein/peptides) or inhibitor sitagliptan (100µM). The reaction was subsequently started by adding 50µl of the substrate (5mM) in each well and incubated at 37°C for 30 minutes. Fluorescence signals were measured in a multimode plate reader (Ensight, Perkin Elmer) using appropriate wavelength settings (Excitation wavelength: 350nm and emission wavelength: 460nm). Control (100% initial activity) was measured by the addition of

vehicle instead of inhibitors. Background absorbance of samples without enzyme and substrate were also measured. Sitagliptan, a standard DPP4 enzyme inhibitor was used as positive control in the assay. DPP4 activity of (%) sample/inhibitor was calculated as:

$$DPP4\ activity\ (\%) = \frac{(sample\ or\ inhibitor\ fluorescence - background\ fluorescence)\ X\ 100}{(Control\ fluorescence - background\ fluorescence)}$$

5.3.9 α-glucosidase activity assay

α-glucosidase enzyme cleaves terminal non-reducing α-1,4 glycosidic linked glucose residue in polysaccharides (starch) or disaccharides and releases α-D-glucose units. In this assay, chromogenic substrate p-nitrophenol-α-D-glucopyranoside (pNPG) is used to measure α-glucosidase activity. The enzyme cleaves the α1,4 linked glycosidic bond in the substrate and releases yellow coloured product (p-nitrophenol) which has maximal absorbance at 400nm.

α-glucosidase inhibition assay was performed according to standard methods with minor modifications [251]. The assay was carried out in triplicates in 96-well plate. The reaction mixture was prepared by adding reagents in the wells in the following order: 30µl of sodium phosphate (50mM) pH 6.86 assay buffer, 25µl of α-glucosidase enzyme (0.15U/ml) containing BSA (0.2%), 25µl of the sample (γ-conglutin protein / peptides) or inhibitor acarbose (0.001-25mM). The reaction was subsequently started by adding 25µl of pNPG (5mM) substrate in each well and incubated at 37°C for 15minutes. Later, 100µl of sodium carbonate (200mM) was added to stop the reaction. α-glucosidase activity was determined by measuring the absorbance at 400nm using multimode plate reader (Ensight, Perkin Elmer). Background absorbance of samples without enzyme and substrate pNPG were also measured. Acarbose (50mM) was used as a positive control in the inhibition study. α-glucosidase activity (%) of sample/inhibitor was calculated as:

$$\alpha - glucosidase\ activity\ (\%)$$
$$= \frac{(sample\ or\ inhibitor\ absorbance - background\ absorbance)\ X\ 100}{(Control\ absorbance - background\ absorbance)}$$

5.3.10 Statistical analysis

All statistical analyses were performed as described in section 4.3.11 using GraphPad Prism v.6.0 software. $P \leq 0.05$ was considered statistically significant.

5.4 RESULTS AND DISCUSSIONS

5.4.1 Characterisation and enzymatic hydrolysis of purified γ-conglutin

γ-conglutin protein fraction was purified from lupin protein extract using cation exchange chromatography (section 3.5.2; chapter 3). At first, the eluted protein fraction from cation exchange chromatography was identified to be specifically γ-conglutin protein by western blot (section 3.5.3.2; chapter 3) and mass spectrometry (section 3.5.3.4; chapter 3). Next, the purity of eluted γ-conglutin was found to be ~100% by SDS-PAGE (section 3.5.3.1; chapter 3) and 95% based on RP-HPLC analysis (section 3.5.3.3; chapter 3). In order to evaluate the anti-diabetic potential of γ-conglutin as an oral anti-diabetic agent, it was hydrolysed under gastrointestinal digestion condition using proteolytic enzymes pepsin and pancreatin (section 3.5.4; chapter 3). After achieving a maximum degree of hydrolysis, the enzymes and high molecular weight proteins were removed by filtering the hydrolysate (peptides) through 3KDa MWCO membrane. Permeate, a mixture of γ-conglutin peptides with molecular weight ≤6.5KDa was further investigated for its potential anti-diabetic activities.

5.4.2 γ-conglutin peptides did not exhibit acute insulinotropic action in pancreatic β cells (BRIN-BD11 and INS-1E)

The introduction of incretin-based therapeutics have widely promoted screening and development of different plant and animal-derived peptides for their glucose-dependent insulinotropic action in β cells [252]. In chapter 4, it was observed that lupin protein extract hydrolysate exhibited glucose permissive insulinotropic action by enhancing glucose metabolism and stimulating Gα$_q$/PLC/PKC pathway in pancreatic β cell BRIN-BD11 [246]. However, bio-molecule(s) responsible for this action was not determined. As a result, peptides generated from the hydrolysis of purified lupin protein γ-conglutin were screened *in-vitro* for their insulinotropic action. Different *in-vitro* models like the perfused pancreas, isolated pancreatic islets and derived β cell

lines are generally used as screening tools for assessing insulin secretion property. BRIN-BD11 derived from electrofusion of rat pancreatic islets with rat insulinoma cells and INS-1E derived from X-ray induced rat insulinoma cells were selected for investigating the insulinotropic property of γ-conglutin peptides [253].

At first, the cell viability of BRIN-BD11 and INS-1E cells in the presence of γ-conglutin peptides was studied to determine if peptides resulted in any release of insulin by cell death. A significant increase in cell viability over 24 hours was observed in BRIN-BD11 cells (500μg/ml) and INS-1E cells (500-100μg/ml) indicating beneficial effects of the peptides on cell growth and proliferation (Figure 5.2A and 5.2B). Acute (20minutes) insulin secretions from both BRIN-BD11 and INS-1E cells at 16.7mM glucose in presence of different peptide concentration of γ-conglutin hydrolysate (200 - 20μg/ml) were insignificant as compared to control (Figure 5.2C and 5.2D). Moreover, these secretion values were significantly lower than the lupin extract hydrolysate (200μg/ml) and positive control alanine (10mM). This indicated that some other biomolecule(s) were responsible for the potent insulinotropic action of extract hydrolysate. Overall, γ-conglutin peptides did not exhibit insulinotropic action in either of the cell models.
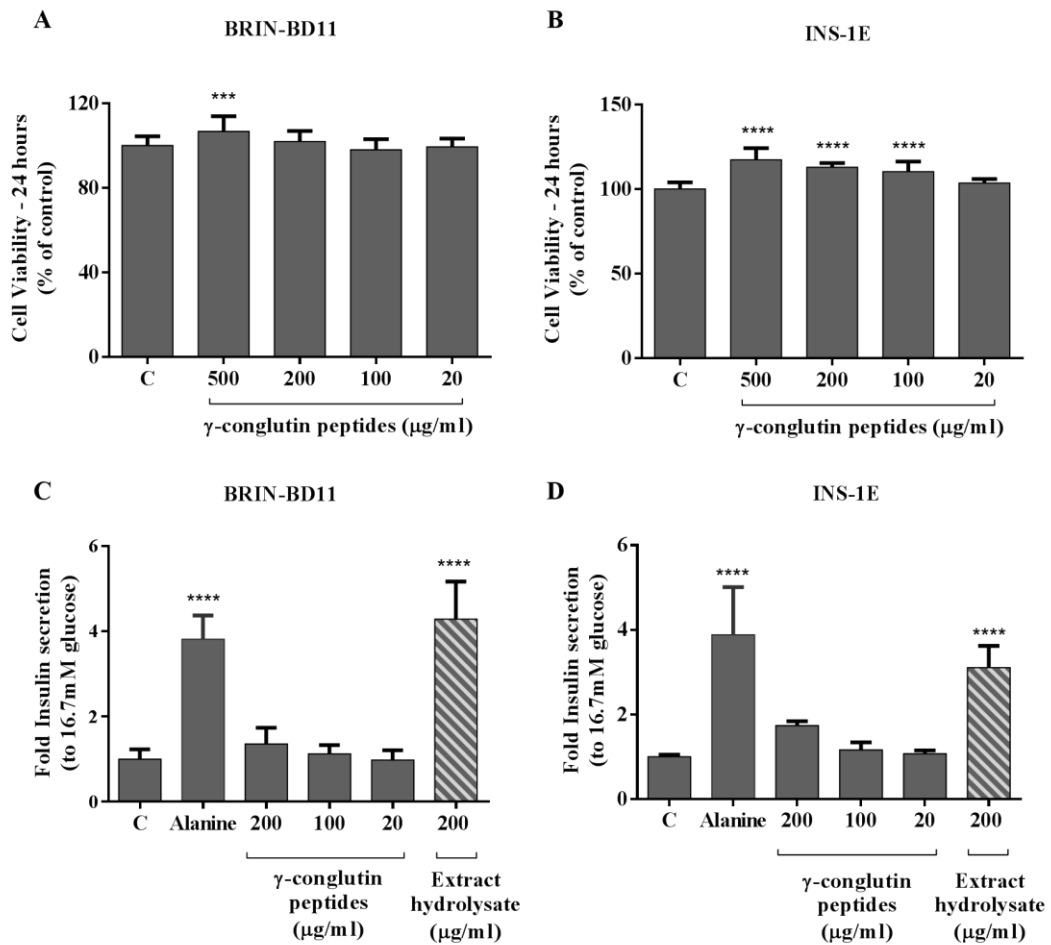
*Figure 5.2 Cell viability and γ-conglutin peptide stimulated insulin secretion. (A) BRIN-BD11 and (B) INS-1E cell viability at different γ-conglutin peptide concentrations (500-20µg/ml) over 24 hours. Cell viability is reported as a percentage of control 'C'. Dose-dependent effect of γ-conglutin peptides in 16.7mM glucose on acute (20 minutes) insulin secretion from (C) BRIN-BD11 and (D) INS-1E cells. The response was compared with control (16.7mM glucose) referred as 'C', positive control (10mM L-alanine in 16.7mM glucose) referred as 'Alanine' and lupin extract hydrolysate (200µg/ml). Insulin secretion is reported as values normalised with control. Values are mean ± standard deviation of three independent experiments; ****p ≤0.0001 and ***p ≤0.001 are significantly different as compared to control.*

5.4.3 γ-conglutin peptides exhibited insulin-mimetic behaviour in primary human skeletal muscle myotubes.

Skeletal muscle is one of the major glucose hemostasis regulators, mainly due to its large mass. Insulin is a key factor required for the transfer, metabolism and storage of blood glucose in the muscle cells [254]. It enhances glucose uptake, increases the rate of glycolysis and stimulates glycogen synthesis in the cells. Also, insulin increases the transport of amino acids across the membrane and cascades activation of protein

111

synthesis in cells [255]. Like insulin, γ-conglutin has been reported to regulate glucose transportation, protein synthesis, and muscle energy metabolism through phosphorylation and activation of proteins involved in insulin signal transduction in derived muscle myoblasts (C2C12) [41]. However, these reported results of γ-conglutin were explored only in one cell line. Due to the induced modification in derived cell lines, the target therapeutic response should preferably be validated in primary cells isolated directly from the donor. Primary cells present an environment resemblance relatively closer to *in vivo* cells than immortal cell lines. As a result, healthy primary human skeletal muscle myoblasts differentiated into myotubes (*in-vitro)* were used to study the insulin-mimetic action of γ-conglutin peptides. The viability of the cells in presence of γ-conglutin peptides (200µg/ml) was not affected. The percentage of γ-conglutin peptides treated live cells was found to be 95.27% (±1.05%) as calculated from the fluorescence obtained from propidium iodide negative stained singlet (live) cells in flow cytometer.

5.4.3.1 γ-conglutin peptides stimulated PI3K/Akt/mTOR signaling pathway

Binding of insulin to extracellular α subunit of IR results in activation of intracellular IR tyrosine kinase. The phosphorylated tyrosine kinases are recognised by different substrate adaptor proteins such as IRS-1. The phosphorylated IRS-1 serves as binding site for various signaling proteins, the most important being PI3K, which subsequently activates 3-phosphoinositide-dependent protein kinase 1 (PDK-1) [256]. Further, PDK-1 phosphorylates and activates downstream Akt and protein kinase C cascades. Phosphorylation of Akt at Ser-473 residue by mammalian target of rapamycin (mTOR) complex 2 (mTORC2) is also required for its complete activation. PDK-1 and mTORC2 mediated Akt phosphorylation triggers activation of multiple downstream proteins/enzymes involved in regulating protein, lipid and glycogen synthesis, translocating glucose transporters to the cell surface, controlling cell cycle and survival [257]. In the mouse subclone muscle myoblast model (C2C12 cell line), γ-conglutin protein has been reported to activate insulin signaling cascade through the IRS-1/PI3K/Akt pathway required for glucose homeostasis [41].

Herein, the effect of γ-conglutin peptides in an *in-vitro* model of primary human skeletal muscle myotubes on phosphorylation/activation of proteins involved in insulin

signaling pathway was studied. Acute exposure of cells to γ-conglutin peptides (200µg/ml) resulted in an increase (~2 fold) in phosphorylation levels of mTOR (Figure 5.3A) and Akt (Figure 5.3B) compared to control. This indicated that peptide(s) can mediate different metabolic actions of insulin by stimulating the central PI3K/Akt/mTOR signaling pathway.
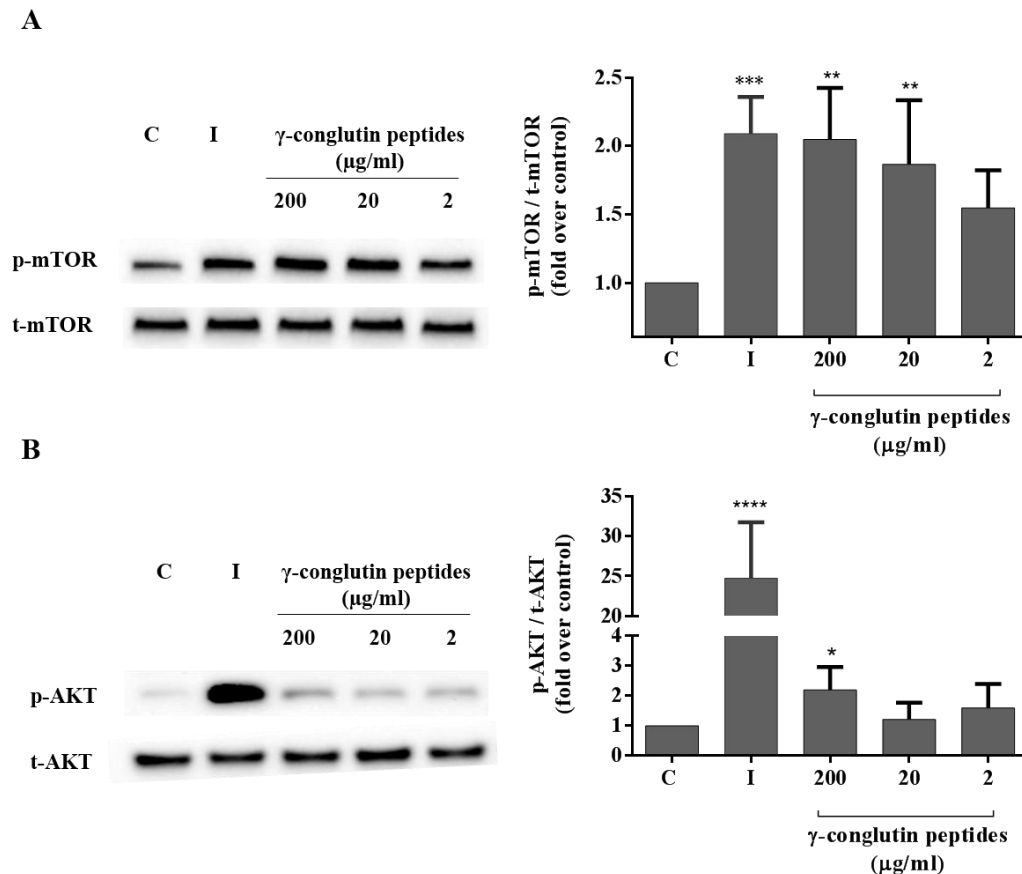
*Figure 5.3 Western blot analysis of (A) mammalian target of rapamycin (mTOR) and (B) protein kinase B (Akt) in in human skeletal muscle myotube cell extract and ratio of their band intensities (phosphorylated / total) in presence of vehicle (control referred to as 'C'), insulin (100nM) (referred as 'I'), γ-conglutin peptides (200 - 2µg/ml). The ratio of band intensities is reported as values normalised with control. Phosphorylated and total form of proteins is mentioned with prefix 'p' and 't' respectively. Values are mean ± standard deviation of three or more independent experiments; ****p ≤0.0001, ***p ≤0.001, **p ≤0.01 and *p ≤0.05 are significantly different as compared to control. Immunoblot protein bands shown are representative of three or more independent experiments.*

5.4.3.2 γ-conglutin peptides regulated cellular glucose metabolism

On activation, Akt triggers the phosphorylation of GSK3β at serine residues that block and prevent the enzymatic action of GSK3β. The inactivation of GSK3β leads to subsequent dephosphorylation and activation of Glycogen Synthase (GS) that catalyses the conversion of glucose monomers into glycogen units, thus, eliciting cellular glycogen synthesis process [258]. γ-conglutin peptides stimulated the phosphorylation of GSK3β (~1.4 folds; Figure 5.4A) and escalated cellular glycogen synthesis as evident from increased glycogen content in the cells treated with peptides (2.8 folds; Figure 5.4B).
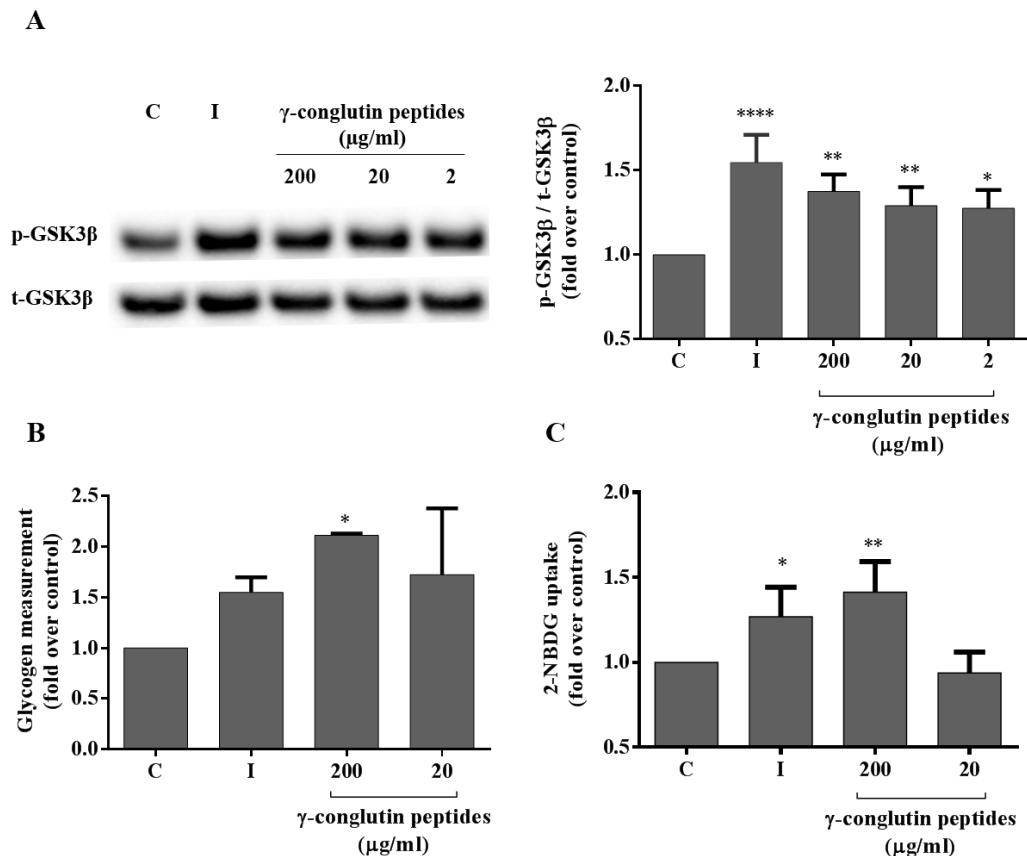
Figure 5.4 Effect of γ-conglutin peptides on glucose metabolism in human skeletal muscle myotubes (HSMM) : (A) Western blot analysis of Glucose Kinase 3 β (GSK3β) in HSMM cell extract and ratio of their band intensities (phosphorylated / total) in presence of vehicle (control referred to as 'C'), insulin (100nM) (referred as 'I'), γ-conglutin peptides (200 - 2μg/ml). The ratio of band intensities is reported as values normalised with control. Phosphorylated and total form of proteins is mentioned with prefix 'p' and 't' respectively. Immunoblot protein bands shown are representative of three or more independent experiments. (B) Glycogen content and (C) 2-(N-(7-nitrobenz-2-oxa-1,3-diazol-4-yl)amino)-2-deoxyglucose (2-NBDG) uptake in HSMM cells in presence of vehicle (control referred as 'C'), insulin (100nM) (referred as 'I'),

114

Insulin-mediated phosphorylation of Akt activates Caveolin-3 and flotillin-2 mediated GLUT-4 receptor translocation from cytoplasm to the cell membrane. In the early phase of insulin signal transduction, phosphorylated Akt stimulates the movement of flotillin-2/GLUT-4 containing domain from perinuclear region to the cytoplasm. In the next phase, caveolin-3 domain, containing caveolin-3 and IR, move away from the plasma membrane to the cytoplasm where they interact with flotillin-2/GLUT-4 domain. IR moves from caveolin-3 domain to flotillin-2 domain. Further, insulin-stimulated phosphorylated Cbl protein promotes the translocation of GLUT-4 along with flotillin-2 domain to the membrane. The fusion of GLUT-4/flottilin-2 domain with the plasma membrane facilitates blood glucose transportation into the cells [259]. In the same context, γ-conglutin peptides have been reported to increase concentrations of flotillin-2 and caveolin-3 and phosphorylation of Cbl in C2C12 myoblasts, thus, playing a role in translocation of GLUT-4 vesicles to the cell membrane in C2C12 myoblasts [41]. However, the end effect of blood glucose transportation into the cells was not reported. In the present study, an increase in glucose uptake (~1.4 folds) in cells treated with γ-conglutin peptides was observed (Figure 5.4C), thus, validating the hypothesis of glucose transportation into cells via GLUT-4 translocation. Similarly, γ-conglutin increased glucose consumption in HepG2 hepatocytes [92] and 3T3-L1 adipocytes [40] when exposed to high glucose concentration medium. No significant increase in glucose consumption was observed when HepG2 cells were cultured in normal glucose concentrations. Moreover, a synergistic effect of γ-conglutin peptides with insulin on cellular glucose consumption was reported in these studies. Altogether, the dataset presented herein displayed that γ-conglutin peptides were able to stimulate AKT/GSK3β signaling axis with an increase in glycogen synthesis and glucose uptake response in HSMM.

5.4.3.3 γ-conglutin peptides modulated protein metabolism

Insulin enhances the transportation of amino acids into the cells, inhibits proteolysis and triggers protein synthesis [111]. Akt stimulates activation of multiple substrates

involved in insulin action. Akt phosphorylates and inactivates Tuberous Sclerosis Complex (TSC1/2), a negative regulator of mTORC1, subsequently activating mTORC1 downstream proteins [260]. The two predominant mTORC1 downstream targets are eIF4E and p70S6K. Phosphorylation by mTORC1 leads to inhibition of eIF4E and activation p70S6K which further instigates the protein synthesis process. Phosphorylated p70S6K subsequently activates ribosomal protein S6 and initiates the translation process [261]. The present data in Figure 5 showed that γ-conglutin peptides induced an increase in phosphorylation of p70S6K (~3.6 folds; Figure 5.5A) and S6 (~2.5 folds; Figure 5.5B) proteins. This indicated that incubation of myotubes with γ-conglutin peptides triggered Akt/mTOR/70S6K/S6 signaling axis responsible for cellular protein synthesis. These results are in parallel with the previous study reporting similar phosphorylation and stimulation of p70S6K and eIF4E in C2C12 myoblasts cultures with γ-conglutin protein [41].
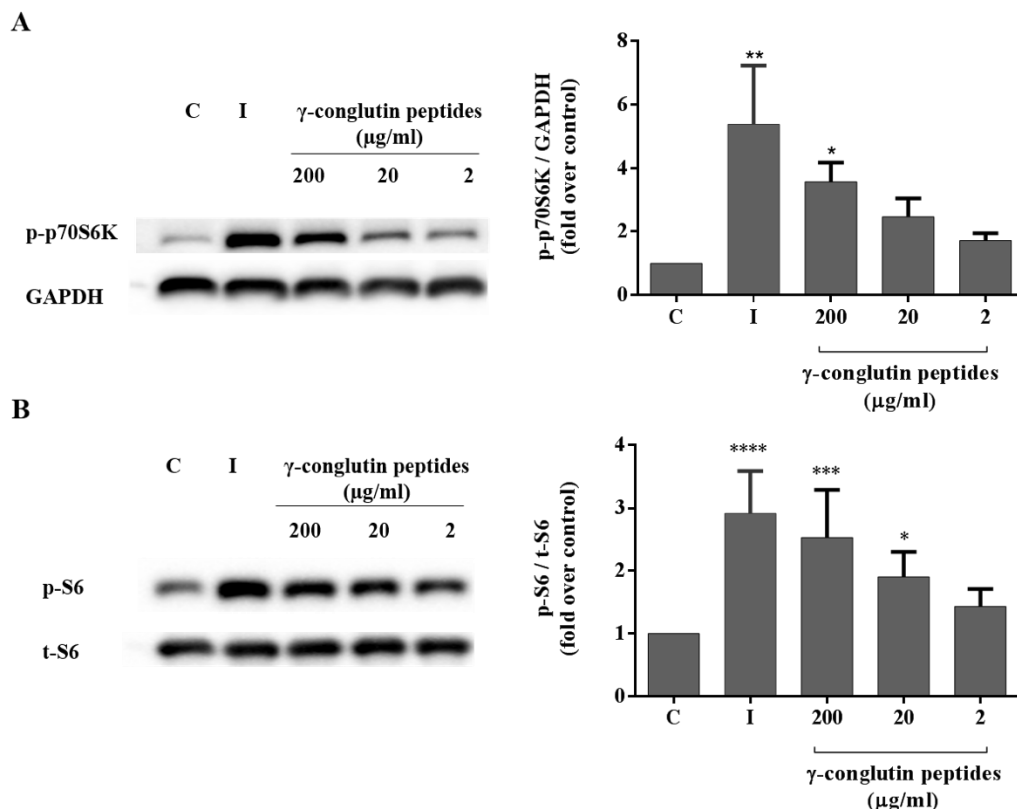
Figure 5.5 Western blot analysis of (A) 70KDa ribosomal protein S6 kinase (p70S6K) and (B) ribosomal protein S6 (S6) in human skeletal muscle myotubes cell extract in presence of vehicle (control referred to as 'C'), insulin (100nM) (referred as 'I'), γ-conglutin peptides (200 - 2µg/ml). The band intensities of phosphorylated p70S6K (p-p70S6K) were normalised with glyceraldehyde-3-phosphate dehydrogenase (GAPDH), a housekeeping protein used as loading control for protein normalisation,

Protein synthesis is the fundamental biological process where the cells synthesise their own proteins. This process comprises mainly two important steps: transcription and translation. The first step is initiated in the nucleus where the information encoded in DNA is copied to messenger ribonucleic acid (mRNA) molecules. In skeletal muscle cells, insulin exerts its anabolic effect by increasing the rate of protein synthesis and decreasing the rate of degradation [262]. Insulin enhances the protein gene expression as reflected by an increase in mRNA levels and stimulates the translation process by triggering the initiation of peptide chain synthesis [263-266]. Thus, insulin overall increases the capacity of protein synthesis and produces specific proteins required for cellular metabolism.

In the above dataset, γ-conglutin peptides increased the phosphorylation of p70S6K and S6 proteins responsible for activation of protein synthesis and, thus, the next step was to detect and quantify the increase in nascent protein synthesis in presence of peptides. Differentiated HSMM were co-incubated with γ-conglutin peptides/insulin and OPP aminonucleoside antibiotic. The OPP conjugated nascent polypeptide chains were fluorescently labeled with AF594 - AlexaFluor® 594 picolyl azide (combination of picolyl azide and alkyne moieties) for visualisation by fluorescence microscopy. As an additional control, conditions inhibiting protein synthesis were also introduced by co-incubating cells with OPP and cycloheximide, an inhibitor of translation elongation process in the protein synthesis. Figure 5.6, merged images (subset: a-f) display the images captured at two wavelengths to detect nascent synthesized protein (561nm, AlexaFluor®; subset: g-l) and nuclei (402nm; HCS Nuclear Mask® blue stain; subset: m-r). As observed the nascent protein synthesised in presence of γ-conglutin or insulin were more fluorescent as compared to the control (vehicle/media).

	Merged image	Nascent protein (AlexaFluor 594)	DNA (HCS Nuclear Mask Blue stain)

Blank — a, g, m

Control — b, h, n

Insulin (100nM) — c, i, o

γ-conglutin peptides (200μg/ml) — d, j, p

γ-conglutin peptides (20μg/ml) — e, k, q

Cycloheximide (10μM) — f, l, r

118
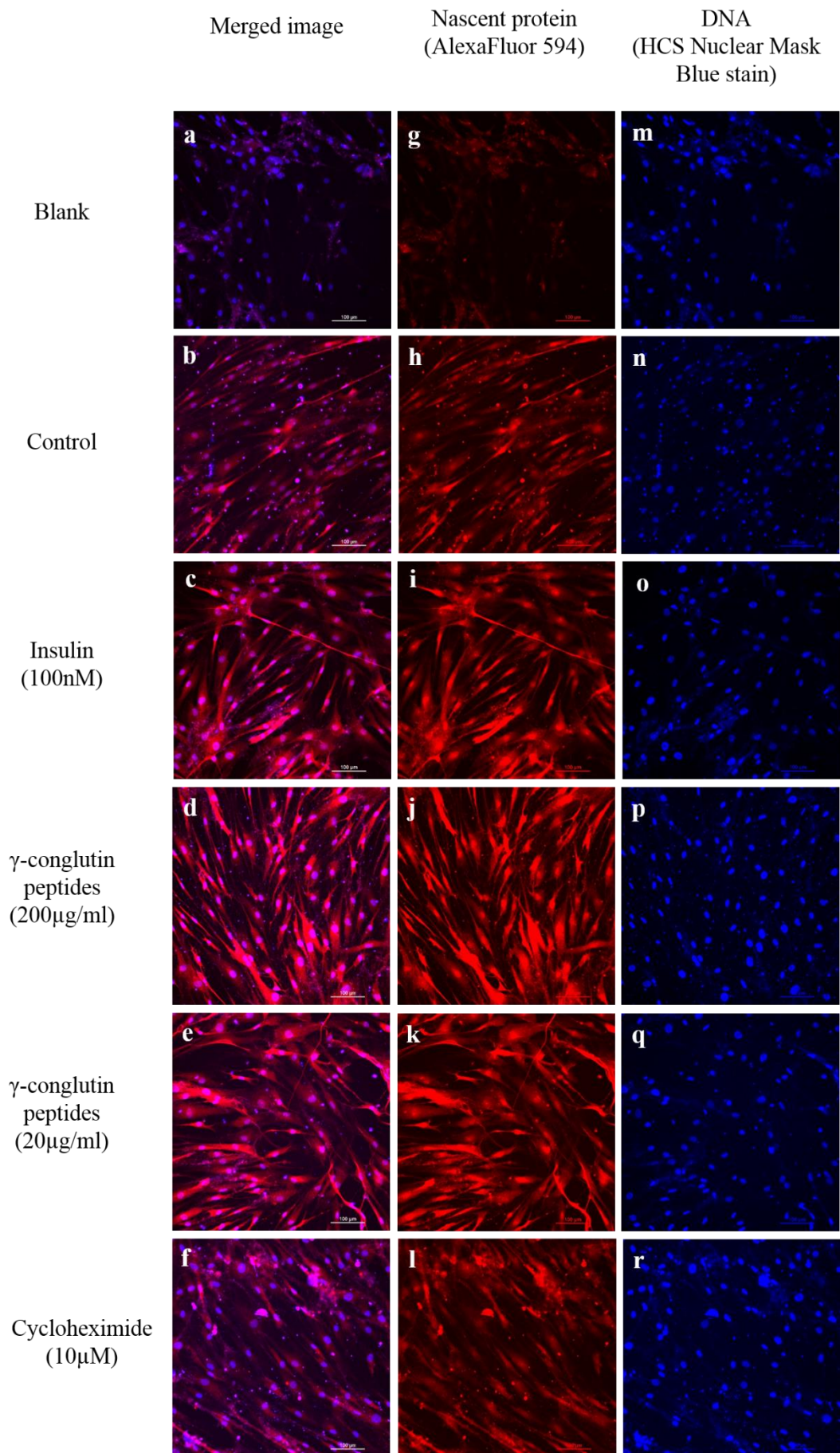
Figure 5. 6 Effect of γ-conglutin peptides on protein synthesis in human skeletal muscle myotubes (HSMM): Confocal laser scanning microscopy images of nascent proteins in cells co-cultured with OPP and different treatments. 'Blank' represents cells unlabelled with OPP, 'C - control' refers the OPP treatment only, and 'I - insulin (100nM) / γ-conglutin peptides (200µg/ml and 20µg/ml) / CHX - cycloheximide (10µM) refers to OPP labelled cells with the respective treatments. The cells are stained with AlexaFlour594 (nascent protein) and HCS NuclearMask® Blue stain (DNA). Images shown are representative of three independent experiments.

AlexaFluor® fluorescence of nascent protein was quantified as the integrated density of pixel per unit area (mean) and reported as fold increase to control (Figure 5.7). Insulin, γ-conglutin peptides at 200µg/ml and 20µg/ml exhibited an increase in protein synthesis (~1.56, ~1.55, and ~1.34 folds respectively) compared to control. As predicted, cycloheximide abolished the protein synthesis process (~0.6 folds) compared to control. Altogether, like insulin, γ-conglutin peptides activated 70S6K and S6 protein signalling resulting in enhancement of protein synthesis process.
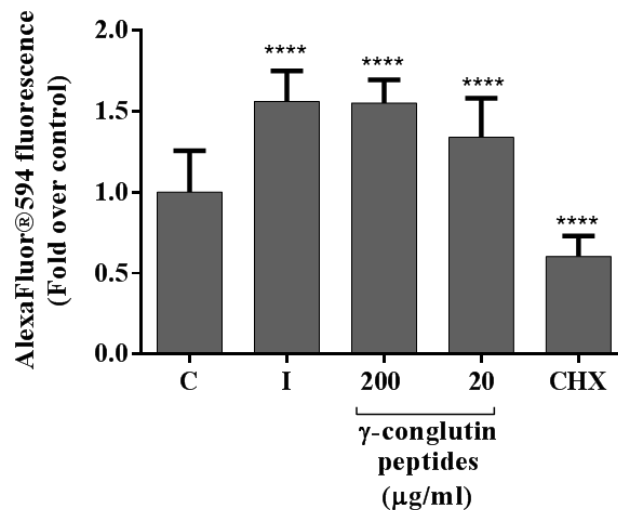
*Figure 5.7 Quantification of AlexaFlour®594 fluorescence intensity (integrated density of pixels /area from Figure 5.6) reported as fold over control. 'C' refers to control, I refers to insulin, CHX refers to cycloheximide. Values are mean ± standard deviation of three independent experiments; ****p ≤0.0001 is significantly different as compared to control*

5.4.3.4 γ-conglutin peptides activated Extracellular Signal-Regulated Kinase (ERK) 1 and 2.

Insulin receptor activation results in balanced signaling of two independent pathways: (a) PI3K/AKT pathway (metabolic arm) and (b) Ras/ Mitogen-Activated Protein Kinase (MAPK) pathway (mitogenic arm) [267]. IRS protein recruit's cytoplasmic growth factor receptor bound 2 (Grb2) adaptor proteins. Grb2 on association with son-of-sevenless (SOS) protein activates membrane-bound GTPase protein, Ras which subsequently binds to Raf kinase. Later, the phosphorylated Raf activates MAPK / ERK 1 and 2 signaling pathway that eventually cascades downstream targets involved in cellular proliferation, differentiation, and survival [268]. In this study, γ-conglutin peptides induced phosphorylation of ERK 1/2 (1.7 folds; Figure 5.8) similar to the response produced by insulin. This indicated that γ-conglutin peptides, like insulin, have potential to affect proliferation and differentiation of muscle cells. However, one of the limitations of this study was that the increase in myoblast count and myotube size in presence of peptides was not determined.
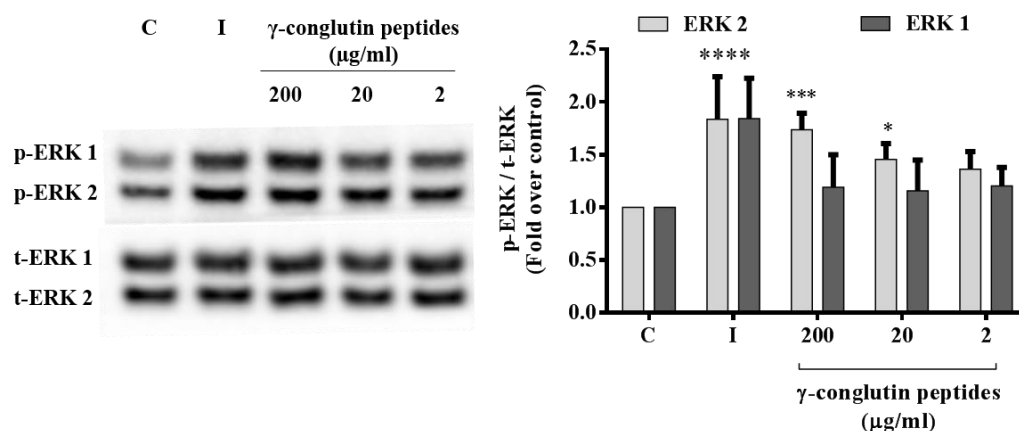
*Figure 5.8 Western blot analysis of Extracellular Signal-Regulated Kinase (ERK) 1 and 2 in human skeletal muscle myotube cell extract and ratio of their band intensities (phosphorylated / total) in presence of vehicle (control referred to as 'C'), insulin (100nM) (referred as 'I'), γ-conglutin peptides (200 - 2μg/ml). The band intensities ratio is reported as fold change over control. Phosphorylated and total form of proteins is mentioned with prefix 'p' and 't' respectively. Values are mean ± standard deviation of three or more independent experiments; ****p ≤0.0001, ***p ≤0.001, and *p ≤0.05 are significantly different as compared to control. Immunoblot protein bands shown are representative of three or more independent experiments.*

The present data indicated that γ-conglutin peptides, like insulin, phosphorylated and activated Akt, the central mediator responsible for stimulating a range of metabolic

processes. γ-conglutin peptides increased glucose uptake in the cells, promoted glycogen synthesis mediating through AKT/GSK3β pathway, induced protein synthesis by activating AKT/mTOR/70S6K/S6 pathway and also has potential of influencing muscle growth and differentiation by activating ERK. Overall, as depicted in Figure 5.9, γ-conglutin peptides partially share properties of insulin suggesting its potential therapeutic application as an insulin-mimetic agent.
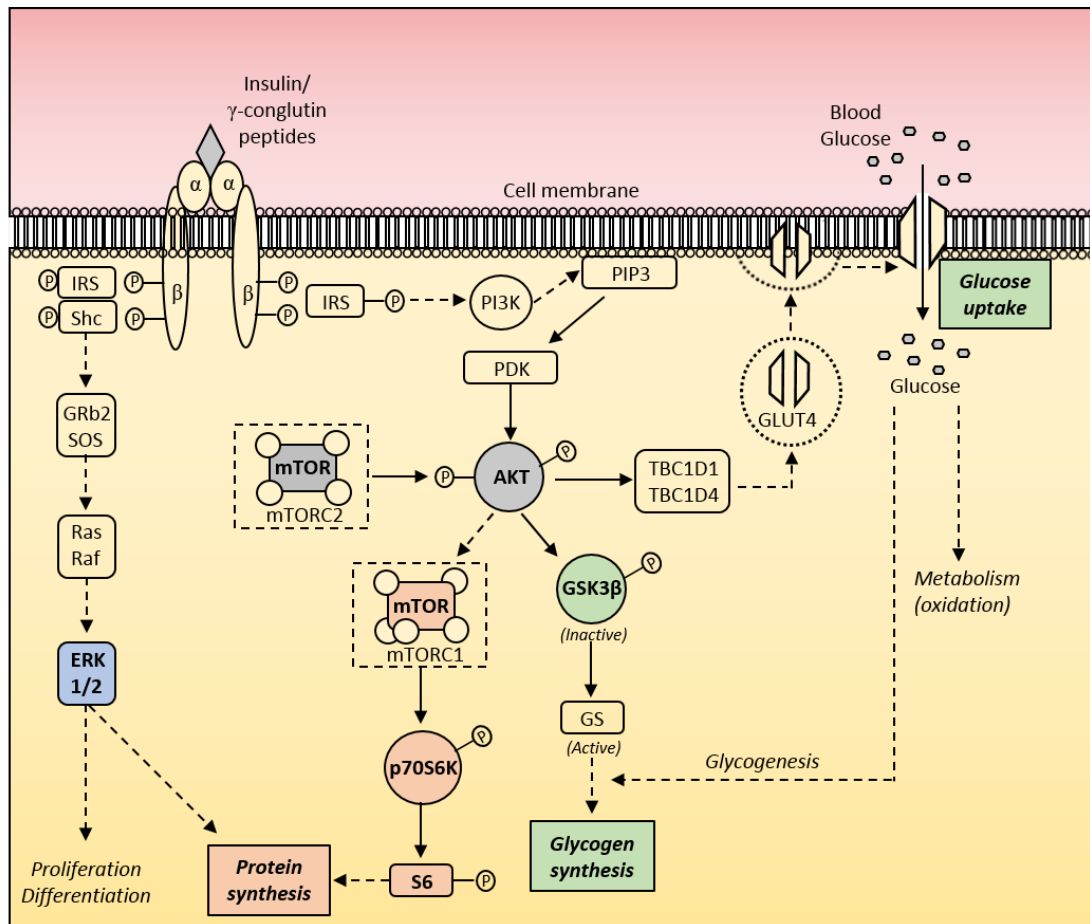
Figure 5.9 Activation of insulin signaling pathway by γ-conglutin peptides: Insulin on binding to its receptor leads to phosphorylation of IRS and Shc proteins which further activates metabolic arm (PI3K/AKT pathway) and mitogenic arm (Ras/Raf/MAPK pathway) respectively. In the metabolic arm, IRS proteins mostly recruit and activate PI3K that leads to the generation of secondary messenger PIP3. Membrane-bound PIP3 activates PDK. Both mTORC2 and PDK are required for complete activation of Akt complex. Activated Akt is the central mediator responsible for regulating insulin's metabolic effects, glycogen and protein synthesis, glucose transport into the cells. Akt mediates protein synthesis by activating mTORC1/p70S6K/S6 pathway ultimately leading to protein synthesis. Also, Akt directly activates GSK3β/GS pathway leading to glycogen synthesis. AKT activates TBC1D1/4 proteins and stimulates modulation of caveolin-3 and flotillin-2 domain within the cell resulting in GLUT-4 translocation to the cell membrane. The mitogenic arm Ras/Raf/MAPK pathway is mostly responsible for cellular growth, differentiation and gene transcription. γ-conglutin

peptides activate the central PI3K/Akt/mTOR signaling pathway further activating pathways responsible for glycogen and protein synthesis. The peptides also affect mitogenic arm by activating ERK1/2 proteins. Thus, γ-conglutin exhibits insulin-mimetic behaviour.

IRS: insulin receptor substrate; PI3K: phosphoinositide-3-kinase; PIP3: phosphatidylinositol (3,4,5)-triphosphate; PDK: 3-phosphoinositide-dependent protein kinase 1; mTORC: mammalian target of rapamycin complex; Akt: protein kinase B; GSK3 β: glucose kinase 3 β; GS: glycogen synthase; GLUT-4: glucose transporter 4; p70S6K: 70KDa ribosomal protein S6 kinase; S6: ribosomal protein S6; MAPK: mitogen-activated protein kinase; ERK: extracellular signal-regulated kinase; TBC1D1/4: TBC1 domain family member 1/4.

5.4.4 γ-conglutin peptides as DPP4 and α-glucosidase enzyme inhibitors

5.4.4.1 DPP4 enzyme inhibition

After food intake, GLP-1 and gastric inhibitory peptide (GIP) incretin hormones are secreted by distal small intestine L cells and proximal small intestine K cells respectively [7]. These hormones stimulate synthesis of insulin and are responsible for ~70% of insulin secretion from pancreatic β cells [269, 270]. Circulating GLP-1 and GIP are rapidly degraded by DPP4 enzyme (half-life less than 2 minutes). Since DPP4 enzyme (serine endopeptidase) cleaves peptides with proline or alanine at the second position from N-terminal, the incretin hormones are its excellent substrates [271]. DPP4 inhibitors, like sitagliptin and saxagliptin, suppresses the activity of DPP4 enzyme and increases the half-life of circulating incretins in blood. Since the introduction of synthetic DPP4 inhibitors as an oral anti-diabetic therapeutic agent, food derived proteins have been isolated, hydrolysed and characterised for evaluation of their inhibitory property [272]. Lupin and soy-derived peptides have been reported to inhibit DPP4 enzyme released from human intestinal epithelial cell line (Caco-2) and circulating in human serum [114].

As a preliminary study, γ-conglutin peptides were investigated for their potential DPP4 inhibitory activity using an *in-vitro* biochemical screening kit. As observed in Figure 5.10, positive control Sitagliptin at 100μM (manufacturer recommended concentration) completely inhibited DPP4 activity [273]. γ-conglutin protein (non-hydrolysed) did not exhibit its inhibitory action, whereas, the hydrolysed form of the protein (γ-conglutin peptides) inhibited the enzyme in a dose-dependent manner. This indicated that the protein had to be digested by pepsin and pancreatin enzymes to

produce peptides having DPP4 inhibitory action. In order to eliminate the fact that inhibition is a resultant of a mixture of peptides competing with the enzyme substrate (H-Gly-Pro-aminomethylcoumarin), a standard peptide digest (500µg/ml) obtained from ThermoFisher Scientific was used as a negative control and exhibited no inhibitory action.
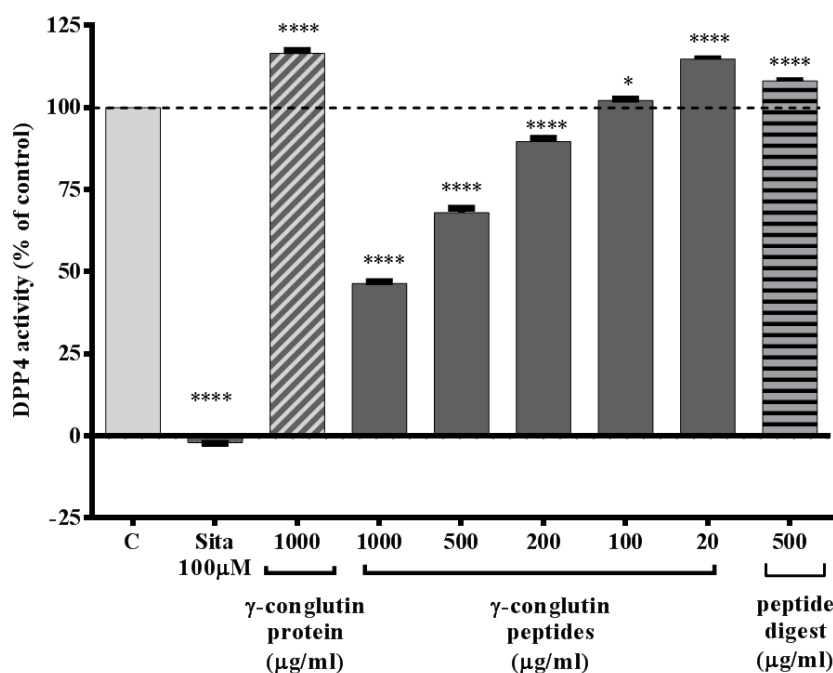
Figure 5.10 Inhibitory effect of different concentration of γ-conglutin peptides (1000-20µg/ml) on the enzymatic activity of dipeptidyl peptidase 4 (DPP4) compared to control referred to as 'C'. Sitagliptan (100µM) referred to as 'Sita' was used as positive control. A standard peptide digest (500µg/ml) obtained from ThermoFisher Scientific was used as a negative control. Values are mean ± standard deviation of three independent experiments; ****p ≤0.0001 and *p ≤0.05 are significantly different as compared to control.

Similar results were also reported by Munoz et al. where γ-conglutin peptides at higher concentration (5mg/ml) completely inhibited DPP4 enzyme [40]. However, in this report, the purity of γ-conglutin protein (non-hydrolysed) was not stated and the SDS-PAGE profile of the purified γ-conglutin also displayed different protein impurity bands between 56-100KDa and 56-21KDa. As a result, there was a possibility that other impurity proteins might be responsible for DPP4 inhibition. The results, herein, confirm the inhibition of DPP4 by peptides obtained from hydrolysis of γ-conglutin protein having purity 100% based on SDS-PAGE (section 3.5.3.1; chapter 3) and 95% based on RP-HPLC (section 3.5.3.3; chapter 3) analysis.

The above results provide preliminary evidence that γ-conglutin peptides might be a potential DPP4 inhibitor. However, *in-vitro* biochemical screening assays do not consider the influence of several factors like bioavailability and stability of peptides, the interaction of peptides with serum components, the effect of serum proteases, *in–vivo* fluid dynamics affecting the inhibition kinetics. As a result, further studies for validating these inhibitory results are required. Considering, the ethical issues associated with *in-vivo* studies, a cell-based *in-situ* DPP4 activity assay can be performed to screen potential inhibitors. Human colon carcinoma Caco-2 cell model is known to express mRNAs translating to active DPP4 enzyme on the apical cell membrane [274, 275]. Also, this cell model is often used as an intestinal barrier in the bioavailability studies as it expresses various morphological and functional features of intestinal cells [276]. Thus, incubating peptides with Caco-2 cells and analysing DPP4 activity can be the next proposed step to evaluate the inhibitory property of γ-conglutin peptides *in situ* followed by *in-vivo* studies [277].

5.4.4.2 α-glucosidase enzyme inhibition

α-glucosidase inhibitors, also known as starch blockers, are another unique type of oral anti-diabetic agents. α-glucosidase is a small intestinal brush border enzyme that cleaves α-1,4 glycosidic linkage in carbohydrates. The enzyme digests starch, oligosaccharides, and disaccharides into glucose monomeric units which are then absorbed into the bloodstream [8]. Inhibitors of α-glucosidase, thus, delay the digestion of α-1,4 linkage carbohydrates (starch and table sugar) and alleviates post-prandial hyperglycemia. Acarbose and Miglitol are the commercial available α-glucosidase inhibitors prescribed mostly to type 2 diabetic patients in combination with other anti-diabetic medications (sulphonylureas, DPP4 inhibitor, metformin) [278]. Plant-derived biomolecules like flavonoids, alkaloids, quinones, phenols, tannins, and terpenes have been reported to exhibit α-glucosidase inhibitor properties [279-281]. Different di, tri, and oligopeptides isolated from plants, animals, and microorganism having a molecular weight from 234 to 1970 Da (2 amino acid residue to 18 amino acid residue) are identified as potential α-glucosidase inhibitors [247]. Analysis of these peptides revealed that the most potent peptides are with 3 to 6 amino acid residues with hydroxyl or basic side chain residue at the N terminal. Since the

hydrolysate of γ-conglutin protein is a mixture of low molecular weight oligopeptides, their α-glucosidase inhibitory potential was investigated.

The inhibitory action of acarbose was evaluated at different concentration (0.001-25mM) in the optimised assay condition (Figure 5.11A). Maximum inhibition of α-glucosidase activity was observed at 10mM acarbose concentration. γ-conglutin peptides from 100μg/ml to 1000μg/ml concentration exhibited a minimal reduction in enzyme activity (6%) (Figure 5.11B). Thus, no prominent α-glucosidase inhibitory action was displayed by γ-conglutin protein (1000μg/ml) and peptides (1000-100μg/ml).
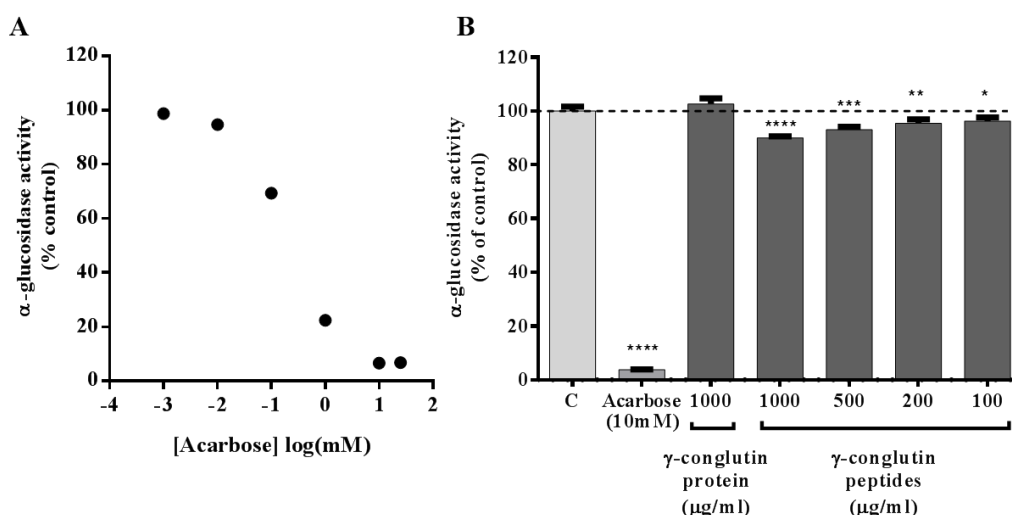
Figure 5.11: Effect of different concentrations of acarbose and γ-conglutin peptides on the enzymatic activity of α-glucosidase enzyme. (A) Dose-response curve of the inhibitory action of acarbose (0.001-25mM) (B) Inhibitory effect of γ-conglutin protein (1000μg/ml) compared to control referred to as 'C'. Acarbose (10mM) used as positive control. Values are mean ± standard deviation of three independent experiments; ****p ≤0.0001, ***p ≤0.001, **p ≤0.01 and *p ≤0.05 are significantly different as compared to control.

5.5 CONCLUSION

Most common current and effective anti-diabetic therapeutics comprise drugs that (A) stimulate pancreatic β cells to secrete more insulin; (B) functions like insulin and improve insulin receptor sensitivity; (C) inhibit DPP4 and α-glucosidase enzymes (D) decrease glucose production in liver (E) are incretin-mimetics and activate GLP-1

receptor in the pancreatic β cell. In this chapter, γ-conglutin peptides were evaluated for their insulinotropic action in pancreatic β cells (BRIN-BD11 and INS-1E), insulin-mimetic action in primary human skeletal muscle cells and enzyme (DPP4 and α-glucosidase) inhibitory effects. γ-conglutin peptides did not exhibit insulinotropic action in pancreatic β cells. The *in-vitro* results demonstrated that, like insulin, γ-conglutin peptides activated insulin signaling pathways responsible for glycogen and protein synthesis. The peptides increased glucose transport into the cells and also activated ERK1/2 proteins that are key regulators of cellular proliferation and differentiation. In addition, the peptides exhibited DPP4 enzyme inhibitory action in static conditions but did not inhibit activity of α-glucosidase enzyme.

Altogether, γ-conglutin peptides have the potential of regulating glucose metabolism by inhibiting DPP4 enzyme activity and functionally behaving like insulin (insulin-mimetics). Further fractionation and screening of particular γ-conglutin peptide(s) responsible for insulin-mimetic and DPP4 inhibitory actions maybe important to refine their hypoglycaemic effects such that they could potentially be used in treatment of type 2 diabetes.

Chapter 6
Conclusions and future work

6.1 CONCLUSIONS

The results presented in this thesis provide evidence that lupin seed proteins may play a beneficial role in regulating blood glucose levels. At first, the proteins were extracted from defatted lupin seed flour and γ-conglutin was purified from this extract. Both lupin protein extract and pure γ-conglutin were subjected to a 'gastrointestinal proteolytic digestion' process. Lupin extract hydrolysate exhibited insulinotropic action by activating intracellular Gα$_q$ signal transduction mechanism in pancreatic β cells. γ-conglutin hydrolysate (peptides) regulated glucose metabolism by activating insulin signal transduction pathway in muscle cells and inhibited DPP4 enzyme activity. The following sections summarise the conclusions of each experimental research chapters in this thesis.

6.1.1 Purification, characterization and hydrolysis of lupin proteins (Chapter 3)

Proteins were extracted from defatted lupin flour and cation exchange chromatography was applied for purification of γ-conglutin from the extract. The elution method was optimised to obtain purified γ-conglutin. The eluted γ-conglutin was characterised using SDS-PAGE, western blot, RP-HPLC and mass spectrometry techniques. The purity of γ-conglutin was found to be ~100% based on SDS-PAGE and ~95% based on RP-HPLC analysis. Both the extract and pure γ-conglutin protein were hydrolysed by gastrointestinal digestive enzymes, pepsin and pancreatin. Degree of hydrolysis achieved for the extract and γ-conglutin was 22% and 18% respectively. It was observed that pepsin hydrolysed the proteins into polypeptides with molecular weight ≤22KDa for extract and ≤30kDa for γ-conglutin, while pancreatin hydrolysed large peptides into small peptides (≤6.5KDa). In order to separate the enzymes from the digestion products, hydrolysate was filtered through 3KDa centrifugal filters. The permeate consisting of mixture of oligopeptides, di-tripeptides and amino acids was evaluated for its anti-diabetic mechanism in different cell lines.

127

6.1.2 Insulinotropic mechanism of action of lupin extract hydrolysate (Chapter 4)

Insulin releasing property of the lupin extract hydrolysate was explored in rat derived pancreatic β cells (BRIN-BD11 and INS-1E). The hydrolysate displayed a dose dependent glucose permissive insulin secretion from β cells. Also, lupin hydrolysate improved insulin secretion in palmitate-induced lipotoxic β cells highlighting its potential application in a physiological environment frequently observed in type 2 diabetes patients. Hydrolysate promoted glucose metabolism by enhancing glucose uptake and rate of glycolysis which later promoted closure of K-ATP channels and membrane depolarisation in β cells. Its mechanism of action in β cells was further investigated in detail. It was found that hydrolysate did not mediate its action through activation of prominent secondary messenger cAMP/PKA signalling pathway. A novel insulin secretory mechanism of lupin hydrolysate mediating through $G\alpha_q$ protein signalling transduction by activating PLC-PKC pathway was established. The proposed hydrolysate induced insulin secretion pathways increased the downstream intracellular Ca^{2+} levels causing insulin exocytosis from β cells.

6.1.3 Anti-diabetic mechanisms of action of γ-conglutin peptides (Chapter 5)

Hydrolysis of purified γ-conglutin resulted in mixture of di-tri and oligopeptides in range of 8.4 to 0.6KDa molecular weight. Insulinotropic action in pancreatic β cells (BRIN-BD11 and INS-1E), insulin-mimetic action in primary human skeletal muscle cells, and enzyme (DPP4 and α-glucosidase) inhibitory effect of γ-conglutin peptides were evaluated. It was found that these peptides did not stimulate insulin secretion in β cells, however, they exhibited potent insulin-mimetic action by regulating glucose and protein metabolism in human muscle cells. Peptides activated Akt protein, a central mediator that stimulates a range of metabolic processes and enhanced glucose transport into the cells. Peptides were also found to activate the downstream targets p70S6K/S6 and GSK3β resulting in increased cellular protein and glycogen synthesis respectively. Moreover, these peptides, like insulin, also activated ERK and have potential of regulating cell proliferation and differentiation. Thus, γ-conglutin peptides displayed functional characteristics of insulin by activating insulin signal transduction suggesting a possible therapeutic application as an insulin-mimetic agent. In addition, peptides (1mg/ml) inhibited DPP4 enzyme activity (by 55%) as evaluated with *in-vitro*

bioassay. However, further investigations in validating the latter inhibitory results are now required.

The present research provides scientific substantiation of the mechanisms associated with health benefits related to lupin seed proteins. The results presented herein are one of the preliminary steps in improvement in the current market of lupins as stockfeed, towards lupin-based food products for human consumption as well as the inclusion of lupin proteins in nutraceuticals and functional food.

6.2 RECOMMENDATIONS FOR FUTURE WORK

This thesis provides comprehensive information related to *in-vitro* anti-diabetic action of lupin proteins and peptides explored in different cell lines. Nevertheless, there are various areas where further research is required.

6.2.1 *Ex-vivo* and *in-vivo* animal studies

The proposed biological / biochemical mechanisms outlined in Chapter 4 of this thesis offer a novel perspective for the insulinotropic action of lupin hydrolysate in β-cells. This mechanism of action was preliminarily investigated in insulinoma derived pancreatic β cell models (BRIN-BD11 and INS-1E). The next step would be to confirm hydrolysate induced insulin secretion in primary islets *ex-vivo* isolated from rat/mouse pancreas. The insulin-mimetic action of γ-conglutin peptides was investigated in primary human skeletal muscle cells isolated directly from a donor (chapter 5). It would be useful to validate this glucose modulatory property of γ-conglutin peptides in normal (healthy) and diabetic animal models *in-vivo*.

6.2.2 Large scale manufacturing of high purity γ-conglutin

Currently, the developed process on 5ml HiScreen CaptoS column has been successfully implemented at lab scale for producing ~250mg of γ-conglutin in ~22hours. However, the yield (4.8% w/w of load proteins) of the process can be improved by optimising method to prevent loss of γ-conglutin in flow through. The protein concentration of the load should be increased by concentrating the load (feed) using membrane filtration. The concentrated protein load will reduce the load volume

and the process time, thus, increasing the process productivity. This would also be beneficial for scaling up the process on 20 ml CaptoS column.

The exact content of γ-conglutin in seeds varies because of genetic and environmental effects [282]. As a result, calculating the process recovery (extraction and purification) based on γ-conglutin in seed is difficult. Therefore, reliable methods for quantification of γ-conglutin in lupin seeds are required. An isotope labelled multiple reaction monitoring mass spectrometry (MRM-MS) method for absolute quantification of γ-conglutin is currently being developed and validated for different lupin species and varieties in our laboratories.

6.2.3 Gastrointestinal digestion and bioavailability of lupin proteins and peptides

The extract proteins and γ-conglutin were hydrolysed using gastrointestinal proteolytic enzymes i.e. pepsin and pancreatin (section 3.5.4; chapter 3). It would be interesting to hydrolyse extract proteins and γ-conglutin using simulated gastrointestinal digestion protocol containing enzymes that breakdown carbohydrate, proteins and lipids at different digestion stages. In this way, the carbohydrate moieties attached to proteins (glycoproteins) can also be digested into monomeric sugar forms and bioactivity of the peptides in presence of these hydrolysed sugars can be studied together. The next step would be to fractionate the extract and γ-conglutin hydrolysate peptides based on their size, hydrophobicity and charge using membrane filtration, RP-HPLC and ion exchange chromatography techniques respectively [283]. The fractionated peptides can then be assessed for potential bioavailability. Caco-2 cell model is often used as an intestinal barrier in the bioavailability studies as it expresses various morphological and functional features of intestinal cells [277]. As a result, the peptide fraction can be subjected to a dual cell culture system with Caco-2 cell monolayer (apical) and pancreatic β cells or human skeletal muscle cells (basal) to mimic *in-vitro* gastrointestinal absorption condition and to substantiate the bioactivity of the peptides that may enter circulation *in vivo* [175]. Further, mass spectrometry can be used to elucidate the profile and structure of the bioactive peptides passing through Caco2 cell monolayer (apical). The screened peptides can be incubated in plasma in order to assess their resistance to endopeptidase and the peptide structure can be tailored to prevent them from degradation or prolong their half-life in circulating plasma without

losing bioactivity. This approach will lead to development of peptide-based food ingredients and nutraceutical from lupin.

6.2.4 Insulin signal transduction

Insulin-mimetic action of γ-conglutin peptides was explored in Chapter 5. γ-conglutin peptides promoted an increase in glucose uptake/transport in muscle cells. However, the impact of peptides on activation of signalling pathway associated with glucose receptor 4 (GLUT-4) translocation to the membrane requires further investigation. This will enable a deeper insight into γ-conglutin peptide regulated muscle energy and glucose metabolism and will substantiate data obtained from glycolytic flux and mitochondrial respiration in muscle cells (Seahorse based technology).

Like insulin, peptides also induced activation of ERK 1/2 in muscle cells. However, activation of other cellular proteins involved in Ras/MAPK mitogenic pathway requires further investigation with respect to the effect of peptides on cellular growth and differentiation.

6.2.5 Interaction of γ-conglutin peptides with insulin

γ-conglutin protein exhibits an electrostatic binding interaction with insulin immobilised on agarose gel matrix and the equilibrium dissociation constant of this interaction is in moderate affinity range of protein-ligand interaction as recorded by real-time SPR analysis of γ-conglutin with insulin [100]. It would be interesting to study the influence of γ-conglutin peptides on insulin-insulin receptor interaction by immobilising insulin receptors (IR) obtained from IR-overexpressing Chinese hamster ovary cells on SPR biosensor chips. Also, this strategy can be used to determine if any particular peptide fragment of γ-conglutin interacts specifically with insulin.

6.2.6 DPP4 inhibitory action

DPP4 inhibitory action of γ-conglutin peptides were evaluated using *in-vitro* biochemical screening assay. However, *in-vitro* enzymatic assays do not account for factors that influence the stability and bioactivity of peptides *in vivo*. As a result, the inhibitory action of peptides in a cell-based DPP4 activity assay should be further

examined. Human colon carcinoma Caco-2 cell model is known to express mRNAs translating to active DPP4 enzyme on the apical cell membrane [274, 275]. Thus, the peptides can be incubated with Caco-2 cells and activity of DPP4 expressed by the cells can be analysed. [277]. Also, the inhibitory action of peptides on a circulating form of DPP4 in human serum can be evaluated.

6.2.7 Lupin proteins as human supplements

After studying hypoglycaemic effects of lupin proteins in animals (*in-vivo*) and exploring its mechanism of action in cell lines (*in-vitro*) and animal tissues (*ex-vivo*), lupin protein extract and/or γ-conglutin can be tested as supplements for diabetes treatment in humans. A placebo-controlled clinical trial can be conducted by administering dry extract/ γ-conglutin in form of sachets or tablets to volunteers (healthy/type 2 diabetes) for 6-8 weeks. Alternatively, the volunteers can be administered with extract/ γ-conglutin enriched meal or beverages. The glucose and insulin blood levels should be monitored during the course of this study. Also, appetite and fluid intake, haemodynamic parameters and any side-effects or adverse effects during the course should be recorded.

Altogether, the knowledge obtained from this research can be beneficial to several sectors of the community. The nutraceutical/biopharmaceutical industries would benefit with the developed process strategy for purification of glycaemic modulating protein - γ-conglutin. Increase in demand of purified γ-conglutin or lupin-based products can create a surge in lupin production and markets which will motivate farmers to grow this nitrogen-fixing lupin rotation crop. With the increase in lupin cultivation, agriculture industries would profit from the increased demand and return on lupin crops. Eventually, health professional, nutritionist, and dieticians would benefit through the availability of new natural source derived glucose modulating agent which may have lesser side effects as compared to traditional synthetic drugs. Diabetic consumers can gain advantage by a potential reduction in healthcare cost. All these factors can promote sustainable production of lupin, a crop well suited to deep acid sandy soil environment of Western Australian wheat belt, in turn making a high-value health beneficial economic product for the society.

REFERENCES

1.   Cnop, M., et al., *Mechanisms of pancreatic β-cell death in type 1 and type 2 diabetes: many differences, few similarities.* Diabetes, 2005. **54**(suppl 2): p. S97-S107.

2.   Fonseca, V.A., *Defining and characterizing the progression of type 2 diabetes.* Diabetes care, 2009. **32**(suppl 2): p. S151-S156.

3.   Gerich, J.E. *Contributions of insulin-resistance and insulin-secretory defects to the pathogenesis of type 2 diabetes mellitus*. in *Mayo Clinic Proceedings*. 2003. Elsevier.

4.   DiabetesAustralia, *Living with diabetes, preventing complications.* https://www.diabetesaustralia.com.au/preventing-complications, 2015.

5.   Australia, D., *General practice management of type 2 diabetes.* The Royal Austalian College of General Practitioners, 2014. **2**: p. 10-12.

6.   Bolen, S., et al., *Systematic review: comparative effectiveness and safety of oral medications for type 2 diabetes mellitus.* Annals of internal medicine, 2007. **147**(6): p. 386-399.

7.   Drucker, D.J. and M.A. Nauck, *The incretin system: glucagon-like peptide-1 receptor agonists and dipeptidyl peptidase-4 inhibitors in type 2 diabetes.* The Lancet, 2006. **368**(9548): p. 1696-1705.

8.   Lebovitz, H.E., *Alpha-glucosidase inhibitors.* Endocrinology and metabolism clinics of North America, 1997. **26**(3): p. 539-551.

9.   WHO, *World Diabetes Day 2018.* World health organisation, 2018. **https://www.who.int/diabetes/world-diabetes-day-2018/en/**.

10.   IDF, *International Diabetes Federation.* IDF Diabetes Atlas 2017. **8th edition**.

11.   Association, A.D., *Economic costs of diabetes in the US in 2017.* Diabetes care, 2018. **41**(5): p. 917-928.

12.   Gannon, M.C., et al., *An increase in dietary protein improves the blood glucose response in persons with type 2 diabetes.* The American journal of clinical nutrition, 2003. **78**(4): p. 734-741.

13.   Chandalia, M., et al., *Beneficial effects of high dietary fiber intake in patients with type 2 diabetes mellitus.* New England Journal of Medicine, 2000. **342**(19): p. 1392-1398.

14.   Asif, M., *The prevention and control the type-2 diabetes by changing lifestyle and dietary pattern.* Journal of education and health promotion, 2014. **3**.

15.   Bösenberg, L.H. and D.G. van Zyl, *The mechanism of action of oral antidiabetic drugs: A review of recent literature.* Journal of Endocrinology, Metabolism and Diabetes of South Africa, 2008. **13**(3): p. 80-88.

16.   Gurib-Fakim, A., *Medicinal plants: traditions of yesterday and drugs of tomorrow.* Molecular aspects of Medicine, 2006. **27**(1): p. 1-93.

17.   Gray, A.M. and P.R. Flatt, *Nature's own pharmacy: The diabetes perspective.* Proceedings of the Nutrition Society, 1997. **56**(1B): p. 507-517.

18. Arumugam, G., P. Manjula, and N. Paari, *A review: Anti diabetic medicinal plants used for diabetes mellitus.* Journal of Acute Disease, 2013. **2**(3): p. 196-200.

19. Surya, S., et al., *Diabetes mellitus and medicinal plants-a review.* Asian Pacific Journal of Tropical Disease, 2014. **4**(5): p. 337-347.

20. Yeh, G.Y., et al., *Systematic review of herbs and dietary supplements for glycemic control in diabetes.* Diabetes care, 2003. **26**(4): p. 1277-1294.

21. Atanasov, A.G., et al., *Discovery and resupply of pharmacologically active plant-derived natural products: A review.* Biotechnology advances, 2015. **33**(8): p. 1582-1614.

22. Chang, C.L., et al., *Herbal therapies for type 2 diabetes mellitus: chemistry, biology, and potential application of selected plants and compounds.* Evidence-Based Complementary and Alternative Medicine, 2013. **2013**.

23. Tharanathan, R. and S. Mahadevamma, *Grain legumes—a boon to human nutrition.* Trends in Food Science & Technology, 2003. **14**(12): p. 507-518.

24. DPIRD, *Lupin in Western Australian Farming.* Department of Primary Industries and Regional Development, Agriculture and Food, Government of WA, 2017. **https://www.agric.wa.gov.au/lupins/lupin-western-australian-farming**.

25. DPIRD, *Lupin essentials – growing a successful lupin crop.* Department of Primary Industries and Regional Development, Agriculture and Food, Government of WA, 2018. **https://www.agric.wa.gov.au/lupins/lupin-essentials-%E2%80%93-growing-successful-lupin-crop**.

26. Duranti, M., *Grain legume proteins and nutraceutical properties.* Fitoterapia, 2006. **77**(2): p. 67-82.

27. DAFWA, *Australian Sweet Lupin - A very healthy asset.* Department of Agriculture and Food,

Government of Western Australia, 2008.

28. OGTR, *The Biology of Lupinus L. (lupin or lupine).* Department of Health and Ageing, office of the Gene Technology Regulator, 2013. **http://www.ogtr.gov.au**.

29. DPIRD, *Western Australian lupin industry.* Department of Primary Industries and Regional Development, Agriculture and Food, Government of WA, 2018. **https://www.agric.wa.gov.au/crops/grains/lupins**.

30. AgriFutures, *Lupin.* AgriFutures Australia, 2017. **https://www.agrifutures.com.au/farm-diversity/lupin/**.

31. Capraro, J., et al., *Pasta supplemented with isolated lupin protein fractions reduces body weight gain and food intake of rats and decreases plasma glucose concentration upon glucose overload trial.* Food & function, 2014. **5**(2): p. 375-380.

32. Dove, E.R., et al., *Lupin and soya reduce glycaemia acutely in type 2 diabetes.* British Journal of Nutrition, 2011. **106**(7): p. 1045-1051.

33. Hall, R.S., S.J. Thomas, and S.K. Johnson, *Australian sweet lupin flour addition reduces the glycaemic index of a white bread breakfast without affecting palatability in healthy human volunteers.* Asia Pacific journal of clinical nutrition, 2005. **14**(1): p. 91.

34. Keogh, J., et al., *Food intake, postprandial glucose, insulin and subjective satiety responses to three different bread-based test meals.* Appetite, 2011. **57**(3): p. 707-710.

35. Lee, Y.P., et al., *Lupin-enriched bread increases satiety and reduces energy intake acutely–.* The American journal of clinical nutrition, 2006. **84**(5): p. 975-980.

36. Pereira, F.C., et al., *Insulinotropic action of white lupine seeds (Lupinus albus L.): effects on ion fluxes and insulin secretion from isolated pancreatic islets.* Biomedical Research, 2001. **22**(2): p. 103-109.

37. López, P.M.G., et al., *Quinolizidine alkaloids isolated from Lupinus species enhance insulin secretion.* European journal of pharmacology, 2004. **504**(1): p. 139-142.

38. Duranti, M., et al., *The major proteins of lupin seed: characterisation and molecular properties for use as functional and nutraceutical ingredients.* Trends in Food Science & Technology, 2008. **19**(12): p. 624-633.

39. Mane, S., *Isolation and purification of protein (Conglutin-g) from lupin Seeds.* 2018.

40. Muñoz, E.B., et al., *Gamma-conglutin peptides from Andean lupin legume (Lupinus mutabilis Sweet) enhanced glucose uptake and reduced gluconeogenesis in vitro.* Journal of Functional Foods, 2018. **45**: p. 339-347.

41. Terruzzi, I., et al., *Insulin-mimetic action of conglutin-γ, a lupin seed protein, in mouse myoblasts.* Nutrition, Metabolism and Cardiovascular Diseases, 2011. **21**(3): p. 197-205.

42. Wojciechowicz, T., et al., *Suppressive effects of γ-conglutin on differentiation of 3T3-L1 preadipocytes.* International Journal of Food Science & Technology, 2018. **53**(11): p. 2624-2630.

43. Shewry, P.R., J.A. Napier, and A.S. Tatham, *Seed storage proteins: structures and biosynthesis.* The plant cell, 1995. **7**(7): p. 945.

44. USDA, *Lupinus classification*, in *Natural Resources Conservation Services, United States Department of Agriculture*. https://plants.usda.gov/java/ClassificationServlet?source=display&classid=LUPIN.

45. ITIS, *Integrated Taxonomic Information System.* www.itis.gov, 2017.

46. lupins.org, *Lupins information source.* www.lupins.org, 2015.

47. Bermejo, J.E.H. and J. León, *Neglected crops: 1492 from a different perspective*. 1994: Food & Agriculture Org.

48. PulseAustralia, *Lupin.* http://www.pulseaus.com.au/growing-pulses/bmp/lupin#marketing-and-standards, 2019.

49. Magni, C., et al., *Updating lupin seed protein research and development.* Opportunities to give a boost to a wealthy food protein source for human nutrition Agro FOOD Industry Hi Tech, 2014. **25**: p. 39-42.

50. Arnoldi, A., et al., *The health benefits of sweet lupin seed flours and isolated proteins.* Journal of Functional Foods, 2015. **18**: p. 550-563.

51. WHO/IUIS, *Lup a 5 and Lup an 1 allergen.* WHO/IUIS World Health Organisation (WHO) / International Union of Immunological Societies (IUIS), Allergen nomenclature, 2017. **http://www.allergen.org**.

52. Goggin, D.E., et al., *Proteomic analysis of lupin seed proteins to identify conglutin β as an allergen, Lup an 1.* Journal of Agricultural and Food Chemistry, 2008. **56**(15): p. 6370-6377.

53. ASCIA, *Lupin allergy.* Australian society of clinical immunology allergy, 2015. **www.allergy.org.au**.

54. Smith, W.B., D. Gillis, and F.E. Kette, *Lupin: a new hidden food allergen.* 2004.

55. Woo, A., *Lupin in packaged and non-packaged foods–potential for allergic reactions (3158875) BSc Thesis.* The University of New South Wales, School of Chemical Sciences and Engineering, Department of Food Science and Technology, 2008.

56. Foodstandards, *Allergen labelling.* Food standards, Australia New Zealand, 2017. **www.foodstandards.gov.au/allergenlabelling**.

57. Johnson, S.K., et al., *Lupins: Their unique nutritional and health-promoting attributes*, in *Gluten-Free Ancient Grains*. 2017, Elsevier. p. 179-221.

58. Glencross, B.D., *Feeding lupins to fish: A review of the nutritional and biological value of lupins in aquaculture feeds*. 2001: Department of Fisheries--Research Division, Government of Western Australia.

59. Petterson, D., *Composition and food uses of lupins.* Lupins as crop plants: biology, production, and utilization, 1998: p. 353-384.

60. Cowling, W.A. and A. Tarr, *Effect of genotype and environment on seed quality in sweet narrow-leafed lupin (Lupinus angustifolius L.).* Australian Journal of Agricultural Research, 2004. **55**(7): p. 745-751.

61. Uzun, B., et al., *Fat and fatty acids of white lupin (Lupinus albus L.) in comparison to sesame (Sesamum indicum L.).* Food Chemistry, 2007. **102**(1): p. 45-49.

62. Rona, C., F. Vailati, and E. Berardesca, *The cosmetic treatment of wrinkles.* Journal of cosmetic dermatology, 2004. **3**(1): p. 26-34.

63. Kurlovich, B., et al., *Biochemical composition.* Lupins. Geography, classification, genetic resources and breeding. INTAN, St Petersburg, 2002: p. 241-267.

64. Kohajdova, Z., J. Karovičová, and Š. Schmidt, *Lupin composition and possible use in bakery–a review.* Czech J Food Sci, 2011. **29**(3): p. 203-211.

65. Osborne, T., *The vegetable proteins. 1924.* Brown, WL: J. biol. Chem, 1944. **154**: p. 57.

66. Blagrove, R. and J. Gillespie, *Isolation, purification and characterization of the seed globulins of Lupinus angustifolius.* Functional Plant Biology, 1975. **2**(1): p. 13-27.

67. Gueguen, J. and P. Cerletti, *Proteins of some legume seeds: soybean, pea, fababean and lupin*, in *New and developing sources of food proteins*. 1994, Springer. p. 145-193.

68. Casey, R., *Distribution and some properties of seed globulins*, in *Seed proteins*. 1999, Springer. p. 159-169.

69. Duranti, M., et al., *The seed globulins of Lupinus albus.* Phytochemistry, 1981. **20**(9): p. 2071-2075.

70. Duranti, M., et al., *The molecular basis for N-glycosylation in the 11S globulin (legumin) of lupin seed.* Journal of protein chemistry, 1995. **14**(2): p. 107-110.

71. Duranti, M., E. Cucchetti, and P. Cerletti, *Changes in composition and subunits in the storage proteins of germinating lupine seeds.* Journal of Agricultural and Food Chemistry, 1984. **32**(3): p. 490-493.

72. Duranti, M., et al., *Thermal stabilities of lupin seed conglutin γ protomers and tetramers.* Journal of agricultural and food chemistry, 2000. **48**(4): p. 1118-1123.

73. Capraro, J., et al., *Spectroscopic studies on the pH-dependent structural dynamics of γ-conglutin, the blood glucose-lowering protein of lupin seeds.* International journal of biological macromolecules, 2010. **47**(4): p. 502-507.

74. Restani, P., et al., *Subunit composition of the seed globulins of Lupinus albus.* Phytochemistry, 1981.

75. Eaton-Mordas, C.A. and K.G. Moore, *Seed glycoproteins of Lupinus angustifolius.* Phytochemistry, 1978. **17**(4): p. 619-621.

76. Allen, J.G., *Toxins and lupinosis.* Lupines as a crop plant biology, production and utilization, 1998: p. 411-428.

77. Kamel, K.A., et al., *Quantitative and qualitative content of alkaloids in seeds of a narrow-leafed lupin (Lupinus angustifolius L.) collection.* Genetic Resources and Crop Evolution, 2016. **63**(4): p. 711-719.

78. MOSAAD, M.N., et al., *HYPOGLYCEMIC EFFECT OF LUPIN ALKALOIDS AND/OR ROSIGLITAZONE IN PREGNANT DIABETIC RATS IN RELATION TO ATHEROGENIC INDEX.*

79. Baldeón, M.E., et al., *Hypoglycemic effect of cooked Lupinus mutabilis and its purified alkaloids in subjects with type-2 diabetes.* Nutricion hospitalaria, 2012. **27**(4).

80. Bohn, T., *Bioactivity of carotenoids–chasms of knowledge.* Int. J Vitam. Nutr. Res, 2016.

81. Wang, S., S. Errington, and H.H. Yap. *Studies on carotenoids from lupin seeds.* in *Lupins for Health and Wealth'Proceedings of the 12th International Lupin Conference*. 2008.

82. Lampart-Szczapa, E., et al., *Antioxidant properties of lupin seed products.* Food chemistry, 2003. **83**(2): p. 279-285.

83. James, P. and R. McFadden, *Understanding the processes behind the regulation of blood glucose.* Nursing times, 2004. **100**(16): p. 56-58.

84. Layden, B., V. Durai, and W. Lowe Jr, *G-protein-coupled receptors, pancreatic islets, and diabetes.* Nature Education, 2010. **3**(9): p. 13.

85. Komatsu, M., et al., *Glucose-stimulated insulin secretion: A newer perspective.* Journal of diabetes investigation, 2013. **4**(6): p. 511-516.

86. Arnoldi, A. and S. Greco, *Nutritional and nutraceutical characteristics of lupin protein.* Nutrafoods, 2011. **10**(4): p. 23-29.

87. Scarafoni, A., C. Magni, and M. Duranti, *Molecular nutraceutics as a mean to investigate the positive effects of legume seed proteins on human health.* Trends in Food Science & Technology, 2007. **18**(9): p. 454-463.

88. Graham, M.L., et al., *The streptozotocin-induced diabetic nude mouse model: differences between animals from different sources.* Comparative medicine, 2011. **61**(4): p. 356-360.

89. Sah, S.P., et al., *Animal models of insulin resistance: A review.* Pharmacological Reports, 2016. **68**(6): p. 1165-1177.

90. Bouchoucha, R., et al., *Anti-hyperglycemic and Anti-hyperlipidemic Effects of Lupinus albus in Type 2 Diabetic Patients: A Randomized Double-blind, Placebo-controlled Clinical Trial.* International Journal of Pharmacology, 2016. **12**(8): p. 830-837.

91. Khalil, S.S., et al., *COMBINATION OF GLICLAZIDE DRUG AND LUPIN SEEDS POWDER ALLEVIATE HYPERGLYCEMIA ON INDUCED-DIABETIC RATS RECEIVING HIGH-FAT HIGH FRUCTOSE/SUCROSE DIET.* Veterinary Medicine In-between Health & Economy (VMHE)–16-19 October 2018, 2018. **55**(20-Suppl).

92. Lovati, M.R., et al., *Lupin seed γ-conglutin lowers blood glucose in hyperglycaemic rats and increases glucose consumption of HepG2 cells.* British Journal of Nutrition, 2012. **107**(1): p. 67-73.

93. MOSAAD, M.N., et al., *HYPOGLYCEMIC EFFECT OF LUPIN ALKALOIDS AND/OR ROSIGLITAZONE IN PREGNANT DIABETIC RATS IN RELATION TO ATHEROGENIC INDEX.* International Journal of Pharmacy and Pharmaceutical Sciences, 2014. **6**(3): p. 1-8.

94. Wiedemann, M., et al., *Lupanine improves glucose homeostasis by influencing KATP channels and insulin gene expression.* Molecules, 2015. **20**(10): p. 19085-19100.

95. Karamanlis, A., et al., *Effects of protein on glycemic and incretin responses and gastric emptying after oral glucose in healthy subjects–.* The American Journal of Clinical Nutrition, 2007. **86**(5): p. 1364-1368.

96. Gannon, M.C., et al., *The insulin and glucose responses to meals of glucose plus various proteins in type II diabetic subjects.* Metabolism-Clinical and Experimental, 1988. **37**(11): p. 1081-1088.

97. Nuttall, F.Q. and M.C. Gannon, *Plasma glucose and insulin response to macronutrients in nondiabetic and NIDDM subjects.* Diabetes Care, 1991. **14**(9): p. 824-838.

98.   Lima-Cabello, E., et al., *Narrow-leafed lupin (Lupinus angustifolius L.) β-conglutin proteins modulate the insulin signaling pathway as potential type 2 diabetes treatment and inflammatory-related disease amelioration.* Molecular nutrition & food research, 2017. **61**(5).

99.   Lima-Cabello, E., et al., *Narrow-leafed lupin (Lupinus angustifolius L.) seed β-conglutins reverse the induced insulin resistance in pancreatic cells.* Food & function, 2018. **9**(10): p. 5176-5188.

100.   Magni, C., et al., *Conglutin γ, a lupin seed protein, binds insulin in vitro and reduces plasma glucose levels of hyperglycemic rats.* The Journal of nutritional biochemistry, 2004. **15**(11): p. 646-650.

101.   Bertoglio, J.C., et al., *Hypoglycemic effect of lupin seed γ-conglutin in experimental animals and healthy human subjects.* Fitoterapia, 2011. **82**(7): p. 933-938.

102.   Vargas-Guerrero, B., et al., *Administration of lupinus albus gamma conglutin (Cγ) to n5 STZ rats augmented Ins-1 gene expression and pancreatic insulin content.* Plant foods for human nutrition, 2014. **69**(3): p. 241-247.

103.   Rutter, G.A., *Diabetes: the importance of the liver.* Current biology, 2000. **10**(20): p. R736-R738.

104.   Lovati, M.R., et al., *Internalization of intact γ-conglutin, the lupin seed glucoselowering glycoprotein, by Hep G2 cells: biochemical and microscopy studies.* The FASEB Journal, 2013. **27**(1 Supplement): p. 637.14-637.14.

105.   Uldry, M. and B. Thorens, *The SLC2 family of facilitated hexose and polyol transporters.* Pflügers Archiv, 2004. **447**(5): p. 480-489.

106.   Sandoval-Muñíz, R.d.J., et al., *Lupin gamma conglutin protein: effect on Slc2a2, Gck and Pdx-1 gene expression and GLUT2 levels in diabetic rats.* Revista Brasileira de Farmacognosia, 2018. **28**(6): p. 716-723.

107.   Association, A.D., *Standards of medical care in diabetes—2016 abridged for primary care providers.* Clinical diabetes: a publication of the American Diabetes Association, 2016. **34**(1): p. 3.

108.   Van Schaftingen, E. and I. Gerin, *The glucose-6-phosphatase system.* Biochemical Journal, 2002. **362**(3): p. 513-532.

109.   González-Santiago, A.E., et al., *Lupinus albus conglutin gamma modifies the gene expressions of enzymes involved in glucose hepatic production in vivo.* Plant Foods for Human Nutrition, 2017. **72**(2): p. 134-140.

110.   Sirtori, C.R., et al., *Proteins of white lupin seed, a naturally isoflavone-poor legume, reduce cholesterolemia in rats and increase LDL receptor activity in HepG2 cells.* The Journal of nutrition, 2004. **134**(1): p. 18-23.

111.   Saltiel, A.R. and C.R. Kahn, *Insulin signalling and the regulation of glucose and lipid metabolism.* Nature, 2001. **414**(6865): p. 799.

112.   Auwerx, J., et al., *Transcription, adipocyte differentiation, and obesity.* Journal of Molecular Medicine, 1996. **74**(7): p. 347-352.

113.   Ahren, B., *DPP-4 inhibitors.* Best Practice & Research Clinical Endocrinology & Metabolism, 2007. **21**(4): p. 517-533.

114.	Lammi, C., et al., *Soybean-and lupin-derived peptides inhibit DPP-IV activity on in situ human intestinal Caco-2 cells and ex vivo human serum.* Nutrients, 2018. **10**(8): p. 1082.

115.	ZHU, B.C., R.A. LAINE, and M.D. BARKLEY, *Intrinsic tryptophan fluorescence measurements suggest that polylactosaminyl glycosylation affects the protein conformation of the gelatin-binding domain from human placental fibronectin.* European journal of biochemistry, 1990. **189**(3): p. 509-516.

116.	Duranti, M., et al., *The Saccharide Chain of Lupin Seed Conglutin γ is not Responsible for the Protection of the Native Protein from Degradation by Trypsin, but Facilitates the Refolding of the Acid-Treated Protein to the Resistant Conformation.* European journal of biochemistry, 1995. **230**(3): p. 886-891.

117.	Capraro, J., et al., *Susceptibility of lupin γ-conglutin, the plasma glucose-lowering protein of lupin seeds, to proteolytic enzymes.* Journal of agricultural and food chemistry, 2009. **57**(18): p. 8612-8616.

118.	Czubinski, J., et al., *Characterisation of different digestion susceptibility of lupin seed globulins.* Food chemistry, 2014. **143**: p. 418-426.

119.	Czubiński, J., A. Siger, and E. Lampart-Szczapa, *Digestion susceptibility of seed globulins isolated from different lupin species.* European Food Research and Technology, 2016. **242**(3): p. 391-403.

120.	Hughes, T.R. and I.M. Klotz, *Analysis of metal-protein complexes.* Methods of biochemical analysis, 1956: p. 265-299.

121.	Duranti, M., et al., *Interaction of metal ions with lupin seed conglutin γ.* Phytochemistry, 2001. **56**(6): p. 529-533.

122.	Bader, S., et al., *Characterisation of odour-active compounds in lupin flour.* Journal of the Science of Food and Agriculture, 2009. **89**(14): p. 2421-2427.

123.	Bader, S., et al., *Influence of different organic solvents on the functional and sensory properties of lupin (Lupinus angustifolius L.) proteins.* LWT-Food Science and Technology, 2011. **44**(6): p. 1396-1404.

124.	Sironi, E., F. Sessa, and M. Duranti, *A simple procedure of lupin seed protein fractionation for selective food applications.* European Food Research and Technology, 2005. **221**(1-2): p. 145-150.

125.	Bahrami, N., et al., *Comparison of ambient solvent extraction methods for the analysis of fatty acids in non-starch lipids of flour and starch.* Journal of the Science of Food and Agriculture, 2014. **94**(3): p. 415-423.

126.	Wong, A., et al., *Isolation and foaming functionality of acid-soluble protein from lupin (Lupinus angustifolius) kernels.* Journal of the Science of Food and Agriculture, 2013. **93**(15): p. 3755-3762.

127.	Sipsas, S., *New Lupin Products: Final Report of Project DAW00069.* Grains Research and Development Corporation, Barton, ACT, Australia., 2004.

128.	El-Adawy, T., et al., *Nutritional potential and functional properties of sweet and bitter lupin seed protein isolates.* Food Chemistry, 2001. **74**(4): p. 455-462.

129.	Blaicher, F., R. Nolte, and K. Mukherjee, *Lupin protein concentrates by extraction with aqueous alcohols.* Journal of the American Oil Chemists' Society, 1981. **58**(7): p. A761-A765.

130.	Hron Sr, R., S. Koltun, and A. Graci Jr, *Biorenewable solvents for vegetable oil extraction.* Journal of the American Oil Chemists' Society, 1982. **59**(9): p. 674A-684A.

131.	Wäsche, A., K. Müller, and U. Knauf, *New processing of lupin protein isolates and functional properties.* Food/Nahrung, 2001. **45**(6): p. 393-395.

132.	Mane, S.P., et al., *Lupin seed γ-conglutin: Extraction and purification methods-A review.* Trends in Food Science & Technology, 2018. **73**: p. 1-11.

133.	Healthcare, G., *Ion Exchange Chromatography & Chromatofocusing: Principles and Methods.* Edition AA, Amersham Biosciences, 2010: p. 7.

134.	Villarino, C.B.J., *Maximising the nutritional and sensory quality of Lupin bread made using Western Australian bakers flour.* 2014, Curtin University.

135.	Derbyshire, E., D. Wright, and D. Boulter, *Legumin and vicilin, storage proteins of legume seeds.* Phytochemistry, 1976. **15**(1): p. 3-24.

136.	Mane, S., et al., *Reverse phase HPLC method for detection and quantification of lupin seed γ-conglutin.* Journal of Chromatography B, 2017. **1063**: p. 123-129.

137.	Heukeshoven, J. and R. Dernick, *Simplified method for silver staining of proteins in polyacrylamide gels and the mechanism of silver staining.* Electrophoresis, 1985. **6**(3): p. 103-112.

138.	Domon, B. and R. Aebersold, *Mass spectrometry and protein analysis.* science, 2006. **312**(5771): p. 212-217.

139.	Bringans, S., et al., *Proteomic analysis of the venom of Heterometrus longimanus (Asian black scorpion).* Proteomics, 2008. **8**(5): p. 1081-1096.

140.	Spellman, D., et al., *Proteinase and exopeptidase hydrolysis of whey protein: Comparison of the TNBS, OPA and pH stat methods for quantification of degree of hydrolysis.* International Dairy Journal, 2003. **13**(6): p. 447-453.

141.	Adler-Nissen, J., *Determination of the degree of hydrolysis of food protein hydrolysates by trinitrobenzenesulfonic acid.* Journal of agricultural and food chemistry, 1979. **27**(6): p. 1256-1262.

142.	Mane, S., et al., *Extraction of gamma-conglutin from lupin seeds.* Chemeca 2014: Processing excellence; Powering our future, 2014: p. 1503.

143.	Raynal, B., et al., *Quality assessment and optimization of purified protein samples: why and how?* Microbial cell factories, 2014. **13**(1): p. 180.

144.	Pauli, G.F., et al., *Importance of purity evaluation and the potential of quantitative 1H NMR as a purity assay: miniperspective.* Journal of medicinal chemistry, 2014. **57**(22): p. 9220-9231.

145.	Dolan, J.W., *Peak tailing and resolution.* LC GC NORTH AMERICA, 2002. **20**(5): p. 430-437.

146.	Dolan, J.W., *Why do peaks tail.* LCGC Eur, 2003. **16**(9): p. 610-3.

147. Rathore, A. and A. Velayudhan, *Guidelines for optimization and scale-up in preparative chromatography.* Biopharm international, 2003. **16**(1): p. 34-42.

148. Hansen, E.B., *Chromatographic Scale-Up on a Volume Basis.* Preparative Chromatography for Separation of Proteins, 2017: p. 227.

149. KIDAL, S. and O.E. JENSEN, *Using volumetric flow to scaleup chromatographic processes.* Biopharm international, 2006. **19**(3).

150. Carta, G. and A. Jungbauer, *Protein chromatography: process development and scale-up.* 2010: John Wiley & Sons.

151. Den Engelsman, J., et al., *Strategies for the assessment of protein aggregates in pharmaceutical biotech product development.* Pharmaceutical research, 2011. **28**(4): p. 920-933.

152. Baldwin, M.A., *Protein identification by mass spectrometry issues to be considered.* Molecular & Cellular Proteomics, 2004. **3**(1): p. 1-9.

153. MatrixScience, *Understanding Mascot Reports (MS/MS Ion Results).* www.matrixscience.com, 2016.

154. Cottrell, J.S., *Protein identification using MS/MS data.* Journal of proteomics, 2011. **74**(10): p. 1842-1851.

155. Chen, Y.Y., *Preparation of total lupin protein extract and identification of target peptide for absolute quatification of gamma conglutin with isotope dilution liquid chromatography mass spectrometry.* 2018.

156. Islam, M.S., *Lupin seed proteomics for quantifying diversity and analysing food product.* 2012.

157. Carr, S., et al., *The need for guidelines in publication of peptide and protein identification data working group on publication guidelines for peptide and protein identification data.* 2004, ASBMB.

158. Capriotti, A.L., et al., *Identification of potential bioactive peptides generated by simulated gastrointestinal digestion of soybean seeds and soy milk proteins.* Journal of Food Composition and Analysis, 2015. **44**: p. 205-213.

159. Appel, W., *Chymotrypsin: molecular and catalytic properties.* Clinical biochemistry, 1986. **19**(6): p. 317-322.

160. Leiros, H.K.S., et al., *Trypsin specificity as elucidated by LIE calculations, X-ray structures, and association constant measurements.* Protein science, 2004. **13**(4): p. 1056-1070.

161. Morifuji, M., et al., *Comparison of different sources and degrees of hydrolysis of dietary protein: effect on plasma amino acids, dipeptides, and insulin responses in human subjects.* Journal of agricultural and food chemistry, 2010. **58**(15): p. 8788-8797.

162. Korhonen, H. and A. Pihlanto, *Food-derived bioactive peptides-opportunities for designing future foods.* Current pharmaceutical design, 2003. **9**(16): p. 1297-1308.

163. Mosmann, T., *Rapid colorimetric assay for cellular growth and survival: application to proliferation and cytotoxicity assays.* Journal of immunological methods, 1983. **65**(1-2): p. 55-63.

164. Carlessi, R., et al., *GLP-1 receptor signalling promotes β-cell glucose metabolism via mTOR-dependent HIF-1α activation.* Scientific Reports, 2017. **7**.

165. Keane, K.N., et al., *The impact of cryopreservation on human peripheral blood leucocyte bioenergetics.* Clinical science, 2015. **128**(10): p. 723-733.

166. Krause, M., et al., *Elevated levels of extracellular heat-shock protein 72 (eHSP72) are positively correlated with insulin resistance in vivo and cause pancreatic β-cell dysfunction and death in vitro.* Clinical Science, 2014. **126**(10): p. 739-752.

167. Paredes, R.M., et al., *Chemical calcium indicators.* Methods, 2008. **46**(3): p. 143-151.

168. Grimble, G., et al., *Effect of peptide chain length on amino acid and nitrogen absorption from two lactalbumin hydrolysates in the normal human jejunum.* Clinical Science, 1986. **71**(1): p. 65-69.

169. Koopman, R., et al., *Ingestion of a protein hydrolysate is accompanied by an accelerated in vivo digestion and absorption rate when compared with its intact protein.* The American journal of clinical nutrition, 2009. **90**(1): p. 106-115.

170. Adibi, S., et al., *Evidence for two different modes of tripeptide disappearance in human intestine. Uptake by peptide carrier systems and hydrolysis by peptide hydrolases.* Journal of Clinical Investigation, 1975. **56**(6): p. 1355.

171. Geerts, B.F., et al., *Hydrolyzed casein decreases postprandial glucose concentrations in T2DM patients irrespective of leucine content.* Journal of dietary supplements, 2011. **8**(3): p. 280-292.

172. Blachier, F., et al., *Stimulus-secretion coupling of arginine-induced insulin release. Functional response of islets to L-arginine and L-ornithine.* Biochimica et Biophysica Acta (BBA)-Molecular Cell Research, 1989. **1013**(2): p. 144-151.

173. Schwanstecher, C., et al., *Interaction of N‑benzoyl‑D‑phenylalanine and related compounds with the sulphonylurea receptor of β‑cells.* British journal of pharmacology, 1998. **123**(6): p. 1023-1030.

174. Claessens, M., et al., *Glucagon and insulin responses after ingestion of different amounts of intact and hydrolysed proteins.* British journal of nutrition, 2008. 100(1): p. 61-69

175. Gaudel, C., et al., *A whey protein hydrolysate promotes insulinotropic activity in a clonal pancreatic β-cell line and enhances glycemic function in ob/ob mice.* The Journal of nutrition, 2013. **143**(7): p. 1109-1114.

176. Power, O., A. Hallihan, and P. Jakeman, *Human insulinotropic response to oral ingestion of native and hydrolysed whey protein.* Amino acids, 2009. **37**(2): p. 333-339.

177. McClenaghan, N.H., et al., *Characterization of a novel glucose-responsive insulin-secreting cell line, BRIN-BD11, produced by electrofusion.* Diabetes, 1996. **45**(8): p. 1132-1140.

178. McClenaghan, N.H., *Physiological regulation of the pancreatic β-cell: functional insights for understanding and therapy of diabetes.* Experimental physiology, 2007. **92**(3): p. 481-496.

179. Dixon, G., et al., *A comparative study of amino acid consumption by rat islet cells and the clonal beta-cell line BRIN-BD11-the functional significance of L-alanine.* Journal of Endocrinology, 2003. **179**(3): p. 447-454.

180. DeFronzo, R., *Insulin resistance, lipotoxicity, type 2 diabetes and atherosclerosis: the missing links. The Claude Bernard Lecture 2009.* Diabetologia, 2010. **53**(7): p. 1270-1287.

181. Halperin, F., et al., *Insulin augmentation of glucose-stimulated insulin secretion is impaired in insulin-resistant humans.* Diabetes, 2012. **61**(2): p. 301-309.

182. Baggio, L.L. and D.J. Drucker, *Biology of incretins: GLP-1 and GIP.* Gastroenterology, 2007. **132**(6): p. 2131-2157.

183. Merglen, A., et al., *Glucose sensitivity and metabolism secretion coupling studied during two-year continuous culture in INS-1E Insulinoma cell lines.* Endocrinology, 2004. 142(2): p. 667-678.

184. Zhong, D., et al., *The glycolytic inhibitor 2-deoxyglucose activates multiple prosurvival pathways through IGF1R.* Journal of Biological Chemistry, 2009: p. jbc. M109. 005280.

185. Zhao, C., et al., *Expression and distribution of lactate/monocarboxylate transporter isoforms in pancreatic islets and the exocrine pancreas.* Diabetes, 2001. **50**(2): p. 361-366.

186. Carlessi, R., et al., *GLP-1 receptor signalling promotes beta-cell glucose metabolism via mTOR-dependent HIF-1alpha activation.* Sci Rep, 2017. **7**(1): p. 2661.

187. Maro, B., M.-C. Marty, and M. Bornens, *In vivo and in vitro effects of the mitochondrial uncoupler FCCP on microtubules.* The EMBO journal, 1982. **1**(11): p. 1347-1352.

188. AgilentTechnologies, *Agilent Seahorse XF Cell Mito Stress Test kit.* User guide kit 103015-100, 2017.

189. Luni, C., J.D. Marth, and F.J. Doyle III, *Computational modeling of glucose transport in pancreatic β-cells identifies metabolic thresholds and therapeutic targets in diabetes.* PloS one, 2012. **7**(12): p. e53130.

190. Thorens, B., *GLUT2, glucose sensing and glucose homeostasis.* Diabetologia, 2015. **58**(2): p. 221-232.

191. Brereton, M.F., et al., *Hyperglycaemia induces metabolic dysfunction and glycogen accumulation in pancreatic β-cells.* Nature communications, 2016. **7**: p. 13496.

192. Newgard, C.B. and J.D. McGarry, *Metabolic coupling factors in pancreatic β-cell signal transduction.* Annual review of biochemistry, 1995. **64**(1): p. 689-719.

193. Prentki, M., F.M. Matschinsky, and S.M. Madiraju, *Metabolic signaling in fuel-induced insulin secretion.* Cell metabolism, 2013. **18**(2): p. 162-185.

194. Straub, S.G., et al., *Glucose activates both K (ATP) channel-dependent and K (ATP) channel-independent signaling pathways in human islets.* Diabetes, 1998. **47**(5): p. 758-763.

195. Panten, U., et al., *Control of insulin secretion by sulfonylureas, meglitinide and diazoxide in relation to their binding to the sulfonylurea receptor in pancreatic islets.* Biochemical pharmacology, 1989. **38**(8): p. 1217-1229.

196. Ashcroft, F.M. and P. Rorsman, *Electrophysiology of the pancreatic β-cell.* Progress in biophysics and molecular biology, 1989. **54**(2): p. 87-143.

197. Henquin, J.-C., et al., *Hierarchy of the β-cell signals controlling insulin secretion.* European journal of clinical investigation, 2003. **33**(9): p. 742-750.

198. Seino, S. and T. Shibasaki, *PKA-dependent and PKA-independent pathways for cAMP-regulated exocytosis.* Physiological reviews, 2005. **85**(4): p. 1303-1342.

199. Nenquin, M., et al., *Both triggering and amplifying pathways contribute to fuel-induced insulin secretion in the absence of sulfonylurea receptor-1 in pancreatic β-cells.* Journal of Biological Chemistry, 2004. **279**(31): p. 32316-32324.

200. Ravier, M.A., et al., *Glucose controls cytosolic Ca2+ and insulin secretion in mouse islets lacking adenosine triphosphate-sensitive K+ channels owing to a knockout of the pore-forming subunit Kir6. 2.* Endocrinology, 2008. **150**(1): p. 33-45.

201. Hannan, J., et al., *Ocimum sanctum leaf extracts stimulate insulin secretion from perfused pancreas, isolated islets and clonal pancreatic β-cells.* Journal of Endocrinology, 2006. **189**(1): p. 127-136.

202. Hannan, J., et al., *Insulin secretory actions of extracts of Asparagus racemosus root in perfused pancreas, isolated islets and clonal pancreatic β-cells.* Journal of Endocrinology, 2007. **192**(1): p. 159-168.

203. Miller, L., et al., *The class B G-protein-coupled GLP-1 receptor: an important target for the treatment of type-2 diabetes mellitus.* International journal of obesity supplements, 2014. **4**: p. S9-S13.

204. Gembal, M., et al., *Mechanisms by which glucose can control insulin release independently from its action on adenosine triphosphate-sensitive K+ channels in mouse B cells.* Journal of Clinical Investigation, 1993. **91**(3): p. 871.

205. Willard, F.S. and K.W. Sloop, *Physiology and emerging biochemistry of the glucagon-like peptide-1 receptor.* Experimental diabetes research, 2012. **2012**.

206. Sharp, G., *The adenylate cyclase-cyclic AMP system in islets of Langerhans and its role in the control of insulin release.* Diabetologia, 1979. **16**(5): p. 287-296.

207. Seino, S., et al., *Roles of cAMP signalling in insulin granule exocytosis.* Diabetes, Obesity and Metabolism, 2009. **11**(s4): p. 180-188.

208. Light, P.E., et al., *Glucagon-like peptide-1 inhibits pancreatic ATP-sensitive potassium channels via a protein kinase A-and ADP-dependent mechanism.* Molecular endocrinology, 2002. **16**(9): p. 2135-2144.

209. Kang, G., et al., *cAMP sensor Epac as a determinant of ATP-sensitive potassium channel activity in human pancreatic β cells and rat INS-1 cells.* The Journal of physiology, 2006. **573**(3): p. 595-609.

210. MacDonald, P. and M. Wheeler, *Voltage-dependent K+ channels in pancreatic beta cells: role, regulation and potential as therapeutic targets.* Diabetologia, 2003. **46**(8): p. 1046-1062.

211. Gromada, J., et al., *Glucagon-like peptide 1 (7-36) amide stimulates exocytosis in human pancreatic β-cells by both proximal and distal regulatory steps in stimulus-secretion coupling.* Diabetes, 1998. **47**(1): p. 57-65.

212. Doyle, M.E. and J.M. Egan, *Mechanisms of action of glucagon-like peptide 1 in the pancreas.* Pharmacology & therapeutics, 2007. **113**(3): p. 546-593.

213. Kang, G., et al., *A cAMP and Ca2+ coincidence detector in support of Ca2+-induced Ca2+ release in mouse pancreatic β cells.* The Journal of physiology, 2005. **566**(1): p. 173-188.

214. Alasbahi, R. and M. Melzig, *Forskolin and derivatives as tools for studying the role of cAMP.* Die Pharmazie-An International Journal of Pharmaceutical Sciences, 2012. **67**(1): p. 5-13.

215. Chijiwa, T., et al., *Inhibition of forskolin-induced neurite outgrowth and protein phosphorylation by a newly synthesized selective inhibitor of cyclic AMP-dependent protein kinase, N-[2-(p-bromocinnamylamino) ethyl]-5-isoquinolinesulfonamide (H-89), of PC12D pheochromocytoma cells.* Journal of Biological Chemistry, 1990. **265**(9): p. 5267-5272.

216. Fassett, J., D. Tobolt, and L.K. Hansen, *Type I collagen structure regulates cell morphology and EGF signaling in primary rat hepatocytes through cAMP-dependent protein kinase A.* Molecular biology of the cell, 2006. **17**(1): p. 345-356.

217. Ferro, A., et al., *Nitric oxide-dependent β2-adrenergic dilatation of rat aorta is mediated through activation of both protein kinase A and Akt.* British journal of pharmacology, 2004. **143**(3): p. 397-403.

218. Xie, G.-H., et al., *ADP-ribosyl cyclase couples to cyclic AMP signaling in the cardiomyocytes.* Biochemical and biophysical research communications, 2005. **330**(4): p. 1290-1298.

219. Kakita, A., et al., *Possible involvement of p38 MAP kinase in prostaglandin E1-induced ALP activity in osteoblast-like cells.* Prostaglandins, leukotrienes and essential fatty acids, 2004. **70**(5): p. 469-474.

220. Kim, S.H., et al., *Involvement of protein kinase A in cannabinoid receptor-mediated protection from oxidative neuronal injury.* Journal of Pharmacology and Experimental Therapeutics, 2005. **313**(1): p. 88-94.

221. Burvall, K., L. Palmberg, and K. Larsson, *Expression of TNFalpha and its receptors R1 and R2 in human alveolar epithelial cells exposed to organic dust and the effects of 8-bromo-cAMP and protein kinase A modulation.* Inflammation Research, 2005. **54**(7): p. 281-288.

222. Skinn, A.C. and W.K. MacNaughton, *Nitric oxide inhibits cAMP-dependent CFTR trafficking in intestinal epithelial cells.* American Journal of Physiology-Gastrointestinal and Liver Physiology, 2005. **289**(4): p. G739-G744.

223. Dalle, S., et al., *Roles and regulation of the transcription factor CREB in pancreatic β-cells.* Current molecular pharmacology, 2011. **4**(3): p. 187-195.

224. Gilman, A.G., *G proteins: transducers of receptor-generated signals.* Annual review of biochemistry, 1987. **56**(1): p. 615-649.

225. Gilon, P. and J.-C. Henquin, *Mechanisms and physiological significance of the cholinergic control of pancreatic β-cell function.* Endocrine reviews, 2001. **22**(5): p. 565-604.

226. Verspohl, E. and K. Herrmann, *Involvement of G proteins in the effect of carbachol and cholecystokinin in rat pancreatic islets.* American Journal of Physiology-Endocrinology And Metabolism, 1996. **271**(1): p. E65-E72.

227. Lee, B., et al., *Effect of AVP and oxytocin on insulin release: involvement of V1b receptors.* American Journal of Physiology-Endocrinology And Metabolism, 1995. **269**(6): p. E1095-E1100.

228. Gregersen, S., J.L. Thomsen, and K. Hermansen, *Endothelin-1 (ET-1)—potentiated insulin secretion: Involvement of protein kinase C and the ETA receptor subtype.* Metabolism, 2000. **49**(2): p. 264-269.

229. Ahren, B., G. Taborsky, and D. Porte, *Neuropeptidergic versus cholinergic and adrenergic regulation of islet hormone secretion.* Diabetologia, 1986. **29**(12): p. 827-836.

230. Miller, R.E., *Pancreatic neuroendocrinology: peripheral neural mechanisms in the regulation of the islets of Langerhans.* Endocrine Reviews, 1981. **2**(4): p. 471-494.

231. Nishimura, A., et al., *Structural basis for the specific inhibition of heterotrimeric Gq protein by a small molecule.* Proceedings of the National Academy of Sciences, 2010. **107**(31): p. 13666-13671.

232. Schmitz, A.-L., et al., *A cell-permeable inhibitor to trap Gα q proteins in the empty pocket conformation.* Chemistry & biology, 2014. **21**(7): p. 890-902.

233. Biaggioni, I. and D. Robertson, *Adrenoceptor agonists & sympathomimetic drugs.* Basic and Clinical Pharmacology. 11th ed. New York, NY: The McGraw-Hill Companies Inc, 2009.

234. Tian, Y.-M., V. Urquidi, and S. Ashcroft, *Protein kinase C in beta-cells: expression of multiple isoforms and involvement in cholinergic stimulation of insulin secretion.* Molecular and cellular endocrinology, 1996. **119**(2): p. 185-193.

235. Zawalich, W.S. and K.C. Zawalich, *Effects of protein kinase C inhibitors on insulin secretory responses from rodent pancreatic islets.* Molecular and cellular endocrinology, 2001. **177**(1): p. 95-105.

236. Zhang, H., et al., *Bimodal role of conventional protein kinase C in insulin secretion from rat pancreatic β cells.* The Journal of physiology, 2004. **561**(1): p. 133-147.

237. Cheng, K.-C., et al., *Characterization of preptin-induced insulin secretion in pancreatic β-cells.* Journal of Endocrinology, 2012. **215**(1): p. 43-49.

238. Macmillan, D. and J. McCarron, *The phospholipase C inhibitor U-73122 inhibits Ca2+ release from the intracellular sarcoplasmic reticulum Ca2+*

store by inhibiting Ca2+ pumps in smooth muscle. British journal of pharmacology, 2010. **160**(6): p. 1295-1301.

239. Young, L.H., B.J. Balin, and M.T. Weis, *Gö 6983: a fast acting protein kinase C inhibitor that attenuates myocardial ischemia/reperfusion injury.* Cardiovascular Therapeutics, 2005. **23**(3): p. 255-272.

240. Ahrén, B., *Islet G protein-coupled receptors as potential targets for treatment of type 2 diabetes.* Nature reviews Drug discovery, 2009. **8**(5): p. 369-385.

241. Feng, X.-T., H.-M. Duan, and S.-L. Li, *Protective role of Pollen Typhae total flavone against the palmitic acid-induced impairment of glucose-stimulated insulin secretion involving GPR40 signaling in INS-1 cells.* International journal of molecular medicine, 2017. **40**(3): p. 922-930.

242. Veprik, A., et al., *GPR41 modulates insulin secretion and gene expression in pancreatic β-cells and modifies metabolic homeostasis in fed and fasting states.* The FASEB Journal, 2016. **30**(11): p. 3860-3869.

243. Reimann, F. and F.M. Gribble, *G protein-coupled receptors as new therapeutic targets for type 2 diabetes.* Diabetologia, 2016. **59**(2): p. 229-233.

244. Drucker, D.J., *The biology of incretin hormones.* Cell metabolism, 2006. **3**(3): p. 153-165.

245. Ahrén, B., *GLP-1-based therapy of type 2 diabetes: GLP-1 mimetics and DPP-IV inhibitors.* Current diabetes reports, 2007. **7**(5): p. 340-347.

246. Tapadia, M., et al., *Lupin seed hydrolysate promotes G-protein-coupled receptor, intracellular Ca2+ and enhanced glycolytic metabolism-mediated insulin secretion from BRIN-BD11 pancreatic beta cells.* Molecular and cellular endocrinology, 2019. **480**: p. 83-96.

247. Ibrahim, M.A., et al., *Structural properties of bioactive peptides with α-glucosidase inhibitory activity.* Chemical biology & drug design, 2018. **91**(2): p. 370-379.

248. Lammi, C., et al., *Peptides derived from soy and lupin protein as dipeptidyl-peptidase IV inhibitors: in vitro biochemical screening and in silico molecular modeling study.* Journal of agricultural and food chemistry, 2016. **64**(51): p. 9601-9606.

249. Zhang, P., *Analysis of mouse liver glycogen content.* Bio-protocol, 2012. **2**(10): p. e186.

250. Schneider, C.A., W.S. Rasband, and K.W. Eliceiri, *NIH Image to ImageJ: 25 years of image analysis.* Nature methods, 2012. **9**(7): p. 671.

251. Elya, B., et al., *creening of alpha-glucosidase inhibitory activity from some plants of Apocynaceae, Clusiaceae, Euphorbiaceae, and Rubiaceae.* BioMed Research International, 2011. **2012**.

252. Lovshin, J.A. and D.J. Drucker, *Incretin-based therapies for type 2 diabetes mellitus.* Nature Reviews Endocrinology, 2009. **5**(5): p. 262.

253. Skelin, M., M. Rupnik, and A. Cencič, *Pancreatic beta cell lines and their applications in diabetes mellitus research.* ALTEX-Alternatives to animal experimentation, 2010. **27**(2): p. 105-113.

254.   Buczkowska, E. and P. Jarosz-Chobot, *Insulin effect on metabolism in skeletal muscles and the role of muscles in regulation of glucose homeostasis.* Przeglad lekarski, 2001. **58**(7-8): p. 782-787.

255.   Dimitriadis, G., et al., *Insulin effects in muscle and adipose tissue.* Diabetes research and clinical practice, 2011. **93**: p. S52-S59.

256.   Boucher, J., A. Kleinridders, and C.R. Kahn, *Insulin receptor signaling in normal and insulin-resistant states.* Cold Spring Harbor perspectives in biology, 2014. **6**(1): p. a009191.

257.   Mackenzie, R.W. and B.T. Elliott, *Akt/PKB activation and insulin signaling: a novel insulin signaling pathway in the treatment of type 2 diabetes.* Diabetes, metabolic syndrome and obesity: targets and therapy, 2014. **7**: p. 55.

258.   Summers, S.A., et al., *The role of glycogen synthase kinase 3β in insulin-stimulated glucose metabolism.* Journal of Biological Chemistry, 1999. **274**(25): p. 17934-17940.

259.   Fecchi, K., et al., *Spatial and temporal regulation of GLUT4 translocation by flotillin-1 and caveolin-3 in skeletal muscle cells.* The FASEB journal, 2006. **20**(6): p. 705-707.

260.   Yoon, M.-S., *The role of mammalian target of rapamycin (mTOR) in insulin signaling.* Nutrients, 2017. **9**(11): p. 1176.

261.   Shimobayashi, M. and M.N. Hall, *Making new contacts: the mTOR network in metabolism and signalling crosstalk.* Nature reviews Molecular cell biology, 2014. **15**(3): p. 155.

262.   Liu, Z. and E.J. Barrett, *Human protein metabolism: its measurement and regulation.* American Journal of Physiology-Endocrinology and Metabolism, 2002. **283**(6): p. E1105-E1112.

263.   Kimball, S.R. and L.S. Jefferson, *Cellular mechanisms involved in the action of insulin on protein synthesis.* Diabetes/metabolism reviews, 1988. **4**(8): p. 773-787.

264.   Dillmann, W.H., *Diabetes mellitus-induced changes in the concentration of specific mRNAs and proteins.* Diabetes/metabolism reviews, 1988. **4**(8): p. 789-797.

265.   Jefferson, L., et al. *Insulin in the regulation of protein turnover in heart and skeletal muscle.* in *Federation proceedings.* 1974.

266.   Biolo, G. and R.R. Wolfe, *Insulin action on protein metabolism.* Bailliere's clinical endocrinology and metabolism, 1993. **7**(4): p. 989-1005.

267.   D'Oria, R., et al., *PKB/Akt and MAPK/ERK phosphorylation is highly induced by inositols: Novel potential insights in endothelial dysfunction in preeclampsia.* Pregnancy hypertension, 2017. **10**: p. 107-112.

268.   Seger, R. and E.G. Krebs, *The MAPK signaling cascade.* The FASEB journal, 1995. **9**(9): p. 726-735.

269.   Nauck, M.A., B. Baller, and J.J. Meier, *Gastric inhibitory polypeptide and glucagon-like peptide-1 in the pathogenesis of type 2 diabetes.* Diabetes, 2004. **53**(suppl 3): p. S190-S196.

270. Lynn, F.C., et al., *Defective glucose-dependent insulinotropic polypeptide receptor expression in diabetic fatty Zucker rats.* Diabetes, 2001. **50**(5): p. 1004-1011.

271. Vella, A., *Mechanism of action of DPP-4 inhibitors—new insights.* 2012, Oxford University Press.

272. Power, O., et al., *Food protein hydrolysates as a source of dipeptidyl peptidase IV inhibitory peptides for the management of type 2 diabetes.* Proceedings of the Nutrition Society, 2014. **73**(1): p. 34-46.

273. Caymanchemicals, *DPP(IV) Inhibitor Screening Assay kit, 700210.* www.caymanchem.com.

274. Darmoul, D., et al., *Dipeptidyl peptidase IV (CD 26) gene expression in enterocyte-like colon cancer cell lines HT-29 and Caco-2. Cloning of the complete human coding sequence and changes of dipeptidyl peptidase IV mRNA levels during cell differentiation.* Journal of Biological Chemistry, 1992. **267**(7): p. 4824-4833.

275. Yoshioka, M., et al., *Expression of dipeptidyl aminopeptidase IV during enterocytic differentiation of human colon cancer (Caco-2) cells.* International journal of cancer, 1991. **47**(6): p. 916-921.

276. Sambuy, Y., et al., *The Caco-2 cell line as a model of the intestinal barrier: influence of cell and culture-related factors on Caco-2 cell functional characteristics.* Cell biology and toxicology, 2005. **21**(1): p. 1-26.

277. Caron, J., et al., *Using Caco-2 cells as novel identification tool for food-derived DPP-IV inhibitors.* Food Research International, 2017. **92**: p. 113-118.

278. Derosa, G. and P. Maffioli, *α-Glucosidase inhibitors and their use in clinical practice.* Archives of medical science: AMS, 2012. **8**(5): p. 899.

279. Yin, Z., et al., *α-Glucosidase inhibitors isolated from medicinal plants.* Food Science and Human Wellness, 2014. **3**(3-4): p. 136-174.

280. Kumar, S., et al., *α-glucosidase inhibitors from plants: A natural approach to treat diabetes.* Pharmacognosy reviews, 2011. **5**(9): p. 19.

281. Tundis, R., M. Loizzo, and F. Menichini, *Natural products as α-amylase and α-glucosidase inhibitors and their hypoglycaemic potential in the treatment of diabetes: an update.* Mini reviews in medicinal chemistry, 2010. **10**(4): p. 315-331.

282. Annicchiarico, P., et al., *Detection and exploitation of white lupin (Lupinus albus L.) genetic variation for seed γ-conglutin content.* Journal of Applied Botany and Food Quality, 2016. **89**.

283. Nongonierma, A.B., et al., *Insulinotropic properties of whey protein hydrolysates and impact of peptide fractionation on insulinotropic response.* International Dairy Journal, 2013. **32**(2): p. 163-168.